

Iceland
Liechtenstein
Norway grants

GREENCAM for tomorrow



 NTNU
Norwegian University of
Science and Technology

CONTEMPORARY SOLUTION FOR
ADVANCED MATERIALS WITH
HIGH IMPACT ON SOCIETY

CoSolMat

11th – 15th OCTOBER 2021
BUCHAREST, ROMANIA

<https://www.chimie.unibuc.ro/edu/greencam/index.php/workshop-2021>

“Working together for a green,
competitive and inclusive Europe”

**Contemporary Solutions for
Advanced Catalytic Materials
with a High Impact on Society**

CoSolMat

**GREENCAM FOR
TOMORROW**

11th – 15th OCTOBER 2021

BUCHAREST, ROMANIA

Disclaimer: This workshop was realised with the EEA Financial Mechanism 2014-2021 financial support. Its content (text, photos, videos) does not reflect the official opinion of the Programme Operator, the National Contact Point and the Financial Mechanism Office. Responsibility for the information and views expressed therein lies entirely with the author(s).

ORGANIZING COMMITTEE

Elisabeth E. JACOBSEN, Norwegian University of Science and Technology (NOR)

Kristofer G. Paso, Norwegian University of Science and Technology (NOR)

Sulalit BANDYOPADHYAY, Norwegian University of Science and Technology (NOR)

Mădălina TUDORACHE, University of Bucharest (RO)

Simona M. COMAN, University of Bucharest (RO)

Delia POPESCU, University of Bucharest (RO)

SECRETARIAT

Bogdan JURCA, University of Bucharest (RO)

Octavian D. PAVEL, University of Bucharest (RO)

Bogdan COJOCARU, University of Bucharest (RO)

Iunia PODOLEAN, University of Bucharest (RO)

Natalia CANDU, University of Bucharest (RO)

Sabina ION, University of Bucharest (RO)

	Monday	Tuesday	Wednesday	Thursday	Friday
	11-Oct	12-Oct	13-Oct	14-Oct	15-Oct
10:00-10:50		Parvulescu V.I.	Jacobsen E.E.	Coman S.M.	Conclusions
10:50-11:10		Kadela K.	Gheorghita G.	Psarrou M.N.	
11:10-11:30		Patulski P.	Ion S.	Farrando-Perez J.	
11:30-11:50		Oliveira Jardim E.	Ghetu M.C.	El Fergani M.	
11:50-12:10		Badea M.	Lungu C.	Mirica C.	
12:10-14:00		Lunch time	Lunch time	Lunch time	
14:00-14:30	Welcome & Registration	Frunza L.	Paso K.G.	Wegrzyn A.	
14:30-14:50		Antony J.	Olejniak A.	Pasatoiu T.-D.	
14:50-15:10		Stoian G.	Galarda A.	Petcuta O.	
15:10-15:30	Coffee time	Coffee time	Coffee time	Coffee time	
15:30-15:50	Welcome session	Paraschiv C.	El Fergani M.	Ftodiev A.-I.	
15:50-16:10		Guzo N.C.	Stanca M.	Bordeiasu M.	
16:10-16:30		Ejsmont A.	Oprea M.	Bejan S.E.	
16:30-16:50		Sobetkii A.	Mihăilă S.M.	Toderașc A.-T.	
16:50-17:10		Bărar A.	Mitroi P.C.	Voinea D.	
17:10-18:00		Poster session	Poster session	Poster session	

Summary

PLENARIES			Page
PL1	Parvulescu V.I.	<i>Catalysis in the circular economy concept</i>	3
PL2	Jacobsen E.E.	<i>Chemo-enzymatic synthesis of enantiomers for β-antagonists and -agonists</i>	4
PL3	Coman S.M.	<i>Nanoscaled metal fluorides: promising catalysts for the fine chemicals syntheses and biomass valorisation</i>	6
KEYNOTES			
KN1	Frunza L.	<i>Synthesis/deposition and characterization of supported nanostructured/nanopowdered semiconductor oxides</i>	11
KN2	Paso K.G.	<i>Coil-to-Globule Transition and Binding of Pour Point Depressant Polymers to Paraffin Wax Crystals</i>	13
KN3	Węgrzyn A.	<i>Ordered porous silicas modified with tailor made organic functional groups – treatment of wastewater polluted with emerging contaminants</i>	16
ORAL COMMUNICATIONS			
O1	Kadela K.	<i>Optimization of graphene paper surface functionalization by low temperature plasma using the Design of Experiments (DoE) methodology</i>	19
O2	Patulski P.	<i>K-modification of the CoY catalyst for the ethanol steam reforming process</i>	21
O3	Oliveira Jardim E.	<i>Carbons materials prepared from L-cysteine amino acid</i>	23
O4	Badea M.	<i>Complete solutions: Analytical Equipment, Consumables and Support for your applications!</i>	25
O5	Antony J.	<i>Silica-modified Bismutite Nanoparticles for Enhanced Adsorption and Visible Light Photocatalytic Degradation of Methylene Blue</i>	26
O6	Stoian G.	<i>Green strategy for the synthesis of carbon quantum dots (CQDs) from humins wastes</i>	28
O7	Paraschiv C.	<i>Zn(II) coordination polymers with mixed anionic linkers employed as heterogenous photocatalysts</i>	30
O8	Guzo N.C.	<i>From humins wastes to carbon quantum dots (CQDs) based photocatalytic nanocomposites</i>	32
O9	Ejsmont A.	<i>Co₃O₄ nanosheets as efficient cobalt source for spherical Co-based MOFs</i>	34
O10	Sobečkii A.	<i>Deposition and characterization of thin films based on nanostructured NiO as sensorial element for detection gases</i>	36
O11	Bărar A.	<i>Two-diode modeling of perovskite solar cells and parameter extraction using the Lambert W function</i>	38
O12	Gheorghita G.	<i>Biocatalysis based on cold-active lipase for silymarin valorization from vegetal waste of cold-pressed milk thistle oil technology</i>	40
O13	Ion S.	<i>Lignin derivatization using enzymatic pathway</i>	42

O14	Ghețu M.C.	<i>Bienzymatic biocatalyst based on enzyme co-immobilization for monoterpenes valorization</i>	44
O15	Lungu C.	<i>ABL&E – JASCO Româniaabout us</i>	46
O16	Olejnîk A.	<i>Silica materials modified with copper and aminosilane for adsorption and release of hydroxychloroquine</i>	47
O17	Galarda A.	<i>Metal-organic frameworks as diclofenac nanocarriers to treat migraine</i>	49
O18	El Fergani M.	<i>Magnetic core-multi-shell nanocomposites for green oxidation process of glucose</i>	51
O19	Stanca M.	<i>Protein based byproducts conversion into advanced materials</i>	53
O20	Oprea M.	<i>A new generation of polysulfone membrane materials for hemodialysis</i>	55
O21	Mihăilă S.-D.	<i>New approaches in synthesis of 2D LDH-type materials used in the Claisen-Schmidt condensation</i>	57
O22	Mitroi P.C.	<i>New coordination compounds based on Cu(II) and 1,3-bis(4-pyridyl)propane as a divergent ligand</i>	59
O23	Psarrou M.N.	<i>Synthesis of barbituric acid graphene hybrids</i>	61
O24	Farrando-Pérez J.	<i>Imidacloprid removal using activated carbons</i>	63
O25	El Fergani M.	<i>Environmental friendly solid catalytic systems for HMF production</i>	65
O26	Mirică C.	<i>OF SYSTEMS</i>	67
O27	Pasatoiu T.-D.	<i>Synthesis and Characterization of Several New 1-D, 2-D, and 3-D Coordination Polymers</i>	68
O28	Petcuță O.	<i>Synthesis, Characterization, and Bioactivity of New Oxidovanadium(V) Compounds based on Salicylaldehyde-derivatives Schiff Bases</i>	70
O29	Ftodiev A.-I.	<i>Enzymatic degradation of PET</i>	72
O30	Bordeiașu M.	<i>Crystalline Cu(II)-based coordination polymers with Kagomé architecture</i>	74
O31	Bejan S.E.	<i>Hydrothermal Synthesis of Equimolar Multicomponent Rare Earth Oxides</i>	76
O32	Toderașc A.-T.	<i>New highly effective transition-metal-containing MgFe mixed oxides catalysts for benzyl alcohol hydrodeoxygenation</i>	78
O33	Voinea D.	<i>Novel coordination polymers of Co(II) with 4,4'-oxy(bis)benzoic acid and auxiliary N,N'-donor ligands</i>	80

POSTER PRESENTATIONS

P1	Beneș A.E.M.	<i>New extended structures of organotin(IV) with dicarboxylic acids</i>	85
P2	David M.E.	<i>Decorated Multi-Walled Carbon Nanotubes Dispersed in PHBHV for Wood Preservation</i>	87
P3	Eftemie D.-I.	<i>Chiral-copper(II) complexes anchored on carboxylated graphene oxide for catalytic applications</i>	89
P4	Jankowska A.	<i>Removal of Sunset Yellow FCF from aqueous solutions using modified NaX zeolite and MCM-41 silica obtained from fly ash</i>	91
P5	Mihăilescu R.	<i>Photocatalytic decontamination of wastewaters using hybrid organic inorganic magnetic supramolecular catalysts</i>	93
P6	Pîrvu A.-M.	<i>Homo and heteroclusters of Mn(II/III) and Co(II/III) containing aminoalcohols and carboxylate anions</i>	95
P7	Slabu A.	<i>Plant based resins obtained from epoxidized linseed oil using a heterogenous hydrotalcite catalyst</i>	96

P8	Spinciu A.	<i>Copper-based materials – new “green” electrochemical sensors for hydrogen peroxide</i>	98
P9	Țincu R.-A.	<i>Metal-containing ionic liquids used as catalysts in the recycling of PET waste</i>	100

	ALFABETICAL INDEX OF AUTHORS		103
--	-------------------------------------	--	-----

PLENARIES

Catalysis in the circular economy concept

Vasile I. Parvulescu*

University of Bucharest, Center of Catalysts and Catalysis Processes, 4-12 Regina Elisabeta Av., Bucharest, 030018, Romania

e-mail: vasile.parvulescu@chimie.unibuc.ro

Circular economy (also referred to as "circularity") defines an economic system that tackles global challenges like climate change, biodiversity loss, wastes, and pollution. Chemistry is playing an important role in this system since most of the challenges have it at the origin. To limit the negative effects Circular economy operates with a series of concepts such as: reuse, share, repair, refurbish or remanufacture (Fig. 1) [2]. Therefore, its application is expected to eliminate wastes and regenerate natural systems.

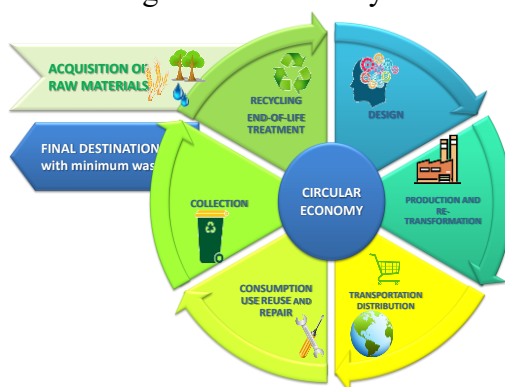


Figure 1. Visualization of the Circular economy concept

Recycling of valuable resources represents a mandatory key instrument of the moments. Catalysis is at “the heart” of the efficient transformations of the molecules and materials and on this basis is a needed important actor for a **circular economy** [3]. Recycling food, agriculture, textile, plastics and carbon dioxide wastes can be efficiently achieved only utilizing catalysis.

To date, reports indicate the use of catalysis in such processes in both the homogeneous catalysis (catalysis with metal complexes and biocatalysis) and biphasic systems (heterogeneous catalysis and photocatalysis). However, heterogeneous catalysis is more preferred due to the possibility to recover catalysts also affording a complete sustainability of catalysts containing expensive metals. This makes even more sense where the catalysts are as well prepared from renewable wastes and can be recycled.

Based on this state of the art, in line with the circular economy concepts, this contribution will focus three aspects: *i)* heterogeneous catalysts from wastes and their efficiency; *ii)* heterogeneous catalysis in valorization of water soluble biowastes and *iii)* valorization of CO₂ following the Circular economy concepts.

References

- [1] Blewitt, J., *Understanding Sustainable Development* (2nd ed.). London: Routledge. ISBN 9780415707824 (2017).
- [2] L'économie circulaire, un nouveau modèle de développement. (2020, 11 juin). ESCadrille Toulouse Junior Conseil. <https://www.escadrille.org/fr/blog/economie-circulaire-nouveau-modele-developpement>.
- [3] Catlow, C.R., Davidson, M., Hutchings, G.J., Mulholland, A., Science to enable the circular economy, *Phil. Trans. R. Soc. A*, 378 (2020), 20200060

Chemo-enzymatic synthesis of enantiomers for β -antagonists and -agonists

Anna Lifen Tennfjord, Kristoffer Klungseth, Susanne Hansen Troøyen, Lucas Hugo Yan Boquin, Elisabeth Egholm Jacobsen*

Norwegian University of Science and Technology, Department of Chemistry, Høgskoleringen 5, 7491 Trondheim, Norway

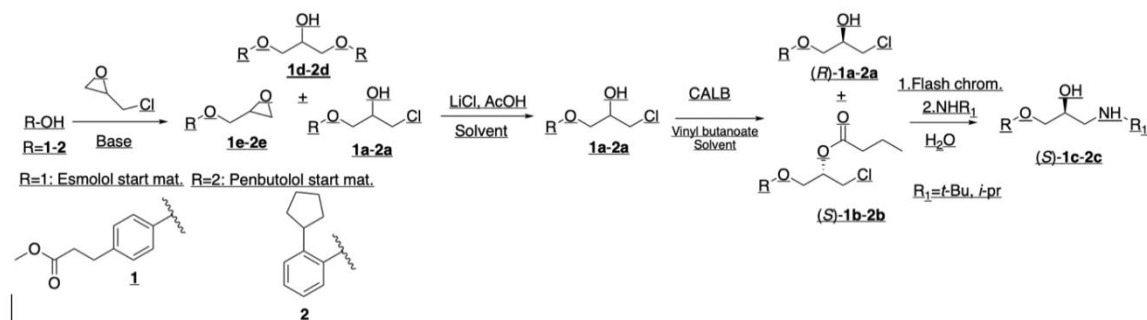
e-mail: elisabeth.e.jacobsen@ntnu.no

Introduction

Many drugs on the market today have active pharmaceutical ingredients (API's) with one or several stereogenic centers. β -Blockers, (drugs that slow down the heart rhythm by blocking or inhibiting the action of hormones, like adrenaline and noradrenaline, also named β -antagonists) have normally one stereogenic center, and then consist of two enantiomers. The enantiomers may have the same effect on the actual receptor in patients, or the enantiomers may have different effects, or worse: one enantiomer may cause several unwanted side effects. The American Food and Drug Administration (FDA) considers the «wrong» enantiomer as an impurity and demands for pure enantiomers as the API in the marketed drugs, not racemates. The demand for enantiomerically pure drugs has increased since FDA demanded manufacturers to evaluate the pharmacokinetics of a single enantiomer or mixture of enantiomers in a chiral drug. Quantitative assays for individual enantiomers should be developed for studies in *in vivo* samples early in drug development. During the last decade, our group has developed environmentally friendly methods for synthesis of enantiomerically pure building blocks for several β -antagonists using lipases in kinetic resolutions of racemates [1-5]. We have also obtained high enantiomeric excess of synthons in asymmetrisations of prochiral compounds with ketoreductases as catalysts [6]. Our ongoing projects on synthesis of enantiomerically pure building blocks for the β -antagonists (*S*)-esmolol and (*S*)-penbutolol will be discussed, and synthesis of building blocks for the β -agonists clenbuterol and sotalol will also briefly be discussed.

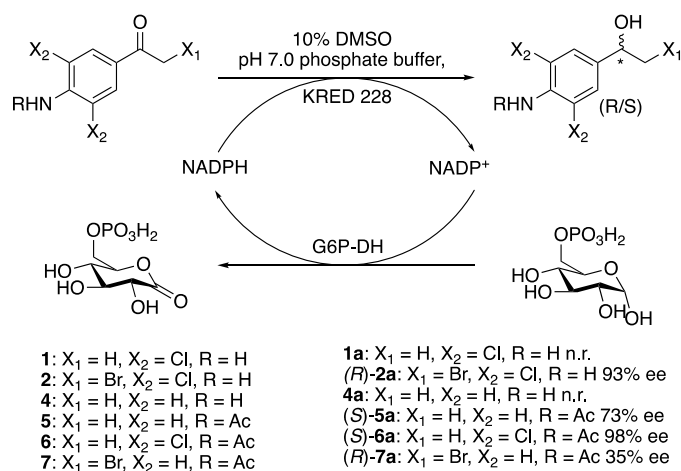
Results and discussion

Chlorohydrin building blocks (*R*)-**1a-2a** for the synthesis of enantiomers of the β -blockers esmolol ((*S*)-**1c**) and penbutolol ((*S*)-**2c**) have been synthesized in 89-96% *ee* by chemo-enzymatic methods (Scheme 1). Since the enzymatic step is kinetic resolution only 50% of the desired enantiomer will be obtained. Dynamic kinetic resolution may be performed in order to obtain full conversion of the starting material.



Scheme 1. Chemo-enzymatic synthesis of enantiomers of esmolol and penbutolol.

Asymmetrisations of ketones with suitable enzymes is another way of obtaining enantiopure compounds. Depending on the stereoselectivity of a catalyst towards a chosen substrate, a theoretical yield of 100% might be obtained. Scheme 2 shows asymmetrisation of ketone **1**, **2** and **4-7** with ketoreductase KRED 228 as catalyst (Syncozymes Co., Ltd., Shanghai, China). Several regeneration systems were tested, in order to find a suitable system to regenerate NADP⁺, and we were successful with glucose-6-phosphate dehydrogenase with glucose-6-phosphate as the co-substrate [7,8]. The co-solvent was dimethyl sulfoxide (DMSO) in all the asymmetrisation reactions.



Scheme 2. Asymmetrisation reactions of prochiral ketones catalysed by ketoreductase 228 (KRED 228) from SyncoZymes, Co LTD.

Conclusions

High enantiomeric excess of synthons as building blocks for several aminoalcohol drugs have been obtained both by kinetic resolutions of racemic mixtures catalysed by lipases and in asymmetrisations of prochiral ketones catalysed by ketoreductases.

Acknowledgements

EEA project 18-COP-0041 GreenCAM is thanked for support and SyncoZymes Co. LTD, Shanghai, China, is thanked for gift of KREDs and CALB.

References

- [1] Jacobsen, E.E., Hoff, B.H., Anthonsen, T., *Chirality*, 12 (2000), 654-659.
- [2] Jacobsen, E.E.; Anthonsen, T., *Canadian Journal of Chemistry*, 80 (2002), 577-581.
- [3] Lund, I.T., Bøckmann, P.L., Jacobsen, E.E., *Tetrahedron*, 72 (2016), 7288-7292.
- [4] Jacobsen, E.E., Anthonsen, T., *Trends in Organic Chemistry*, 18 (2017), 71-83.
- [5] Gundersen, M.A., Austli, G.B., Løvland, S.S., Hansen, M.B., Rødseth, M., Jacobsen, E.E., *Catalysts*, 11 (2021), 503-518.
- [6] Blindheim, F.H., Hansen, M.B., Evjen, S., Zhu, W., Jacobsen, E.E., *Catalysts*, 8 (2018), 516-528.
- [7] Matsuda, T., Yamanaka, R., Nakamura, K., *Tetrahedron: Asymmetry*, 20 (2009), 513-557.
- [8] Faber, K., Fessner, W.-D., Turner, N.J., Eds., *Science of Synthesis: Biocatalysis in Organic Synthesis*, Vol. 2, Georg Thieme Verlag KG, Stuttgart, Germany, (2015), pp. 672.

Nanoscaled metal fluorides: promising catalysts for the fine chemicals syntheses and biomass valorisation

Simona M. Coman^{1,*}, Vasile I. Parvulescu¹, E. Kemnitz²

¹University of Bucharest, Faculty of Chemistry, Department of Organic Chemistry, Biochemistry and Catalysis, 4-12 Regina Elisabeta Av., Bucharest, 030018, Romania

²Humboldt-Universität zu Berlin, Department of Chemistry, Brook-Taylor-Str. 2, 12489 Berlin, Germany

e-mail: simona.coman@chimie.unibuc.ro

Catalysis is clearly one of the foundational pillars of Green Chemistry and it will continue to be one of the main vehicles that take the chemical enterprise into a future of sustainability. For this, the production of chemicals, nowadays based on catalysis (ca. 90% of chemicals produced *via* catalytic routes), should have to move from homogeneous to heterogeneous catalysis (whenever possible) in order to avoid product contamination, reduce the processing costs, enhance the recovery and favor recyclability of catalysts. Therefore, with the aim to improve older industrial processes or to initiate other nowadays new processes under a greener manner, novel selective efficient solid catalysts were created and developed.

For instance, until recently, metal fluorides played a minor role in the field of heterogeneous catalysis but the recent developments of new synthesis approaches toward nanoscaled metal fluorides significantly increased the interest in these materials. Compared to classically metal oxides, metal fluorides just play a minor role in the field of heterogeneous catalysis, but nonetheless, there are several important reactions for which metal fluorides are the only choice as catalysts [1, 2].

Certainly, the classical sol-gel synthesis is one of the most powerful synthesis routes in terms of the wide variety of synthesis approaches and technical applications. Via the *fluorolytic* sol-gel synthesis strongly Lewis acidic nanoscopic metal fluorides, as well as bi-acidic hydroxide fluorides with tuneable Lewis to Brønsted acidity can, for the first time, be synthesized. By tuning the oxygen to fluoride stoichiometry inside these phases the surface side character can be altered from strongly Lewis acidic at high F-content towards weak Lewis but stronger Brønsted acidic or even basic (depending on the metal M at high oxygen content) resulting in optimized solid catalysts with high potential for a wide range of acid-base catalysed reactions [3, 4]. Moreover, the introduction of a second metal into these new compounds allows for further functionalization resulting in unlimited new compounds with high impact on catalytic applications for important industrial sectors, as fine chemicals and pharmaceutical ones.

These nanoscaled metal fluorides and hydroxide fluorides represent not only new, catalytically active classes of compounds with very high surface areas but also are excellent candidates to be used as supports for e.g. precious metals like Au, Pd, Pt etc. [4].

All the metal fluoride based catalysts which will be presented were comprehensively characterized by XRD, TEM, XPS, FTIR-spectroscopy, Solid State NMR, and MS-coupled DTA/TG measurements.

A variety of catalytic reactions performed with these new catalytic materials, in the area of fine chemicals synthesis will be presented. The most important envisaged fine chemicals synthesis were selected from those which still raises environmental problems at industrial level through the generated wastes and high energy consumption, as E and K vitamins synthesis and menthol synthesis [5-9].

But not only the unacceptable high level of wastes and pollution is the nowadays problem of the humanity. The important reduction of fossil fuel reserves on which is based

the current world economy corroborated with the global pollution and climate change is a major political, economic and scientific concern. To survive, our civilization has to make a strategically shift toward renewable fuels/products obtained *via* sustainable processes. In this context, the discovery and development of novel and efficient pathways for the conversion of the valuable bio-polymers (*i.e.*, cellulose, hemicellulose and lignin) into bio-chemicals (also named "platform molecules") are among the big challenges facing heterogeneous catalysis. The successful use of the novel inorganic hydroxylated nanoscopic fluorides catalytic materials in the primary building block production from renewable resources is further evidence of their extraordinary catalytic capabilities. The scientific achievements in the development of these materials and their catalytic properties connected with the catalytic performances will be also discussed [10-13].

References

- [1] Kemnitz, E., Menz, D.-H., Review: Progress in Solid State Chemistry, 26 (1998), 97.
- [2] Kemnitz, E., Winfield, J. M., In Advanced Inorganic Fluorides: Synthesis, Characterization and Applications, T. Nakajima, A. Tressaud, B. Zemva (Eds.), Publ. Elsevier Science S.A., (2000) 367.
- [3] Kemnitz, E., Wuttke, S., Coman, S. M., European Journal of Inorganic Chemistry, 31 (2011), 4773.
- [4] Kemnitz, E., Coman, S. M., Nanoscaled Metal Fluorides in Heterogeneous Catalysis (Chapter 6) in New materials for catalytic applications, V. Parvulescu and E. Kemnitz (Eds.), Elsevier Ltd., Oxford, UK, (2016) 133.
- [5] Coman, S. M., Wuttke, S., Vimont, A., Daturi, M., Kemnitz, E., Advanced Synthesis & Catalysis, 350 (2008), 2517.
- [6] Wuttke, S., Coman, S. M., Scholz, G., Kirmse, H., Vimont, A., Daturi, M., Schroeder, S. L. M., Kemnitz, E., Chemistry – A European Journal, 14 (2008), 11488.
- [7] Coman, S. M., Patil, P., Wuttke, S., Kemnitz, E., Chemical Communications, (2009) 460.
- [8] Coman, S. M., Parvulescu, V. I., Wuttke, S., Kemnitz, E., ChemCatChem, 2 (2010), 92.
- [9] Negoii, A., Wuttke, S., Kemnitz, E., Macovei, D., Parvulescu, V. I., Teodorescu, C.M., Coman, S.M., Angewandte Chemie International Edition, 49 (2010), 8134.
- [10] Troncea, S. B., Wuttke, S., Kemnitz, E., Coman, S.M., Parvulescu, V.I., Applied Catalysis B: Environmental, 107 (2011), 260.
- [11] Wuttke, S., Negoii, A., Gheorghe, N., Kuncser, V., Kemnitz, E., Parvulescu, V.I., Coman, S.M. ChemSusChem, 5 (2012), 1708.
- [12] Coman, S.M., Verziu, M., Tirsoaga, A., Jurca, B., Teodorescu, C., Kuncser, V., Parvulescu, V.I., Scholz, G., Kemnitz, E., ACS Catalysis, 5 (2015), 3013.
- [13] Verziu, M., Serano, M., Jurca, B., Parvulescu, V.I., Coman, S.M., Scholz, G., Kemnitz E., Catalysis Today, 306 (2018), 102.

KEYNOTES

Synthesis/deposition and characterization of supported nanostructured/nanopowdered semiconductor oxides

Ligia Frunzã*, Irina Zgura, Constantin Paul Ganes, Nicoleta Preda, Monica Enculescu
National Institute of Materials Physics, Magurele, Romania
e-mail: lfrunza@infim.ro

Introduction

Composite nanostructured materials containing semiconductors, such as TiO₂, ZnO, CdS, AgS, CdSe became very attractive due to their applications as photocatalysts for decomposing environmental pollutants, as solar cells, in different sensors, in opto-electronics or for transparent conducting films.

Recently we have studied the synthesis of nanoparticles of semiconductor oxides (especially TiO₂ and ZnO) and/or their deposition upon different (unusual, e.g. textiles) supports [1]. In addition, the investigation methods were chosen for these complex systems as well, being adequated to each material component and also to their application as catalytic properties.

The present work brings together some of our results and offers a challenge to enlarge the application area of such multifunctional nanostructured materials.

Experimental

Textiles made from natural or synthetic fibers (as much as possibly by unic components) like polyester, cotton, linen, wool were commercially available.

The semiconductor nanoparticles were deposited by sol-gel, electroless deposition, sputtering etc.

Sometimes one of the semiconductor oxides was used as support for deposition of a second semiconductor.

Several techniques were routinely applied for structural and morphological characterization: optical microscopy, XRD, SEM, TGA, UV-Vis spectroscopy, FTIR-ATR XPS. In addition, dielectric properties, ESR studies, optical examination, wetting and wicking properties were developed and corresponding data obtained when it was necessary. Thus, wetting properties were tested under static conditions by estimating the water contact angle. The sessile drop method was applied. Dielectric spectroscopy was applied in a broadband frequency and temperature range.

Semiconductor adherence on the support was checked by ultra-sonication.

Decolorization of dyes of Rhodamine B or methylene blue type was determined by measuring the variation of characteristic absorption peak at 554 nm wavelength. The percentage of dye photodegradation was estimated by using the known equation:

$$\text{Degradation efficiency} = (C_0 - C)/C_0 \times 100$$

where, C₀ is the initial value of the dye concentration, C is the value of dye concentration at t time.

Illumination was performed with UV or visible light.

Results and discussion

Let speak about some of the obtained materials, especially about those mentioned in Table 1 containing different supports and different deposition methods. Deposition was then successful even at the low temperature asked by the support nature.

Table 1. Temperature and pressure.

Sample	Support	Semiconductor	Deposition	Pretreatment
A	Knitted wool wear	ZnO	sputtering	
B	Knitted wool wear	ZnO	sputtering	Plasma
C	Knitted wool wear	ZnO	Electroless	
E	Knitted wool wear	TiO ₂	Sol-gel	
F	Knitted wool wear	TiO ₂	Sputtering	
G	ZnO	CdS	Wet chemical	

As shown by TG and SEM measurements, the deposited matter represents 3 to 8 wt%, covering rather uniformly the fiber surface.

Treated samples show mostly lower values of contact angle than the pristine ones. XRD Data have shown that TiO₂ layer has either an amorphous structure or is highly dispersed while pure hexagonal wurtzite phase of ZnO was observed for the corresponding samples. As concerning ZnO-CdS composites, they contain ZnO also in hexagonal wurtzite structure and CdS in cubic phase.

Oxide deposition might be conducted by the coordination of the transition metal ion to the protein oxygen atoms, this making a slight shift of the position of the vibration (IR) bands and modifying a bit the shape of these bands. Oxide deposition creates thus composite interfaces of hierarchical roughness since aggregated oxide nanoparticles sit over the periodic structure of microfiber array.

Plasma pretreatment and oxide deposition lead to a decreased hydrophobicity of the wool samples, no matter of their origin.

We have found that the photocatalytic activity of the studied fabric-semiconductor oxide systems could be increased as comparing with the activity of original fabric. Since some photocatalytically active samples did not show either XRD crystalline forms or SEM images of the titanium oxide crystallites we considered that the presence of anatase nanocrystals does no more seem to be a sine qua non photocatalytic element.

Acknowledgements

This work was funded by Ministry of Research, Innovation and Digitization [Project PN19-030101 under 21N Core Program].

References

- [1] Frunza, L., Preda, N., Matei, E., Frunza, S., Ganea, C.P., Vlaicu, A.M., Diamandescu, L., Dorogan, Journal of Polymer Science – Polymer Physics, 51 (2013), 1427-1437.
- [2] Frunza, L., Zgura, I., Enculescu, M., Frunza, S., Ganea, C.P., Rasoga, O., Cotorobai, F., Dorogan, A., Journal of Optoelectronics and Advanced Materials, 16 (2014), 176-181.
- [3] Frunza, L., Diamandescu, L., Zgura, Irina., Frunza, S., Ganea, C.P., Negrila, C.C., Enculescu, M., Birzu, M., Catalysis Today, 306 (2018), 251-259.
- [4] Zgura, I., Preda, N., Socol, G., Ghica, C., Ghica, D., Enculescu, M., Negut, I., Nedelcu, L., Frunza, L., Ganea, C.P., Frunza, S., Materials Research Bulletin, 99 (2018), 174-181.
- [5] Frunza, L., Cotorobai, V.F., Enculescu, M., Zgura, I., Ganea, C. P., Birzu, M., Mănăilă-Maximean, D., Advanced Topics in Optoelectronics, Microelectronics and Nanotechnologies X, 117182W (2020).

Coil-to-Globule Transition and Binding of Pour Point Depressant Polymers to Paraffin Wax Crystals

Muh Kurniawan¹, Jost Ruwoldt², Jens Norrman², Kristofer Gunnar Paso^{3,*}

¹*Ugelstad Laboratory, Department of Chemical Engineering, Norwegian University of Science and Technology, NO-7491 Trondheim, Norway; Research and Development Centre for Oil and Gas Technology, LEMIGAS, Daerah Khusus Ibukota Jakarta 12230, Indonesia*

²*Ugelstad Laboratory, Department of Chemical Engineering, Norwegian University of Science and Technology, NO-7491 Trondheim, Norway*

³*Ugelstad Laboratory, Department of Chemical Engineering, Norwegian University of Science and Technology, NO-7491 Trondheim, Norway*

e-mail: kristofer.g.paso@ntnu.no

Abstract

Paraffin wax crystals precipitate from waxy petroleum fluids upon cooling, leading to various production problems including paraffin wax deposition, gel formation, emulsion stabilization, filter plugging and fluid viscosification. Pristine paraffin wax crystals often adopt platelet-like morphologies with an orthorhombic lattice structure. The paraffin wax crystals generally have a thickness on the order of tens to hundreds of nanometers. Therefore, waxy petroleum fluids are nano-fluids at low temperatures.

The pour point temperature is a physical property which establishes the temperature at which a given fluid loses its ability to flow at short time scales under only the force of gravity. From a rheological perspective, the pour point temperature defines the boundary between a primary solid-like mechanical response and a primary liquid-like mechanical response. Polymer-based fluid additives are used in the petroleum production industry to reduce the pour point of waxy petroleum fluids, including waxy crude oils and waxy gas condensate fluids. Reduction of the fluid pour point temperature allows economic pipe transport of waxy petroleum fluids in cold environments, without incurring economic or energy penalties related to thermal management measures such as insulation or heating. The climate footprint of transporting waxy petroleum fluids is minimized by reducing the pour point using polymer-based chemical additives. Pour point depressants are formulated chemical products that are injected into waxy produced fluid streams to reduce the pour point, enabling low-temperature flowability. Pour point depressant formulations contain specially tailored polymers that physically bind to paraffin wax crystals. The polymers alter the wax crystal morphology and/or impart interparticle repulsions, thereby reducing the pour point.

When polymer molecules are thoroughly dispersed in a petroleum fluid, the chains may adopt a soluble coil conformational state or an insoluble globule conformational state, depending on the relative free energy favorability of intermolecular interactions. In the coil state, physical interactions between fluid molecules and polymer chain segments are favorable and abundant. In the coil state, the chain swells to maximize the favorable physical interactions. Conversely, in the insoluble globule conformational state, physical interactions between fluid molecules and polymer chain segments are unfavorable and sparse. In the insoluble globule state, the polymer chain retracts to minimize unfavorable physical interactions. As such, in the globule conformation, fluid molecules are expelled from the globule, and the polymer loses solubility. The coil-to-globule transition is governed by polymer size and temperature. An equivalency exists between temperature and polymer chain length with respect to the occurrence of the coil-to-globule transition. Low temperatures and long chains favor the insoluble globule state; high temperatures and short chains favor the coil state. Polymer chains must exist in the coil state to effectively bind with wax crystals and

reduce the pour point temperature. Considering only polymer solubility, shorter polymers are more effective in maintaining the fluidized coil conformation necessary for binding to paraffin wax crystals. Commensurately, low molecular weight polymer fractions would be considered preferable for usage in industrial pour point depressant formulations, based solely on solubility considerations.

In addition to polymer solubility constraints, physical binding between polymers and paraffin wax crystals must be considered when tailoring polymer molecular weight fractions for use in pour point depressant formulations. In addition to adopting a soluble coil conformational state (with fluidized polymer chains) in the bulk petroleum fluid at the paraffin wax crystallization temperature, effective pour point depressant polymers must physically bind to wax crystals by adsorption or co-crystallization. The effective binding strength of a polymer to wax crystals is quantified by the Gibbs free energy of binding:

$$\Delta G^\circ = \Delta H^\circ - T\Delta S^\circ$$

The Gibbs free energy of binding is a function of polymer molecular weight and temperature. In fact, there exists an equivalency between polymer molecular weight and temperature with respect to the Gibbs free energy of binding. The overall magnitude of the Gibbs free energy of binding increases monotonically with increasing polymer chain length. Longer polymers bind more strongly to wax crystals than shorter polymers. Accordingly, higher molecular weight fractions of polymer bind more strongly to paraffin wax crystals than lower molecular weight fractions. High molecular weight fractions of polymer can potentially provide improved pour point reduction efficacy in comparison to low molecular weight polymer fractions, based only on binding considerations.

Solubility considerations and binding considerations show opposite predictions regarding the influence of polymer molecular weight on the efficacy of pour point depressant formulations. Solubilization and binding are both essential components of the complete pour point reduction mechanism. Intermediate molecular weight polymer fractions fulfill the necessary conditions of solubilization and binding. Therefore, the intermediate molecular weight polymer fractions provide optimal pour point depressant efficacy.

Commercial pour point depressant polymers typically consist of a polydisperse distribution of polymer chain lengths. Consider a waxy petroleum fluid existing at a specific low temperature and dosed with a highly polydisperse pour point depressant polymer. The high polydispersity implies that polymers of varying chain length will exhibit vastly dissimilar behavior in terms of phase behavior. The entire distribution of polymer chain lengths can be grossly categorized into 3 separate fractions with distinct phase behavior:

- (1) The shortest polymer chains adopt soluble coil conformations in the bulk fluid phase and bind weakly to wax crystals as quantified by a small Gibbs free energy of binding.
- (2) Mid-length polymer chains adopt a soluble coil conformation in the bulk fluid phase and bind strongly to wax crystals as quantified by a larger Gibbs free energy of binding.
- (3) The longest polymer chains adopt an insoluble globule state in the bulk fluid phase. In the globule state, the polymer chains lose fluidity, lose solubility in the bulk fluid, and are prevented from binding to paraffin wax crystals.

This overall phase behavior description with respect to polymer chain length portends a single optimal polymer molecular weight for maximum binding to paraffin wax crystals, applicable at a single defined temperature condition. The optimal polymer length also approximates the polymer solubility threshold with respect to chain length at the defined temperature condition. An additional complication arises in petroleum production systems in the field, where paraffin wax precipitation occurs over a wide range of temperatures, rather than occurring at a single defined temperature condition. As such, non-isothermal crystallization occurring at real field conditions necessitates a somewhat broader polymer chain length distribution in an optimal pour point depressant formulation, characterized by a finite polydispersity. However, such a finite polydispersity of an optimal formulation is substantially smaller than the polydispersity values of currently existing industrial pour point depressant formulations. Hence, substantial improvements in industrial pour point depressant efficacy are achievable by simply tailoring the molecular weight distribution to the targeted petroleum fluid. In this way, inactive low and high molecular weight polymer fractions may be excluded from product formulations, and the formulated product can be restricted to contain only active polymer chains in addition to other required formulation ingredients.

Experimental data is presented to support the unified phase behavior description with respect to polymer chain length and temperature. The experimental methods of scission and fractional precipitation are introduced to alter molecular weight distributions of pour point depressant polymers. For two polymers, identified as polymer alpha and polymer beta, the low molecular weight sub-fractions of the polymer distribution generally exhibit a poorer performance in reducing the yield stress in comparison with the unmodified polymer distribution, which is consistent with a smaller Gibbs free energy of binding for the shorter polymer chains. The performance of a third polymer, identified as polymer tau, shows a complex dependency on chain length, fully consistent with the Gibbs free energy of binding trend as well as competing solubility effects. When crystallization occurs at low temperatures, polymer tau is marginally soluble, and the low molecular mass scission products (of higher solubility) exhibit improved performance in reducing the yield stress in comparison to the unaltered polymer tau. At high temperature conditions, polymer tau retains adequate solubility, and the low molecular weight scission products exhibit poorer performance in reducing the yield stress in comparison to the unaltered polymer tau, which is consistent with a lower magnitude of the Gibbs free energy of binding for shorter polymer chains. The experimental data corroborate a postulated molecular binding mechanism for the activity mode of the pour point depressant polymers alpha, beta, and tau. Therefore, the unified phase behavior description applies to polymers known to be molecularly dispersible in a bulk fluid phase at the respective wax crystallization temperature. In contrast, polymers that are known to self-assemble in the bulk fluid may show entirely different activity modes and mechanisms, such as nucleation templating, which are to a large extent insensitive to polymer molecular weight. Hence, the unified phase behavior description may be inapplicable to self-assembling pour point depressant polymers.

Acknowledgements

Muh Kurniawan acknowledges the Ministry of Energy and Mineral Resources of the Republic of Indonesia for financial support during his Ph.D. studies.

Ordered porous silicas modified with tailor made organic functional groups – treatment of wastewater polluted with emerging contaminants

Agnieszka Węgrzyn*, Dariusz Cież, Marcelina Radko, Dorota Majda, Sylwia Skórkiewicz, Monika Ciszewska

Jagiellonian University in Kraków, Faculty of Chemistry, ul. Gronostajowa 2, 30-387 Kraków, Poland

email: a.m.wegrzyn@uj.edu.pl

Toxic organic and inorganic chemicals are discharged into water, air and soil, severely contaminating the environment. Recently, the so-called emerging contaminants are gaining more and more attention in scientific research, both due to the need to establish legal regulations, the development of analytical methods used in monitoring as well as methods of their disposal. Emerging contaminants (EC) is a wide group of chemical compounds including pharmaceuticals and personal care products (PPCP), endocrine disruptors (ED), pesticides, perfluoroalkylated substances (PFAS), polybrominated diphenyl ethers (PBDEs), polychlorinated biphenyls (PCBs), and so on. Therefore, finding an effective method of their removal or neutralization is a challenge.

The removal of hazardous pollutants from the environment is an issue of the utmost importance and many methods have been investigated lately to resolve it. Adsorption, however, seems to be the best for that purpose and it is widely used due to its low cost, ease of operation and high effectiveness. Wide range of materials such as activated carbons, zeolites, modified clays, polymeric resins and fly ash have been applied in this process. However, ordered porous silicas modified with tailor made organic functional groups is an excellent example of advanced materials whose potential is yet not fully recognized.

Several examples of organically modified silicas used in removal of synthetic dyes, heavy metals and pharmaceuticals will be shown. Also application of standard methods of physicochemical characterization such as XRD, UV-Vis, FTIR as well as an unusual one, thermoporometry, will be presented.

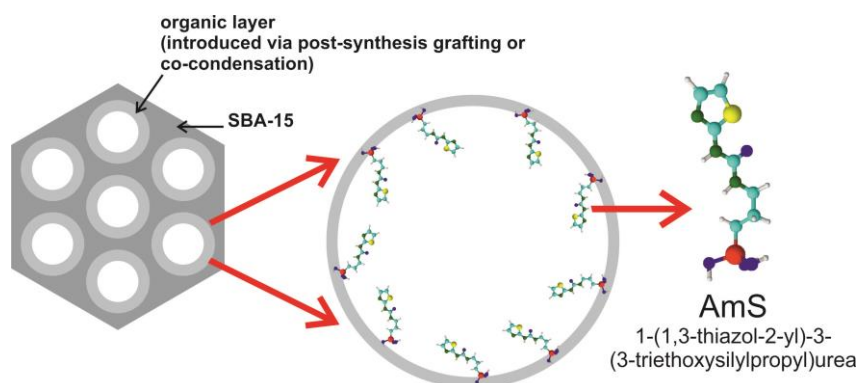


Figure 1. SBA-15 silica modified with aminothiazole [1].

Acknowledgements

Financial support of Talent management POB Anthropocene Minigrant is kindly acknowledged (S. Skórkiewicz).

References

- [1] Węgrzyn, A., Radko, M., Majda, D., Stawiński, W., Skiba, M., Cież, D., *Microporous and Mesoporous Materials*, 268 (2018) 31-38.

ORAL COMMUNICATIONS

Optimization of graphene paper surface functionalization by low temperature plasma using the Design of Experiments (DoE) methodology

Karolina Kadela^{*}, Gabriela Grzybek, Paweł Stelmachowski
Jagiellonian University, Department of Chemistry, Gronostajowa 2 30-387 Kraków, Poland
e-mail: karolina.kadela@student.uj.edu.pl

Introduction

Low temperature plasma was used to introduce oxygen functional groups on the surface of graphene paper. To optimize the degree of graphene paper functionalization the DoE methodology was applied. This method was a key element that helped to indicate which factors (time, plasma generator power, oxygen pressure) have the greatest impact on the modification of graphene paper. DoE is a mathematical methodology used for planning and conducting experiments but also analyzing and interpreting data obtained from the experiments. This is the branch of applied statistics that are used to research a system, process or product in which the input variables have been manipulated to investigate their effect on the measured response variable. [1,2].

Experimental

Graphene paper modification tests were carried out by the DoE application (time, power, pressure in the plasma chamber). For this purpose, 8 experiments were performed following Table 1 and Table 2.

Table 1. Factors and their values used for the DoE methodology.

	FACTOR	MIN VALUE (-1)	MAX VALUE (1)
A	TIME	6 s	15 min
B	POWER	40 W	100 W
C	PRESSURE	0,2 mbar	0,5 mbar

Table 2. The conditions of the experiments

	A	B	C
	TIME	POWER	PRESSURE
1	-1	-1	1
2	-1	1	1
3	1	-1	1
4	1	1	1
5	-1	-1	-1
6	-1	1	-1
7	1	-1	-1
8	1	1	-1

The effect of the modification was measured as the change in the work function (WF) using a Kelvin probe. The work function values exhibit a substantial exponential decay just after the plasma treatment, due an electrostatic charging. The obtained results were thus interpreted for the initial WF changes and after stabilization of the graphene paper in distilled water. X-ray photoelectron spectroscopy was used to determine the nature and surface concentration of surface functional groups.

Results and discussion

The use of the DoE methodology saved time and materials. Thus, with a small number of repeatable measurements, it was found that time and oxygen pressure had the greatest influence on the modification of graphene paper with the use of oxygen plasma. The obtained results are valid both for conditions after stabilization in water and without it. The results are displayed in Fig. 1.

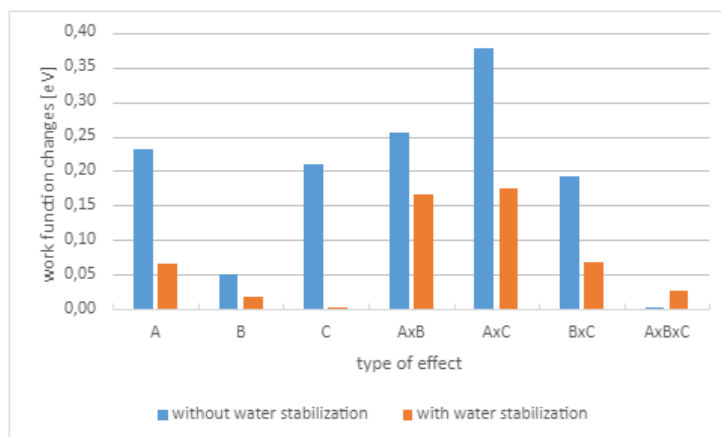


Figure 1. Experimental data collected using the DoE.

The DoE methodology allowed to determine that the factor that have the greatest impact on the level of material modification is plasma treatment time. Thus, treatment time optimization was performed and shown in Fig. 2 and 3.

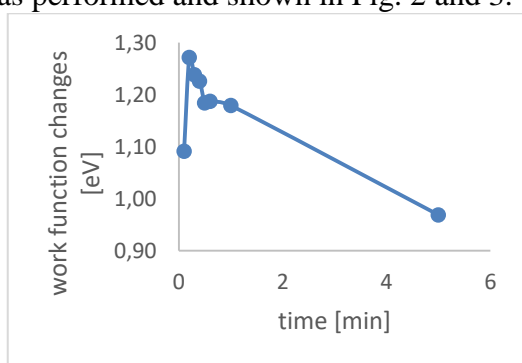


Figure 2. Optimization of the plasma treatment time (without water stabilization)

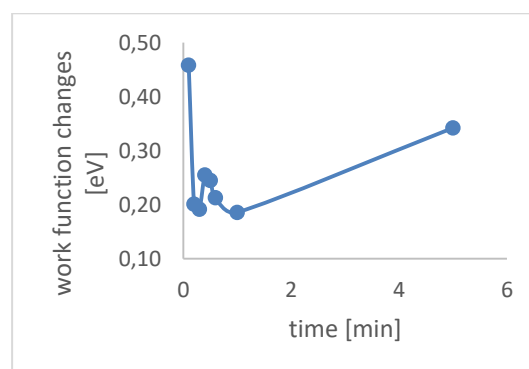


Figure 3. Optimization of the plasma treatment time (using water stabilization)

As shown in Fig. 2, the time at which we achieve the most modified material without stabilization in water is 12 seconds, and with the increase in the time of plasma exposure to graphene paper, this value decreases. It may be related to the more effective charging of the material with the increase of plasma time. For the same material after stabilization in water, the material with the highest work function changes is obtained after applying plasma for 6 seconds. The highest WF represent most effective surface functionalization allowing for the strongest interaction with an adsorbate.

Conclusions

The DoE methodology allowed to determine the optimal conditions to modify the surface of graphene paper with low temperature plasma.

Acknowledgements

This study was financially supported by the National Science Centre, Poland, project number 2020/37/B/ST5/01876.

References

- [1] Eldin, A. B., General Introduction to Design of Experiments (DOE), Sigma Pharmaceutical Corp., Egypt
- [2] Durakovic, B., Design of Experiments Application, Concepts, Examples: State of the Art

K-modification of the CoY catalyst for the ethanol steam reforming process

P. Patulski^{1,*}, G. Grzybek¹, K. Tarach¹, K. Pyra¹, M. Greluk², G. Słowik², M. Rotko², K. Góra-Marek¹, A. Kotarba¹

¹Jagiellonian University in Kraków, Poland

²Maria Curie-Skłodowska University in Lublin, Poland

email: epiotr.patulski@student.uj.edu.pl

Introduction

Ethanol steam reforming (ESR) is a promising and widely researched process for obtaining hydrogen. Although noble metal-based catalysts are very active in the ESR, due to their high cost, equally active systems based on transition metals, e.g. cobalt, are increasingly being investigated [1]. The use of zeolite supports for the ESR catalyst is a promising solution due to their large specific surface area and porosity [2]. This work explored the influence of potassium doping on the structure, surface properties, and efficiency in the ESR process of the cobalt-modified HY zeolite (Si/Al=31) catalyst (CoY).

Experimental

A series of catalysts containing 10 wt.% cobalt phase, with different K content (0 – 4 wt.%) was obtained. The chemical and phase composition, texture, morphology, and reducibility of the catalysts were examined using the methods: ICP, XRD, low-temperature adsorption of N₂, STEM/EDX, and H₂-TPR. The acidity of the catalysts was investigated by FT-IR spectroscopy with the use of probe molecules such as pyridine and carbon monoxide. The tests of catalytic activity in the ESR process were carried out at the temperature of 500 °C for the molar ratio of ethanol to water 1:4 and 1:12.

Results and discussion

The potassium donation to the CoY catalyst caused a slight reduction of its porosity and deterioration of the cobalt dispersion. At the same time, the addition of K caused a drastic reduction in the concentration of acid sites in the system. The strength of the observed effect depends strongly on the nature of potassium in the catalyst. The differences in the influence of potassium on the physicochemical properties of the CoY catalyst are reflected in its performance in the ESR process. 100% ethanol conversion observed for the CoY catalyst is reduced to a value of 75 – 80% upon K introduction in the ion exchange positions, and even to 5 – 10% upon K introduction on the external surface of the system. Importantly, the introduction of potassium significantly lowered the selectivity to the C₂H₄ – a highly undesirable product of the ESR process. The selectivity to C₂H₄ from 65 – 70% decreased to 45 – 55% for the sample with K in the ion-exchange positions and to 0 – 5% for the sample containing K on the external surface of the catalyst.

Conclusions

This study showed the effect of potassium addition on the performance of the zeolite-supported cobalt catalyst (CoY) in the ethanol steam reforming process. The catalytic activity of the studied catalysts was discussed in terms of potassium impact on the structure and acid/redox surface properties of the CoY catalyst.

Acknowledgements

The work was financed by Grant No. 2015/18/E/ST4/00191; 2020/37/B/ST4/01215 from the National Science Centre, Poland.

P.P. acknowledges the funding from the “Talent Management” mini-grant under the program “Excellence Initiative – Research University” at the Jagiellonian University.

References

- [1] Ogo, S., Sekine, Y., *Fuel Processing Technology*, 199 (2020) 106238.
- [2] Chica, A., Sayas, S., *Catalysis Today*, 146 (2009), 37-43.

Carbons materials prepared from L-cysteine amino acid

S. Reljic, C. Cuadrado-Collados, E. Oliveira Jardim, J. Farrando-Perez, M. Martinez-Escandell, J. Silvestre-Albero*

Departamento de Química Inorgánica-Instituto Universitario de Materiales, Universidad de Alicante, Spain

e-mail: joaquin.silvestre@ua.es

Introduction

The activated carbon global market is continuously growing due to the versatility of these materials in industry and municipalities for cleaning purposes. Their main application involves the removal of contaminants in water and air environments [1]. The attractiveness of activated carbon as a universal adsorbent is due to its low cost, the versatility in its production, and the possibility to design the porous structure and surface chemistry upon request. Although the porous structure has a profound impact on the performance of the activated carbons (*e.g.*, microporous activated carbons exhibit an optimum performance for gas and energy storage [2,3]), the presence of surface functionalities, although being also important, has been less explored due to the difficulty to tailor the surface chemistry [4,5]. Non-essential amino acids can be anticipated as potential platforms to obtain carbon materials with a rich surface chemistry. Amino acids are organic compounds that contain amino ($-\text{NH}_2$) and carboxyl ($-\text{COOH}$) functional groups, together with side chains that could contain other functional groups such as sulphur (*e.g.* cysteine & methionine). A priori these platforms could be susceptible to be converted into activated carbon, after a proper activation step, although they have never been evaluated. Based on these premises, the main goal of the present study is the preparation of activated carbon materials combining oxygen, nitrogen and sulphur functionalities starting from L-cysteine as a raw material.

Experimental

In a first step, L-cysteine was spread in the alumina boat and thermally treated in a horizontal furnace at 700 °C for 2 h under a N_2 flow rate of 100 ml/min (heating ramp of 3 °C/min). The reaction process is a simple condensation reaction of L-cysteine under nitrogen atmosphere. After condensation the yield was 5.4 wt.%. In the second step, the condensed material was activated with CO_2 (100 ml/min) at a temperature of 800 °C with the heating ramp of 3 °C/min and the activation time of 1 h, 3 h, 6 h. An additional sample was prepared using 900 °C as activation temperature for 1 h. Four different cysteine-based activated carbons (CAC) were prepared and labelled CAC_xy00, where x = activation time and y = activation temperature. The synthesized samples have been characterized by different techniques, such as N_2 adsorption measurements at -196 °C, CO_2 adsorption at 0 °C, FESEM and XPS.

Results and discussion

The results described in Fig. 1 (right) show that, for a given activation temperature (800 °C), the porous structure of the synthesized samples scales-up with the extend of the activation treatment, *i.e.* activation time from 1 h to 6 h. Sample activated for 1h at 800 °C, *i.e.* CAC1800, exhibits a poorly developed porous structure, with a BET surface area ca. 140 m^2/g . The presence of a scarcely developed porous structure can be clearly appreciated in the N_2 adsorption isotherm (Type I according to the IUPAC classification), with a narrow knee at low relative pressures associated with a purely microporous material. An extension in the activation process to 3 h and 6 h at 800 °C gives rise to a significant development of the porosity with a BET surface area of 600 m^2/g and 1013 m^2/g , respectively. The CAC1900

sample exhibits a moderate BET surface area (ca. 378 m²/g). Interestingly, the N₂ adsorption isotherms confirm that the activation treatment with CO₂ provides purely microporous samples, independently of the activation degree. Despite these large differences in the nitrogen adsorption performance for the three samples synthesized at 800 °C, their CO₂ uptake (Fig. 1 right) at 0 °C and 1 bar is rather similar. This observation anticipates the presence of diffusional restrictions for N₂ to access the inner porous structure in samples with a low activation degree (*e.g.*, CAC1800). The restricted accessibility of nitrogen at -196 °C is confirmed after comparing the micropore volume (V_0) and the narrow micropore volume (V_n) deduced after application of the Dubinin-Radushkevich equation to the N₂ and CO₂ isotherms, respectively. For this specific sample (CAC1800), $V_n \gg V_0$ (0.18 \gg 0.06), thus confirming the presence of diffusional restrictions for nitrogen to access the inner porous structure at cryogenic temperatures. The presence of narrow micropores is also reflected in the more concave shape of the CO₂ isotherm at 0°C. In the specific case of sample CAC3800, $V_n \sim V_0$ (0.24 \gg 0.25), thus reflecting the presence of a narrow micropore size distribution. Only sample CAC6800 possess wider micropores $V_0 \gg V_n$ (0.42 \gg 0.26), although without mesoporosity. Overall, these results show that L-cysteine is an excellent platform to synthesize purely microporous activated carbons with molecular sieving properties. The XPS analysis (not shown) confirm that the synthesized carbons exhibit a rich surface chemistry containing oxygen, nitrogen and sulphur functional groups. Their performance in the adsorption of relevant probes (CH₄, C₂H₄ and CO₂) will be further discussed.

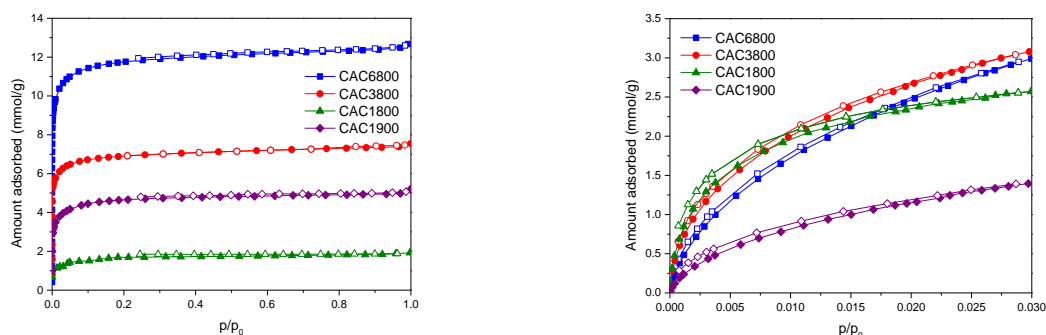


Figure 1. (left) N₂ adsorption/desorption isotherms at -196 °C and (right) CO₂ isotherms at 0 °C in the different carbon materials evaluated.

Conclusions

A series of activated carbon materials have been successfully prepared from a non-essential amino acid, such as L-cysteine. The synthesized carbons combine a widely developed porous structure (BET surface area up to 1000 m²/g) and a rich surface chemistry (mainly oxygen, nitrogen and sulphur functionalities). Furthermore, the synthesized carbons exhibit an excellent adsorption performance for CO₂ (up to 3 mmol/g at 0 °C).

Acknowledgements

Authors acknowledge financial support from the MINECO (Projects PID2019-108453GB-C21 and PCI2020-111968/ERANET-M/3D-Photocat).

References

- [1] Marsh, H., Rodríguez-Reinoso, F., Activated Carbon, Elsevier Science, 2006.
- [2] Sevilla, M., Mokaya, R., Energy & Environmental Science, 7 (2014), 1250-1280.
- [3] Sircar, S., Golden, T.C., Rao, M.B., Carbon, 34 (1996), 1-12.
- [4] Bandoz, T., Surface chemistry of carbon materials, in: Carbon materials for catalysis (P. Serp, J.L. Figueiredo Eds.), Wiley, 2009, pp. 45-92.
- [5] Saha, D., Kienbaum, M.J., Microporous and Mesoporous Materials, 287 (2019), 29-55.

Complete solutions: Analytical Equipment, Consumables and Support for your applications!

Mihaela Badea*

Agilrom, Bucharest, Romania

e-mail: office@agilrom.ro



AGILROM SCIENTIFIC SRL – authorized distributor of AGILENT TECHNOLOGIES in Romania

We are one of the most experienced suppliers of high-end equipment, consumables and accessories for analytical laboratories for more than 20 years on the Romanian market. Since October 2017, our company is the newest member of **ALTIUM Group** - the biggest regional distributor for analytical equipments in Croatia, Czechia, Poland and Turkey. We provide innovative solutions for our customers, from environmental and food laboratories, clinical and pharmaceutical industries to Academia researchers.

Our experienced team – sales, technical support and service engineers - can provide tailored, turnkey solutions and help you to get the highest performance from every system in your lab and work.

Choose high-performance technologies for life science and material characterisation: we bring in your laboratory solutions for healthcare (pharmaceuticals, clinical), energy (petrochemicals), manufacturing new materials/plastics (polymers), and environment (water/ air quality, renewable, and bio-produced materials).

Innovation with purpose!
Intelligent. Intuitive. Innovative
INTUVO 9000 GC/MSMS



FIT-for-purpose!
Next Generation of LC/MSMS
**ULTIVO: Remarkably small -
Screen, Confirm, and Quantify**



Complete solutions: Analytical
Equipment, Consumables
and Support for your
applications!

*All you need in your
lab from an experienced
team!*

... and much more!

Visit us at : www.agilrom.ro

Contact us at: office@agilrom.ro

chem. Eng. Mihaela Badea – General Manager



Address: Bucharest, Grigore Cobalcescu Str. No 39, CP 010193
Phone: +40 21 269 1277; fax: +40 21 269 1299
e-mail: office@agilrom.ro

Silica-modified Bismutite Nanoparticles for Enhanced Adsorption and Visible Light Photocatalytic Degradation of Methylene Blue

Jibin Antony¹, Susana Villa Gonzalez², Sulalit Bandyopadhyay¹, Jia Yang¹, Magnus Rønning^{1,*}

¹Department of Chemical Engineering, Faculty of Natural Sciences, NTNU, Norway

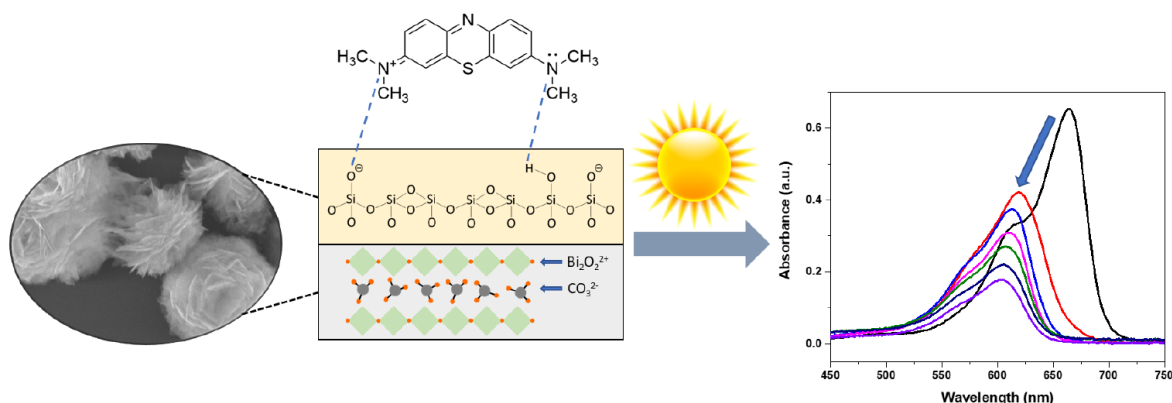
²Department of Chemistry, Faculty of Natural Sciences, NTNU, Norway

e-mail: magnus.ronning@ntnu.no

Introduction

Semiconductors which can be activated under visible light have attracted intense research interest due to their applications in heterogeneous photocatalysis, especially in the degradation of organic pollutants. Bismutite ($\text{Bi}_2\text{O}_2\text{CO}_3$, BSC) nano discs (NDs) have recently emerged as an important candidate in photocatalysis due to its alternate $(\text{Bi}_2\text{O}_2)^{2+}$ and CO_3^{2-} layered anisotropic crystal structure and internal static electric field, which facilitates photoinduced charge transfer and separation [1]. Previous works have reported BSC as an efficient photocatalyst in the degradation of organic dyes such as methylene blue, methyl orange and rhodamine B [2, 3]. However, its use has primarily been limited to the UV spectrum due to the relatively wide bandgap of 3.12 eV. On the other hand, silica, due to porous structure and high surface-to-volume ratio, has attracted attention as a good adsorbent for organic pollutants [4].

In this work, pristine BSC nanoparticles were modified with silica by the addition of different volumes of sodium silicate solution prior to hydrothermal treatment. The presence of silica in the samples was verified by elemental mapping, X-ray diffraction (XRD) and Fourier transform infrared spectroscopy (FT-IR). Increased surface area observed from Brunauer-Emmett-Teller (BET) isotherms and a shift in the zeta potential to more negative values further confirmed the incorporation of silica in BSC NDs. Morphological studies using scanning electron microscope (SEM) revealed the presence of silica to induce thinning and self-assembly of the NDs. The samples were then tested for visible light photocatalytic degradation of methylene blue (MB). Improved adsorption of the cationic MB dye was observed for the samples with higher silica content due to the presence of electrostatic and hydrogen bond interactions with the large amount of silanol groups present on the catalyst surface [5].



Scheme 1. Schematic of visible light photocatalytic degradation of MB by silica-modified bismutite nanoparticles.

Experimental

The enhanced adsorption of MB on silica-modified BSC would ensure better availability of charge carriers for photocatalytic degradation of MB and lead to faster mineralization in the presence of visible light. The mineralization pathway of MB has been reported in literature to occur via intermediates such as Azure B, Azure A, Azure C, thionine etc. [6]. However, an absorbance shift corresponding to these metabolites have not been observed during these reactions, indicating MB to be the primary component still present in the mixture. In contrast, a blue shift in the absorbance peak of MB observed at the start of reaction in the presence of silica-modified BSCs verified quick mineralization of the dye. Further analysis using a mass spectrometer confirmed Azure C and thionine to be the main metabolites after 3 hours of visible light irradiation in silica-modified BSC, whereas heavier metabolites such as Azure B, Azure A and MB itself could be detected with pristine BSC particles. This confirmed faster mineralization of MB in presence of visible light as a result of its stronger adsorption on the catalyst surface. Total organic carbon (TOC) analysis was also performed, and the results indicated 20% better mineralization with silica-modified BSC particles. Hence, this work highlights the importance of incorporating a good adsorbent to the semiconductor photocatalyst for faster mineralization of organic pollutants and is anticipated to lay foundation for future research in obtaining an optimized photocatalyst capable of capturing a wide spectrum of dyes for wastewater remediation.

Acknowledgements

The Research Council of Norway is acknowledged for the support to the Norwegian Micro- and Nano-Fabrication Facility, NorFab, project number 295864. The authors would also like to acknowledge the Mass Spectrometry Lab at the NV Faculty, NTNU for providing the instrumentation and support with mass spectrometry analysis.

References

- [1] Xiao, C., Zhang, X., MacFarlane, D.R., *ACS Sustainable Chemistry & Engineering*, 11 (2017), 10858-10863.
- [2] Cheng, H., Huang, B., Yang, K., Wang, Z., Qin, X., Zhang, X., Dai, Y., *ChemPhysChem*, 11 (2010) 2167-2173.
- [3] Selvamani, T., Raj, B.G.S., Anandan, S., Wu, J.J., Ashokkumar, M., *Physical Chemistry Chemical Physics*, 18 (2016), 7768-7779.
- [4] Dagher, S., Soliman, A., Ziout, A., Tit, N., Hilal-Alnaqbi, A., Khashan, S., Alnaimat, F., Qudeiri, J.A., *Materials Research Express*, 5 (2018), 065518.
- [5] Zych, Ł., Osyczka, A.M., Łacz, A., Różycka, A., Niemiec, W., Rapacz-Kmita, A., Dzierzkowska, E., Stodolak-Zych, E., *Materials*, 14 (2021), 843.
- [6] Gnaser, H., Savina, M.R., Calaway, W.F., Tripa, C.E., Veryovkin, I.V., Pellin, M.J., *International Journal of Mass Spectrometry*, 245 (2005), 61-67.

Green strategy for the synthesis of carbon quantum dots (CQDs) from humins wastes

Giuseppe Stoian¹, Petruta Oancea², Bogdan Cojocaru¹, Madalina Tudorache¹, Vasile I. Parvulescu¹, Simona M. Coman^{1,*}

¹University of Bucharest, Faculty of Chemistry, Department of Organic Chemistry, Biochemistry and Catalysis, 4-12 Regina Elisabeta Blvd., Bucharest, 030018, Romania

²University of Bucharest, Faculty of Chemistry, Department of Physical Chemistry, 4-12 Regina Elisabeta Blvd., Bucharest, 030018, Romania

e-mail: simona.coman@chimie.unibuc.ro

Introduction

Carbon quantum dots (CQD) have recently attracted much attention for their promising applications, especially in photocatalysis [1], bioimaging [2] and bacterial labeling [3]. However, although a huge library of synthetic methods are available for CQDs production, either using the “top-down” or “bottom-up” approaches, their commercial viability is still limited due to the production costs which requires either costly precursors, complex instrumental set-ups or/and post-treatment in the reaction system [4]. Therefore, CQDs must be prepared by green and environmentally friendly methods. In connection with this, an important progress for sustainability was registered with the research focused on low-temperature hydrothermal CQDs synthesis from non-edible biomass or biomass waste streams as feedstock [5]. Humins, for instance, are generated in high amounts in the acid-catalyzed dehydration of carbohydrates [6], as insoluble polyfuranic polymers by-products, thereby severely limiting the utilization efficiency of renewable biomass. In order to improve the process efficiency, humins formation should be avoided but this alternative is quite difficult since it is thermodynamically favored. Fortunately, the presence in a significant amount of the organic functional groups in their structure, humins possess a wide potential for valorization. Nevertheless, information about the use of humins wastes as raw materials for the synthesis of CQDs are almost completely missing in literature in spite of their chemical structure and morphology which recommend them for a such valorization way.

In the post-treatment stage a number of separation methods for the CQDs isolation, including the dialysis process, have been investigated [7] but all these methods have a low efficiency, high complexity, high cost, energy consumption, and produce a large amount of wastewater and by-products. Facile and convenient separation of CQDs by liquid-phase extraction should be developed but the application of this alternative is almost missing in literature reports [8].

Herein, we demonstrate that the worthless humins by-product generated in the glucose acid-dehydration can be successfully transformed into CQDs with ultra-small size, homogeneous size distribution and bright luminescence (PL). Moreover, we demonstrate the efficiency of a biphasic butanol/water system in which the low-temperature hydrothermal synthesis of CQDs is combined with their liquid-phase extraction process in a single step.

Experimental

For the synthesis of CQDs an organic phase/water biphasic system (20 mL) was used. As organic phase n-butanol was used, in the range of 1/1 – 1/5 v/v butanol/water ratio. Humins (20 mg) were added to the biphasic system and the obtained mixture was vigorously stirred at 180-200^oC, for 4-12 h, in an autoclave. After synthesis, the layers were separated and the bottom CQDs rich aqueous layer was collected and further analyzed by techniques as ATR-FTIR, UV-vis and photoluminescence spectroscopy (PL). The relative quantum yields (Qys) of the CQDs were calculated by using fluorescein standard. To reveal the humins

degree of decomposition during the hydrothermal synthesis the top brown organic layer was also analyzed by GPC-SEC chromatography. The obtained CQDs were denoted: CQD_{T-h}, where T – represent the synthesis temperature and h – represent the synthesis time.

Results and discussion

A preliminary study was performed to optimize the synthesis parameters of CQDs in single-phase system (water). The obtained results clearly showed that CQDs with small dimension (< 10 nm), a preponderantly homogeneous size distribution and an intense blue emission may be obtained at either to a high temperature and a short reaction time (ie, CQD₂₀₀₋₄) or to a lower temperature and a longer reaction time (ie, CQD₁₈₀₋₁₂). Therefore, for the biphasic butanol/water system (1/1 vol/vol ratio) the CQDs synthesis and their isolation in a one-pot fashion was applied in these conditions.

It is well known that water and butanol spontaneously form two immiscible phases. However, the wet butanol phase consists of an almost equimolar mixture of butanol and water molecules [9]. The water content inside of butanol is structured and forms inverse micelles [9]. Inside of these water pockets ultra-small polar nanoparticles can be trapped (Fig. 1). Taking into account these statements we can claim that during the one-pot synthesis of CQDs, the most polar CQDs are trapped into n-butanol phase along humin fragments (Figure 1). The same effect was obtained with an increase in water content from 1/1 to 1/2. This supposition was also supported by GPC analysis of the separated butanol phase. The CQDs characteristics, in terms of chemical composition, luminescence properties and QY will be discussed.

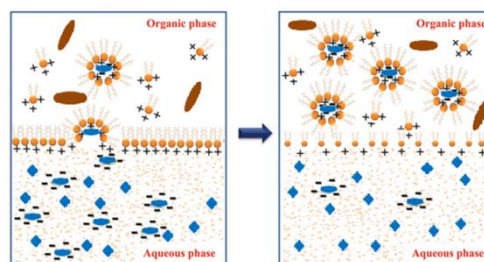


Figure 1. The schematization of the reverse micelles formation and the entrapment of small polar CQDs in it (blue – CQDs, brown – humins fragments)

Conclusions

A novel green biphasic butanol/water system in which the low-temperature hydrothermal synthesis of CQDs is combined with their liquid-phase extraction process in a single step was developed. The developed biphasic butanol/water system methodology is attractive not only in terms of efficiency and simplicity but also in terms of sustainability.

References

- [1] Chang, Q., Li, K.K., Hu, S.L., Dong, Y.G., Yang, J.L., *Materials Letters*, 175 (2016), 44-47.
- [2] Tu, Z., Zhang, Q., Liu, M., Qian, Y., Wang, L., Huang, W.J., *Materials Science*, 51 (2016), 2972-2979.
- [3] Weng, C.I., Chang, H.T., Lin, C.H., Shen, Y.W., Unnikrishnan, B., Li, Y.J., Huang, C., *Biosensors and Bioelectronics*, 68 (2015), 1-6.
- [4] Zhao, S., Song, X., Chai, X., Zhao, P., He, H., Liu, Z., *Journal of Cleaner Production*, 263 (2020), 121561.
- [5] Wongso, V., Sambudi, N.S., Sufian, S., *Biomass Conversion and Biorefinery*, (2020), <https://doi.org/10.1007/s13399-020-00662-9>
- [6] Candu, N., El Fergani, M., Verziu, M., Cojocaru, B., Jurca, B., Apostol, N., Teodorescu, C., Parvulescu, V.I., Coman, S.M., *Catalysis Today*, 325 (2019), 109-116.
- [7] Kokorina, A.A., Sapelkin, A.V., Sukhorukov, G.B., Goryacheva, I.Y., *Advances in Colloid and Interface Science*, (2018), <https://doi.org/10.1016/j.cis.2019.102043>
- [8] Uthirakumar, P., Devendiran, M., Kim, T.H., Lee, I.-H., *New Journal of Chemistry*, 42 (2018), 18312.
- [9] König, G., Reetz, M.T., Thiel, W., *The Journal of Physical Chemistry B*, 122 (2018), 6975-6988.

Zn(II) coordination polymers with mixed anionic linkers employed as heterogenous photocatalysts

Carmen Paraschiv^{1,*}, Andrei Cucos¹, Sergiu Shova², Bogdan Cojocaru³, Vasile I. Parvulescu³
¹National Institute for R&D in Electrical Engineering ICPE-CA, 030138, Bucharest, Romania

²“Petru Poni” Institute of Macromolecular Chemistry, 700487, Iasi, Romania

³Department of Organic Chemistry, Biochemistry and Catalysis, University of Bucharest, 030018, Bucharest, Romania

e-mail: carmenparaschiv@yahoo.com

Introduction

Coordination polymers are infinite systems build up with metal ions and organic ligands as main elementary units linked via coordination bonds and other weak chemical bonds [1]. Numerous multitopic organic ligands with specific binding strength and directionality have been used to obtain coordination polymers. Among them, polycarboxylic acids have been extensively employed, due to the tunability of the obtained structures and their suitability for hydrogen storage, sorption, separation and sensing [2]. On the other hand, amino-alcohols have received much less attention, in spite of the variety of coordination modes or their capability for formation of hydrogen bonds [3,4].

In the present work we report on the synthesis and characterization of a MOF synthesized under solvothermal conditions from zinc(II) nitrate, triethanolamine (TEA) and isophthalic acid. Owing to its porous network, the obtained MOF was tested in two selective reactions: photo-oxidation of phenol to hydroquinone and aerobic photo-oxidative condensation of benzylamine to *N*-benzylidenebenzylamine.

Experimental

Selective photo-oxidation of phenol to hydroquinone. 15 mg of photocatalyst were added to 10 mL aqueous solution of 40 ppm phenol. Samples were irradiated for three hours and 30 μ L of solution were collected at 30 min intervals for HPLC investigation.

Photo-oxidative condensation of benzylamine to N-benzylidenebenzylamine. The benzylamine selective photo-oxidation experiments were solvent free. In a typical experiment 50 mg of photocatalyst were added to 2 mL of benzylamine. Samples were irradiated for two hours, with 30 μ L collected after each hour for gas chromatography analysis.

Both sets of reactions were carried out by irradiation in the following conditions: under UV with a UV lamp centered at 365 nm (2x120W Vilber Lourmat VL-340.BL, 11520 Lm, 33672 lx), and under visible with a visible lamp (150W Philips Master Colour CDM-T 150W/830, 13500 Lm, 5810 lx). Control experiments were carried out testing substrates irradiated without catalysts and with catalysts stirred in the darkness. In all these cases the conversion of substrates was zero.

Results and discussion

Photo-oxidation of phenol to hydroquinone. The evolution of phenol photo-oxidation is presented in Figure 1. A conversion of about 20% was achieved after 180 minutes disregarding the irradiation source (UV or Vis).

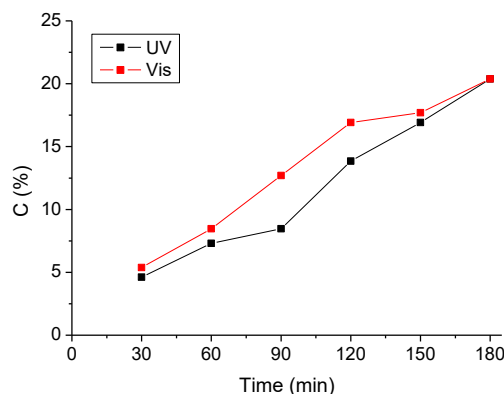


Figure 1. Photo-oxidation of phenol under UV and visible light irradiation.

Photo-oxidative condensation of benzylamine to N-benzylidenebenzylamine. The photo-oxidative condensation was performed under both UV and Vis irradiation. Time evolution of the content of benzaldehyde in the reaction mixture is presented in Figure 2.

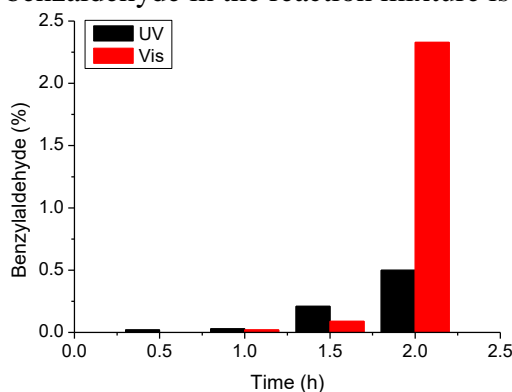


Figure 2. Time evolution of the content of benzaldehyde in the reaction mixture.

Conclusions

The synthesized MOF proved to be active in the selective photo-oxidation of phenol and, even more remarkably, in the selective photo-oxidation of benzylamine to form *N*-benzylidenebenzylamine. The results are promising and highlight the potential application of this kind of materials in photocatalysis.

Acknowledgements

Financial support from the Romanian Ministry of Education CNCS-UEFISCDI (Project PN-II-RU-TE-2012-3-0390) is gratefully acknowledged.

References

- [1] Bailar Jr., J.C., *Preparative Inorganic Reactions*, 1 (1964), 1.
- [2] Sudik, A.C., Ockwig, N.W., Millward, A.R., Côté, A.P., Yaghi, O.M., *Journal of the American Chemical Society*, 127 (2005), 7110-7118.
- [3] Chen, S.M., Zhang, J., Wu, T., Feng, P.Y., Bu, X.H., *Journal of the American Chemical Society*, 131 (2009), 16027- 16029.
- [4] Manos, M.J., Moushi, E.E., Papaefstathiou, G.S., Tasiopoulos, A.J., *Crystal Growth & Design*, 12 (2012), 5471-5480.

From humins wastes to carbon quantum dots (CQDs) based photocatalytic nanocomposites

Nicolae Cristian Guzo¹, Magdi El Fergani¹, Bogdan Cojocaru¹, Joanna Gościańska², Vasile I. Parvulescu¹, Simona M. Coman^{1,*}

¹University of Bucharest, Faculty of Chemistry, Department of Organic Chemistry, Biochemistry and Catalysis, 4-12 Regina Elisabeta Blvd., Bucharest 030018, Romania

²Adam Mickiewicz University, in Poznań, Uniwersytetu Poznańskiego 8, Poznań, Faculty of Chemistry, Department of Chemical Technology, 61-614, Poland

email: simona.coman@chimie.unibuc.ro

Introduction

Photocatalytic reactions driven by sunlight represent a promising way to address the increasing environmental and energy concerns. Therefore, developing and optimizing highly efficient photocatalysts under visible light has attracted worldwide attention. In particular, the modification of TiO₂ with carbon nanomaterials such as CNTs, fullerenes and graphene, have been used for the production of such photocatalysts [1]. However, CNTs and graphene easily aggregate and are difficult to disperse in common solvents, limiting their wide applications [2]. In this context, a new member of carbon family, namely carbon quantum dots (CQDs), have recently attracted considerable attention as the next-generation of green multifunctional nanomaterial with promising applications in photocatalysis. However, although CQD@TiO₂ composites have been intensively investigated [3], their practical application it remains challenging. This is the result of either costly precursors, complex instrumental set-ups or/and post-treatment in the reaction system of most of the applied methodologies for CQDs synthesis [4]. An important progress for sustainability was registered with the research focused on low-temperature hydrothermal CQDs synthesis from non-edible biomass or biomass waste streams as feedstock [5].

Here we report the development of CQD@TiO₂ composites in which CQDs were synthesized by the low-temperature hydrothermal decomposition of humins wastes generated during the glucose dehydration process. Their photocatalytic efficiency was evaluated in methylene blue (MB) dye adsorption and degradation under visible light irradiation.

Experimental

Humins were prepared in agree with a recently reported hydrothermal decomposition of D-glucose [6]. CQDs were synthesized by applying a hydrothermal treatment at temperatures of 160-200 °C, for 4-12 h. The obtained CQDs were denoted as CQD_{T-h}, where T – represent the synthesis temperature and h – represent the synthesis time. CQDs@TiO₂ composites were obtained by a hydrothermal method, following a reported methodology by Zhang and co-workers [7]. Prepared materials were exhaustively characterized by adsorption-desorption isotherms of liquid nitrogen at 77K, XRD, DRIFT spectroscopy, UV-vis spectroscopy, elemental analysis, TG-DTA, SEM, TEM and STEM-EDS.

For MB discoloration, blue LED lamps (112W), emitting at 445-465 nm, and red LED lamps (112W), emitting at 630-650 nm, were used as light source. To reach the adsorption equilibrium prior illuminating all the systems were kept in darkness for 20 min. The dye concentration was determined from a standard curve using the absorbance values measured by the UV-visible spectrophotometer (SPECORD 250-222P108), which was adjusted at 664 nm (wavelength corresponding to the maximum absorption of MB).

Results and discussion

As XRD and ATR-IR measurements showed, the as-prepared CQDs possess different structures and sizes of the carbon core, as a function of the hydrothermal synthesis parameters. Moreover, the fluorescence emission study found that CQDs with brightest luminescence were obtained at 200 °C and 4 h (CQD₂₀₀₋₄) or at 180 °C and 12 h (CQD₁₈₀₋₁₂). Not the last, these CQDs exhibited excitation-independent photoluminescence for $\lambda_{\text{ex}} = 240\text{--}340$ nm, while a red-shifted fluorescence emission was identified with an increase in the excitation wavelength in the range 360–420 nm. This behavior indicates a relatively uniform size distribution of CQDs but also the presence of a high amount of polar groups (such as –OH and –COOH) in the shell of the CQDs.

The XRD patterns of the CQD@TiO₂ samples did not evidence diffraction lines characteristic to CQDs, indicating their small loading weight, poor crystallinity, small size and their high dispersion in the CQD@TiO₂ composites. This is also confirmed by STEM analyses which evidenced the presence of ultra-small CQDs particles on the TiO₂ surface, with a size of 2 nm, for CQD₂₀₀₋₄ and 8 nm for CQD₁₈₀₋₁₂. Moreover, the identical XRD patterns with that of the TiO₂ carrier, without diffraction lines shifting, demonstrate that the CQDs were just well deposited on the surface of the TiO₂ and not incorporated into its lattice. This is also confirmed by DRIFT analysis which evidenced the presence of bands corresponding to –COOTi- group. When coupling CQDs with TiO₂, the CQDs anchored on the surface of TiO₂ increases its surface roughness, resulting in the formation of a heterointerface between CQDs and TiO₂.

Conclusions

In summary, we succeeded to synthesize CQD@TiO₂ photocatalytic composites in which carbon quantum dots (CQDs) were produced by hydrothermal decomposition of humins wastes. The materials display a high adsorption capacity of MB and its photocatalytic decomposition. The CQDs play an important role in the visible light photocatalytic process. First of all, the electrons photogenerated from TiO₂ can be trapped by the CQDs and retard the recombination of photoexcited electron-hole pairs. What's more, these heterostructures formed between CQDs and TiO₂ can greatly prolong the life of the photoexcited electron and hole pairs. All this aspects will be presented and discussed in detail.

Acknowledgements

This work was financially supported by The Education, Scholarship, Apprenticeships and Youth Entrepreneurship Programmer—EEA Grants 2014-2021, Project No. 18-Cop-0041. Authors are grateful to Dr. Petruta Oancea for the photoluminescence measurements.

References

- [1] Zhang, H., Lv, X. J., Li, Y. M., Wang, Y., Li, J. H., ACS Nano, 4 (2010), 380.
- [2] Zhang, Z. P., Zhang, J., Chen, N., Qu, L. T., Energy & Environmental Science, 5 (2012), 8869.
- [3] Tian J., Leng Y., Zhao Z., Xia Y., Sang Y., Hao P., Zhan J., Li M., Liu H., Nano Energy, 11 (2015), 419.
- [4] Zhao, S. X. Song, X. Chai, P. Zhao, H. He Z. Liu, Journal of Cleaner Production, 263 (2020), 121561.
- [5] Wongso, V., Sambudi, N.S., Sufian, S., Biomass Conversion and Biorefinery (2020), <https://doi.org/10.1007/s13399-020-00662-9>
- [6] El Fergani, M., Candu, N., Tudorache, M., Bucur, C., Djelal, N., Granger, P., Coman, S. M., Applied Catalysis A: General, 618 (2021), 118130.
- [7] Yu, H., Zhao, Y., Zhou, C., Shang, L., Peng, Y., Cao, Y., Wu, L.-Z., Tunga, C.-H., Zhang, T., Journal of Materials Chemistry A, 2 (2014), 3344.

Co₃O₄ nanosheets as efficient cobalt source for spherical Co-based MOFs

Aleksander Ejsmont^{*}, Martyna Kotula, Joanna Goscianska^{*}

Adam Mickiewicz University in Poznań, Faculty of Chemistry, Department of Chemical Technology, Uniwersytetu Poznańskiego 8, 61-614 Poznań, Poland

e-mails: aleksander.ejsmont@amu.edu.pl, joanna.goscianska@amu.edu.pl

Introduction

Searching for novel synthetic procedures which enable control over particle shape, size and crystallinity is highly demanded. Intensely studied metal–organic frameworks (MOFs) known for their high porosity and sophisticated structures distinguish from other materials with a unique morphology. MOFs are reticular structures, where building blocks are made up of organic linkers, and metallic nodes. The morphology of MOF crystallites is mainly determined by their composition. It is proven that particles shape and size affect material properties which further can influence its broad application in different fields. In conventional MOF syntheses, salts are used as metal reservoirs, however easily soluble particles cannot maintain their shape. A novel attempt to gain control over particle shape and size is using metal oxides which simultaneously can be structure-direct agents and a metal source. Metal oxides' low solubility and shape preservation facilitate better control over metal ions diffusion and MOF growth. Therefore, metal oxide conversion to MOF qualifies as an alternative synthetic route. Careful optimization of synthesis parameters can lead to efficient metal oxide conversion resulting in new MOF materials. The recent reports present mostly zinc or copper oxides as substructures for ZIF-8 and HKUST-1, respectively [1]. Concurrently, there is a multitude of other MOFs which offer a variety of applications. For instance, cobalt-based MOFs (Co-MOFs) are famed for their catalytic activity or use in energy storage [2]. However, Co₃O₄, which is the potential foundation for obtaining these materials, has not been explored due to its high stability and insolubility in aqueous solutions.

In the presented work, the aim was to obtain unique Co₃O₄ particles and apply them in the Co-MOF synthesis. The optimization of the Co₃O₄ transition to Co-MOF was conducted. All materials obtained were characterized with the use of different analytical techniques including X-ray diffraction, elemental analysis, thermogravimetric analysis, and scanning electron microscopy with energy dispersive X-ray spectroscopy.

Experimental

Firstly, Co₃O₄ was synthesized *via* a hydrothermal approach. Different salts were used as a metal source, such as CoCl₂ and Co(NO₃)₂ in the presence of urea and surfactant hexadecyltrimethylammonium bromide (CTAB) as a capping agent. The aqueous solution was subjected to a thermal treatment at 120 °C for 12 h. In the end, the obtained precipitates of cobalt hydroxides were calcined in various temperatures in the range of 300-500 °C.

As synthesized Co₃O₄ were subsequently applied as cobalt cations source, along with 1,3,5-benzenetricarboxylic acid as a linker in the solvothermal synthesis of Co-MOF. They were dispersed in a mixture of solvents (water, dimethylformamide, and ethanol) with a small addition of inorganic acids (HF and HNO₃). Final solutions were placed in the Teflon-sealed autoclave and heated at 120 °C at various times (6-48 h). The materials obtained were filtered and dried.

Results and discussion

It was established that the synthetic routes have led to the formation of Co₃O₄ nanosheets and spherical Co-based MOF (Fig. 1). The diffractograms showed crystalline phase for Co₃O₄, and also for Co-MOF. The Co₃O₄ obtained indicated a dependence of

particles size and sheet width on the type of salt and temperature of calcination. Co_3O_4 synthesized from nitrates and using low-temperature calcination resulted in smaller particles and thin sheets. Moreover, the study indicated that cobalt oxide particles of different sizes influence the efficiency of conversion to Co-MOF. It was established based on reducing intensity of Co_3O_4 reflections in MOF diffractograms and also on the results of elemental analysis and the increasing amount of carbon. The highest conversion was achieved using metal oxides with small crystallites. Also, the time of the solvothermal reaction was crucial, indicating that longer syntheses (over 24 h) are more effective leading to nearly full Co_3O_4 to MOF transition.

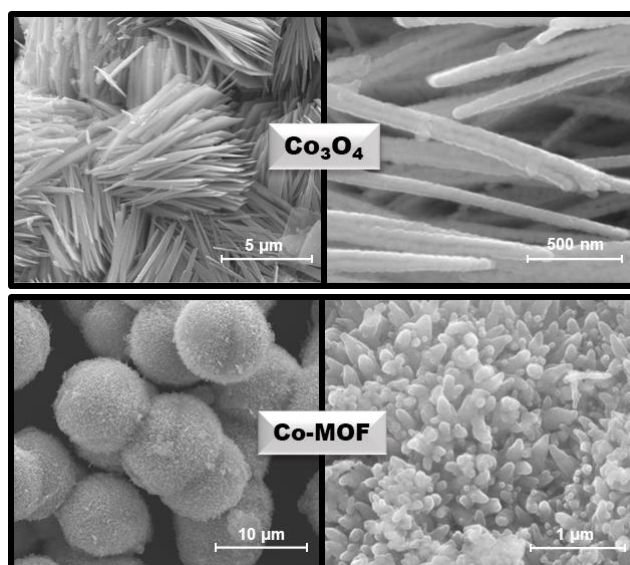


Figure 1. SEM images of Co_3O_4 nanosheets and Co-MOF spheres.

Conclusions

The presented solvothermal methods can be successfully applied for preparation of Co-MOF from Co_3O_4 nanosheets. By optimization of synthetic parameters such as the temperature of Co_3O_4 calcination and time of its reaction with organic linker it is possible to control metal oxide–MOF conversion. It is an alternative for cobalt-based MOF syntheses, which opens a new pathway for obtaining highly applicable materials *e.g.* in catalysis or energy storage.

References

- [1] Hwang, J., Ejsmont, A., Freund, R., Goscianska, J., Schmidt, B.V.K.J., Wuttke, S., *Chemical Society Reviews*, 49 (2020), 3348-3422.
- [2] Ejsmont, A., Andreo, J., Lanza, A., Galarda, A., Macreadie, L., Wuttke, S., Canossa, S., Ploetz, E., Goscianska, J., *Coordination Chemistry Reviews*, 430 (2021), 213655.

Deposition and characterization of thin films based on nanostructured NiO as sensorial element for detection gases

A. Sobetkii^{1±}, R.E. Irimescu^{1±}, A.E. Slobozeanu^{1±}, C.F. Ciobota¹, L. Österlund², J. Montero Amenedo², A. Stănoiu³, C.E. Simion³, R.M. Piticescu^{1*}

¹National Research & Development Institute for Non-ferrous and Rare Metals, High PT Met and Laboratory of Advanced and Nanostructured Materials, Biruinței, 102, Pantelimon, Ilfov, 077145, România

²Uppsala University, Department of Engineering Sciences, The Ångström Laboratory, SE-751 21 Uppsala, PO Box 534, SWEDEN

³National Institute of Materials Physics, Atomîștilor 405A, Măgurele, 077125, România

[±]These authors have equally contributed to the paper

email: rpiticescu@imnr.ro

Introduction

With the rapid development of economy, there are more and more toxic gases generated in the environment. That is why various sensor-based technologies are needed to ensure the safety of industrial production and improve the public health conditions [1]. Sensors based on metal oxide semiconductors (MOSs) such as WO₃ [2], CuO [3], ZnO [4], SnO₂ [5], In₂O₃ [6], and NiO [7] have been extensively used to monitor air quality [8], food safety [9], aerospace [10], and medical diagnosis [11] because of their excellent properties including easy production, low power consumption, and high security [1].

Experimental

The metal oxide considered in this study, i.e., nickel oxide, is a p-type semiconductor with a face centered cubic structure and a reported band gap energy between 3.6 and 4.0 eV [12,13]. It is an attractive material well known for its chemical stability as well as for its excellent optical and electrical properties [13]. NiO is an attractive material for gas sensor [14] applications as well as in other areas [12,13].

It is well known that the preparation method and the deposition parameters play an important role in the physical properties of metal oxide-based gas-sensing layers.

Therefore, we present some original results to demonstrate the potential use of NiO thin films as gas sensors. This study highlights the properties of thin films obtained by two different deposition techniques: DC Reactive Sputtering and Advanced Gas Deposition (AGD).

Films have been characterized by SEM and XRD. Also, sensing measurements on the NiO structures to different test gases (H₂S, CO₂ and NO₂) were performed. Figure 1 illustrates the sensing properties.

Results and discussion

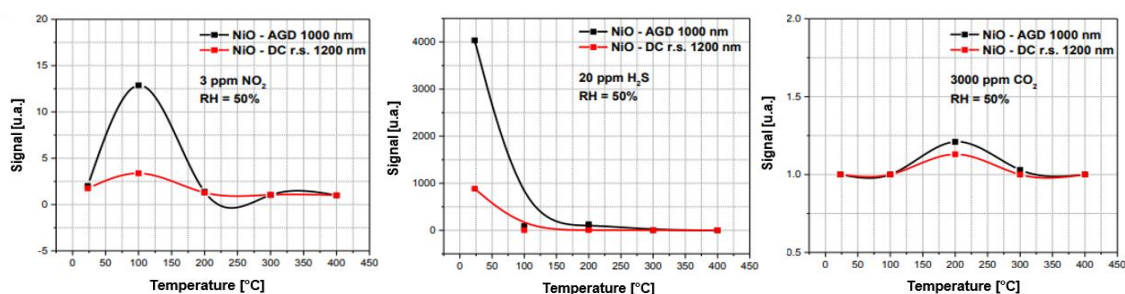


Figure 1. Sensing properties modulated by the operating temperature.

The best results were obtained in the case of the H₂S gas tests. When operated at ~ 25 ° C, NiO-AGD has a pronounced selectivity of S ~4000 and for NiO-DC Reactive Sputtering at the same operating temperature an S ~900 response was recorded. For NO₂ and CO₂ test gases the signal is negligible. The results presented in this paper are promising for further development of gas sensing devices.

Acknowledgements

This work was carried out by a grant of Ministry of Research, Innovation, and Digitization CNCS/CCDI-UEFISCDI through the project MSCA-RISE-2014: Marie Skłodowska-Curie Actions (MSCA) – Research and Innovation Staff Exchange (RISE), Grant no. 645758 (2015 – 2019) – TROPSENSE, and the project PN-III-P4-ID-PCE-2020-0506 (contract no. 116/2021) within PNCDI III and by Romanian National Authority for Scientific Research through the Core Program PN19-03 (contract no. 21 N/08.02.2019).

References

- [1] Wang, Q., Bai, J., Hu, Q., Hao, J., Cheng, X., Li, J., Xie, E., Wang, Y., Pan, X., *Sensors & Actuators: B. Chemical*, 308 (2020), 127668.
- [2] Ma, J., Ren, Y., Zhou, X., Liu, L., Zhu, Y., Cheng, X., Xu, P., Li, X., Deng, Y., Zhao, D., *Advanced Functional Materials*, 28 (2018), 1705268.
- [3] Volanti, D.P., Felix, A.A., Orlandi, M.O., Whitfield, G., Yang, D.-J., Longo, E., Tuller, H.L., Varela, J.A., *Advanced Functional Materials*, 23 (2013), 1759-1766.
- [4] Zhou, X., Zhu, Y., Luo, W., Ren, Y., Xu, P., Elzatahry, A.A., Cheng, X., Alghamdi, A., Deng, Y., Zhao, D., *Journal of Materials Chemistry A*, 4 (2016), 15064-15071.
- [5] Park, S., An, S., Mun, Y., Lee, C., *ACS Applied Materials & Interfaces*, 5 (2013), 4285-4292.
- [6] Jia, L., Cai, W., *Advanced Functional Materials*, 20 (2010), 3765-3773.
- [7] Kim, H.J., Yoon, J.W., Choi, K.I., Jang, H.W., Umar, A., Lee, J.H., *Nanoscale*, 5 (2013), 7066-7073.
- [8] Wang, T., Hao, J., Zheng, S., Sun, Q., Zhang, D., Wang, Y., *Nano Research*, 11 (2017), 791-803.
- [9] Ma, Z., Chen, P., Cheng, W., Yan, K., Pan, L., Shi, Y., Yu, G., *Nano Letters*, 18 (2018), 4570-4575.
- [10] Hunter, G.W., Neudeck, P.G., Liu, C., Ward, B., Wu, Q., Dutta, P., Frank, M., Trimbol, J., Fulkerson, M., Patton, B., *Sensors*, 2002 IEEE, IEEE, 2002, 1126-1133.
- [11] Liu, C., Tai, H., Zhang, P., Yuan, Z., Du, X., Xie, G., Jiang, Y., *Sensors and Actuators B: Chemical*, 261 (2018), 587-597.
- [12] Cindemir, U., Topalian, Z., Granqvist, C.G., Österlund, L., Niklasson, G.A., *Materials Chemistry and Physics*, 227 (2019), 98-104.
- [13] Kuanr, S.K., Vinothkumar, G., Babu, K.S., *Materials Science in Semiconductor Processing*, 75 (2018), 26-30.
- [14] Predanocy, M., Hotovy, I., Caplovicova, M., *Applied Surface Science*, 395 (2017), 208-213.

Two-diode modeling of perovskite solar cells and parameter extraction using the Lambert W function

Ana Bărar^{1,*}, Maria Bălăsoiu^{2,3}, Cristian Boscornea⁴, Doina Mănăilă-Maximean⁵

¹University POLITEHNICA of Bucharest, Faculty of Electronics, Department of Electronic Technology and Reliability, Telecommunication and Information Technology, Romania

²Joint Institute for Nuclear Research, Dubna, Russia

³Horia Hulubei Institute of Physics and Nuclear Engineering, Bucharest, Romania

⁴University POLITEHNICA of Bucharest, Faculty of Applied Chemistry and Materials Science, Department of Bioresources and Polymer Science, Romania

⁵University POLITEHNICA of Bucharest, Faculty of Applied Physics, Physics Department, Romania

e-mail: ana.barar@upb.ro

Introduction

Perovskite solar cells (PSC) have been reported to yield outstanding power conversion efficiencies [1-3]. This performance is due to the perovskite active layer, which exhibits excellent optical absorption properties, as well as long charge carrier diffusion length and direct bandgap transition [4]. However, there are still several drawbacks [5-7] that must be overcome in PSC technology and fabrication, before they may be considered as a viable alternative to silicon solar cells, the main solar energy converters marketed today. Accurate device and material characterizations are crucial for resolving these shortcomings.

The two most widely used models in solar cell device characterization are the one diode equivalent model (see Fig. 1a), respectively its more complex derivation, the two-diode model (see Fig. 1b).

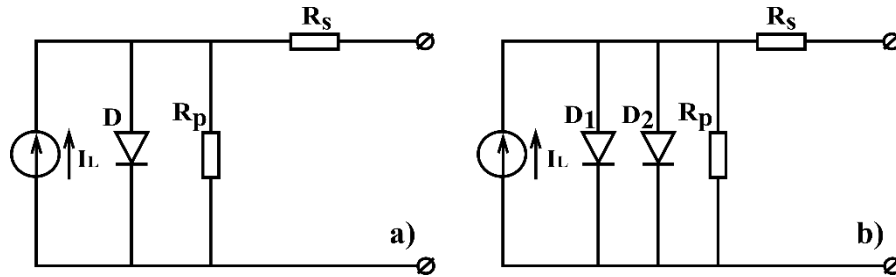


Figure 1. Equivalent circuit models used for solar cell device characterization: a) the one diode model, and b) the two-diode model, where I_L is the current source which models the photocurrent generated within the cell under illumination, diodes D and D_1 model the p-n junction in the cell, diode D_2 represents the charge carriers recombination that takes place in the junction at low voltages, the series resistance R_s models the interface defects found between the active layer and the electrodes, and the parallel (or shunt) resistance R_p models the bulk defects in the active layer of the cell.

Experimental

This paper focuses on the two-diode model, which provides a more accurate approximation of device parameters. Each component in the two-diode equivalent circuit models a certain effect that appears in the solar cell under illumination, as follows: the current source I_L models the photocurrent generated within the cell under illumination, diode D_1 models the p-n junction in the cell, diode D_2 represents the charge carriers recombination that takes place in the junction at low voltages, the series resistance R_s models the interface defects found between the active layer and the electrodes, and the parallel (or shunt)

resistance R_p models the bulk defects in the active layer of the cell. The current I yielded by this circuit represents the current yielded by the cell under illumination, and it is described by the following equation:

$$I = I_L - I_{o1} \left\{ \exp \left[\frac{e(U+R_s I)}{\gamma_1 k T} \right] - 1 \right\} - I_{o2} \left\{ \exp \left[\frac{e(U+R_s I)}{\gamma_2 k T} \right] - 1 \right\} - \frac{U+R_s I}{R_p} \quad (1)$$

where e is the elementary electron charge, U is the voltage yielded by the cell, k is the Boltzmann constant, T is the temperature, I_{o1} is the dark saturation current of diode D_1 , γ_1 is the ideality factor of diode D_1 , I_{o2} is the dark saturation current of diode D_2 , γ_2 is the ideality factor of diode D_2 , respectively. The seven circuit parameters necessary for solar cell characterization are: I_L , R_s , R_p , γ_1 , γ_2 , I_{o1} , I_{o2} , and they must be extracted from Equation 1. However, equation 1 is implicit, therefore it cannot be resolved analytically, numerical methods must be considered for parameter extraction. Based on previous work conducted on the one diode model [8-10], this paper proposes a method involving the Lambert W function, tailored for extracting the parameters of interest. The method is applied on the experimental data obtained for a perovskite solar cell, and the results are compared with the values obtained using other parameter extraction methods, in order to demonstrate accuracy.

Acknowledgements

The authors acknowledge the support of Project RO-JINR, position 64 in IUCN Order no.365/11.05.2021, Theme 04-4-1141-2020/2022.

References

- [1] Jeong, J., Kim, M., Seo, J., Lu, H., Ahlawat, P., Mishra, A., Yang, Y., Hope, M.A., Eickemeyer, F.T., Kim, M., Yoon, Y.J., Choi, I.W., Darwich, B.P., Choi, S.J., Jo, Y., Lee, J.H., Walker, B., Zakeeruddin, S.M., Emsley, L., Rothlisberger, U., Hagfeldt, A., Kim, D.S., Grätzel, M., Kim, J.Y., *Nature* 592 (2021), 381-385.
- [2] Yoo, J.J., Seo, G., Chua, M.R., Park, T.G., Lu, Y., Rotermund, F., Kim, Y.-K., Moon, C.S., Jeon, N.J., Correa-Baena, J.-P., Bulović, V., Shin, S.S., Bawendi, M.G., Seo, J., *Nature*, 590 (2021), 587-593.
- [3] Kim, G., Min, H., Lee, K.S., Lee, D.Y., Yoon, S.M., Seok, S.I., *Science*, 370 (2020), 108-112.
- [4] Kim, J.Y., Lee, J.-W., Jung, H.S., Shin, H., Park, N.-G., *Chemical Review*, 120 (2020), 7867-7918.
- [5] Krishnan, U., Kaur, M., Kumar, M., Kumar, A., *Journal of Photonics for Energy*, 9 (2019), 021001.
- [6] Leguy, A.M.A., Hu, Y., Campoy-Quiles, M., Alonso, M.I., Weber, O.J., Azarhoosh, P., van Schilfgaardem M., Weller, M.T., Bein, T., Nelson, J., Docampo, P., Barnes, P.R.F., *Chemistry of Materials*, 27 (2015), 3397-3407.
- [7] Goyer, R.A., *Environmental Health Perspectives*, 100 (1993), 177-187.
- [8] Del Pozo, G., Romero, B., Arredondo, B., *Proceedings of SPIE – The International Society for Optical Engineering*, (2012) 8435
- [9] Barar, A., Manaila-Maximean, D., Danila, O., Vladescu, M., *Proc. SPIE – The International Society for Optical Engineering*, (2016) 10010.
- [10] Barar, A., Vladescu, M., Schiopu, P., *UPB Scientific Bulletin, Series A*, 80 (2018), 217-226.

Biocatalysis based on cold-active lipase for silymarin valorization from vegetal waste of cold-pressed milk thistle oil technology

Giulia Gheorghita^{1,2,*}, Cristina Purcarea², Madalina Tudorache¹

¹University of Bucharest, Faculty of Chemistry, Department of Organic Chemistry, Biochemistry and Catalysis, 4-12 Regina Elisabeta Blvd., 030018 Bucharest, Romania

²Institute of Biology Bucharest, Romanian Academy, Department of Microbiology, 296 Splaiul Independentei, 060031 Bucharest, Romania

email: gheorghita.giulia@yahoo.com

Introduction

Silymarin (*Silybum marianum*), a natural mixture of flavonolignans with valuable worldwide-known medicinal properties, is slightly soluble in both organic and aqueous media, thus consisting of its drawback on cellular adsorption and bioavailability. Silybins (A and B, 1:1) are one of the most biologically active compounds from silymarin [1]. Structurally, these are responsible for weak acidic properties due to the chromone ring that enables donor-acceptor interactions with basic counterparts. Meanwhile, the presence of polyphenol hydroxyls sustains the ability to form complexes with transitional metal ions, imprinting high oxidant activity to the molecule [2].

In the frame of drug and cosmetic formulations, we propose a biocatalytic cold-active lipase-mediated system for the acylation of silybin A/B, with proper fatty acids or esters to improve the initial liposolubility. The biocatalyst is founded on the protein material extracellularly produced by a novel *Psychrobacter sp.* Extracted from Scarisoara Ice Cave (Romania) [3].

Experimental

Structural analysis was conducted through bioinformatic tools and plate screening assays evidenced the existence of lipases outside the bacterial cell. The relative enzyme activity was evaluated for both free and immobilized biocatalysts using the standard method of *p*-nitro phenylbutyrate hydrolysis, while the immobilization performance was evaluated through FT-IR and SEM techniques. The performance of the biocatalytic system was followed up through HPLC-DAD method of detection and quantified in terms of substrate conversion for silybin (trans)esterification. The conditions of the experiments regarding the biocatalytic transformation are listed in Table 1.

Table 1. Conditions of the biocatalytic system.

2 mM Silybin A/B	60 mM Octanoic Acid	10% biocatalyst (v/v)	25 °C, 24h, 1000 rpm
	30 mM Oleic Acid		
	45 mM Me-decanoate		
	40 mM Me-laurate		
	35 mM Me-miristate		
	30 mM Me-plamitate		

Results and discussion

Genome of *Psychrobacter sp.* Of Scarisoara Ice Cave revealed the existence of bacterial lipases from Family IV and V, and through plate screening tests on Tween 80 and olive oil substrates the extracellular lipolytic activity of the strain was evidenced. Total protein material was partially purified with 80% acetone precipitation procedure and concentration ranged between 5-7 mg/mL.

The protein material was immobilized on different nano-/micro-sized magnetic and polymeric resin supports through covalent bonding, and FT-IR interferograms and SEM micrographs revealed good protein attachment. Finally, five potential biocatalysts were obtained, whose functionality based on lipase activity was further studied in contrast to the unimmobilized biocatalyst.

Good lipolytic activity was established in terms of Km and catalytic efficiency on *p*-nitrophenyl butyrate substrate at two different temperatures (25 °C, 40 °C) to highlight the cold-active character preservation during multiple-step process of biocatalyst design.

Silybin esters were produced when silybin substrate reacted with different acylating agents: octanoic acid, oleic acid, methyl decanoate/laurate/myristate/palmitate. Performance of the biocatalytic system was evaluated as substrate conversion via HPLC-DAD with percentages of success of 40% for free biocatalyst and 70% for immobilized specimens. Increased activity for immobilized specimens is attributed to lipase stabilization in the solvent and the interfacial activation is promoted. Part of the results are displayed in Fig. 1.

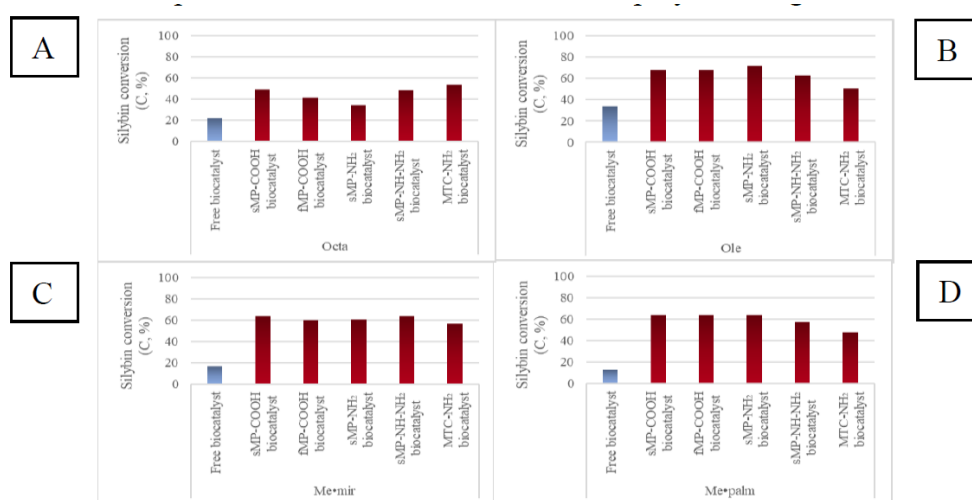


Figure 1. Experimental data. A, B: esterification process of silybin with octanoic and oleic acid. C, D: transesterification process of silybin with methyl myristate and palmitate.

Conclusions

A valuable biocatalytic process was successfully elaborated for silymarin improved bioavailability. Acylation of silybin to corresponding esters was achieved by cold-active biocatalysts, free or immobilized. The cold-active biocatalysts were wisely chosen to promote energy saving mode from the cold-pressed milk thistle oil technology to produce and improve silymarin.

Acknowledgements

This work was financially supported by PNCDI III PED project (contract no. 356PED/2020) from UEFISCDI, Romania.

References

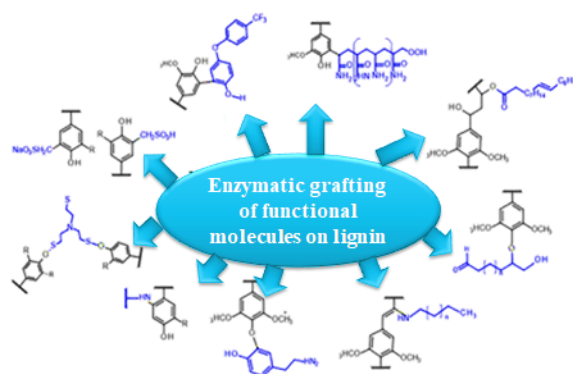
- [1] Di Costanzo, A., Angelico, R., *Molecules*, 24 (2019), 2155.
- [2] Csupor, D., Csorba, A., Hohmann, J., *Journal of Pharmaceutical and Biomedical Analysis*, 130 (2016), 301-317.
- [3] Ramnath, L., Sithole B., Govinden, R., *Biotechnology Reports*, 15 (2017), 114-124.

Lignin derivatization using enzymatic pathway

Sabina Ion^{*}, Bogdan Cojocaru, Madalina Tudorache^{*}, Vasile I. Parvulescu
University of Bucharest, Faculty of Chemistry, Department of Organic Chemistry, Biochemistry and Catalysis, Soseaua Panduri 90, sector 5, 050663 Bucharest, Romania
 e-mail: ion.sabina.gabriela@chimie.unibuc.ro

Introduction

Lignin is a component of lignocellulosic plants which can be an alternative raw material with enormous potential to replace diminishing fossil-based resources for the sustainable production of many chemicals and materials, including petroleum-based products. It is one of the most abundant natural bio-polymers with high heterogeneity, strong intra- and intermolecular hydrogen interactions and modifications introduced during the pulping process which represent a challenge for researchers. Key enzymes can be used to tailor lignin properties such as composition or functional groups in order to obtain new polymers with predictable properties (Scheme 1) [1].



Scheme 1. Enzymatic pathways leading to lignin derivatization [1].

In this study, we investigated biocatalytic routes for the derivatization of lignin. Firstly, lignin was reacted with aniline in the presence of various peroxidase enzymes and H_2O_2 as oxidation reagent. The oxi-polymerization process led to an amino-derivatized lignin with controlled properties (e.g., conductivity, acidity/basicity, thermostability) [2-3]. The grafting bioprocess was optimized working with different concentrations of biocatalyst and different types of lignins. Secondly, the lignin was grafted with a carboxymethylation agent (dimethylcarbonate-DMC) using lipases as biocatalysts. Both free and immobilized lipases were investigated and temperature/DMC concentration was varied.

Experimental

Different types of lignins and peroxidases were tested in the grafting process with aniline. A phosphate buffer saline (PBS) solution (10 mM pH=7.4) and 30 wt % solution of hydrogen peroxide (H_2O_2), methanol (MeOH), Na_2CO_3 , Folin-Ciocalteu reagents of analytical purities were purchased from Sigma-Aldrich. The reaction was set up at 40 °C temperature, 24 h and 1000 rpm. For the carboxymethylation process, different types of free and immobilized lipases were tested in the presence of DMC (also from Sigma Aldrich) and PBS buffer at different reaction temperatures, 24 h and 1000 rpm.

Results and discussion

The derivatized lignins were characterized in order to identify the resulted chemical structure and the induced properties. Thus, the insertion of the amine groups was certified by

¹H-NMR technique, where NH protons were detected in the range of 5.01–4.99 ppm and carboxymethylation process was demonstrated by ¹³C-NMR, where carbonate carbonyl carbons were detected at 154 ppm respectively. The FTIR spectra collected before and after the grafting/carboxymethylation bioprocess evidenced as well the lignin modification. Additionally, the grafted/carboxymethylated lignin was characterized using conductivity measurements, gel permeation chromatography (GPC), thermogravimetric analysis (TGA), temperature-programmed desorption (TPD-NH₃/CO₂), scanning electron microscopy (SEM), and nuclear magnetic resonance (NMR) analyses. All these characterizations provided clearly evidences for a successful bicatalytic derivatization.

Conclusions

A new strategy for the derivatization of lignins using a biocatalytic alternative was demonstrated considering as modifiers amino and carboxymethyl groups. The produced changes afforded suitable characteristics for industrial applications, such as ion-exchange resins, cationic surfactants, flocculants, coagulants, heavy metal adsorbents or support for protein immobilization [4].

Acknowledgements

This work was financially supported by UB project, contract no. 143. We thank to dr. Miguel Alcalde (Institute of Catalysis, CSIC, Madrid, Spain) for mutants of versatile peroxidases.

References

- [1] Weiss, R., Guebitz, G. M., Pellis, A., & Nyanhongo, G. S., *Trends in Biotechnology*, 38 (2020), 1215-1231.
- [2] Ion, S., Opris, C., Cojocaru, B., Tudorache, M., Zgura, I., Galca, A., Bodescu, A., Enache, M., Maria, G., Parvulescu, V.I., *Frontiers in Chemistry*, 6 (2018), 124.
- [3] Ion, S., Brudiu, T., Hanganu, A., Munteanu, F., Enache, M., Maria, G.M., Tudorache, M., Parvulescu, V., *Molecules*, 25 (2020), 4921.
- [4] Lite, C., Ion, S., Tudorache, M., Zgura I., Galca, A.C., Enache, M., Maria, G.M., Parvulescu, V.I., *Catalysis Today*, 379 (2021), 222-229.

Bienzymatic biocatalyst based on enzyme co-immobilization for monoterpenes valorization

Maria Cristina Ghetu*, Madalina Tudorache

University of Bucharest, Faculty of Chemistry, 90-92 Panduri, 5th district, Romania

e-mail: maria.cristina.ghetu@gmail.com

Introduction

Monoterpenes are a class of compounds with wide occurrence in nature, acting as natural defense against herbivores, and to attract pollinators. Terpenoids are the corresponding oxygenated derivatives and are used as flavor and fragrance products [1]. Therefore, an increased interest for developing methods for monoterpenes valorization, and previous studies showed the bioconversion of limonene to limonene-1,2-diol is achievable using whole cell biocatalysis [2]. However, this method has some drawbacks, such as: difficulty of controlling the process, low tolerance of substrate concentration, and high chances of side reactions [3]. Therefore, we propose a bienzymatic cascade pathway that overcomes the mentioned disadvantages.

Experimental

The material was characterized using infrared and ultraviolet-visible spectroscopy before and after co-immobilization. For the applications of the bienzymatic biocatalyst samples were prepared with the following components: 1.6 mols/ L monocyclic monoterpene, 1.6 mols/L octanoic acid, 0.1 mols/L phosphate-buffer saline with pH of around 8, 11 mg biocomposite, 0.3 milimols trisodium citrate. Gas chromatography was used for analysis.

Results and discussion

We analyzed the bienzymatic biocatalyst using IR and near UV spectroscopy, and the resulting data showed that the immobilization was successful. We tested the system using lipase – hydrolase enzymes couple for different substrates transformation, eg I-(+)-limonene and α -phellandrene. The experiments were performed with Novozym®435 (Candida antarctica B lipase immobilized on acrylic support), Novozym®435 in the presence of free hydrolase, and hydrolase@Novozyme®435 biocomposite. Novozym®435 in the presence of free hydrolase (CH55-LEH) allowed achieving a conversion of 45% I-(+)-limonene and a diol yield of 27%. On the other hand, the biocomposite transformed 74% of I-(+)-limonene with 39% yield in limonene-1,2-diol. Additionally, the biocomposite offered 47% of α -phellandrene conversion with 31% yield in p-menth-5-ene-1,2-diol. In all the cases, the enantiomeric excess was above 90% for (1S, 2S, 4R)-(+)-limonene-1,2-diol and (1S, 2S, 4R)-p-menth-5-ene-1,2-diol. The results are displayed in Fig. 1.

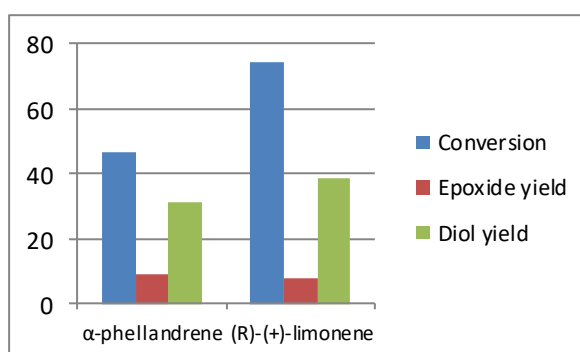


Figure 1. Bienzymatic biocatalyst efficiency.

Conclusions

The developed bienzymatic system exhibited an efficient enantio-biotransformation of I-(+)-limonene/ α -phellandrene into diol derivatives which find many applications in the industrial field.

Acknowledgements

This work was financially supported by The Education, Scholarship, Apprenticeships and Youth Entrepreneurship Programmer-EEA Grants 2014-2021, Project No. 18-Cop-0041.

References

- [1] De Carvalho, C.C.C.R., Da Fonseca, M.M.R., *Biotechnology Advances*, 24 (2006), 134-142.
- [2] Sales, A., Pastore G.M., Bicas, J.L., *Process Biochemistry*, 86 (2019), 25-31.
- [3] Faber, K., *Biotransformations in Organic Chemistry*, 5th Ed. Berlin, Springer, 2004.

ABL&E-JASCO Româniaabout us

Cristina Lungu*

ABL&E – JASCO România Comerț și Servicii SRL, Bucharest, Romania

e-mail: ablerom@ablelab.com

”ABL&E-JASCO România Comerț și Servicii S.R.L.” operates on the laboratory equipment market since 1996, offering complete sales and maintenance services for equipment as well as user consulting and training, with qualified and authorized employees.

The main manufacturers represented are in the field of spectroscopy (JASCO, Metertech), HPLC (JASCO, Teknokroma, ANTEC), analysis of pharmaceutical (Teledyne-Hanson Research), organic synthesis and separation (Biotage) and SPR-surface plasmon resonance spectroscopy (Reichert).

The equipment offered is available in a wide range of models and accessories, from those designed for routine analysis with applications in quality control or education, to those with advanced specifications that meet the most demanding requirements in the field of Research – Development.

ABL & E-JASCO Romania Trade and Services S.R.L. is open to collaboration with young college graduates, offering a dynamic environment of personal and professional development, ensuring regular training and a friendly work climate.

Silica materials modified with copper and aminosilane for adsorption and release of hydroxychloroquine

Anna Olejnik^{*}, Joanna Goscianska^{*}

Adam Mickiewicz University in Poznań, Faculty of Chemistry, Department of Chemical Technology, Uniwersytetu Poznańskiego 8, 61-614 Poznań, Poland

e-mails: annamar@amu.edu.pl, asiagosc@amu.edu.pl

Introduction

In recent years, considerable attention has been paid to hydroxychloroquine (HCQ) that antiviral activity was tested against the HIV-1, poliovirus, Ebola virus, hepatitis A, SARS-CoV-1, and SARS-CoV-2 [1,2]. This drug is effective for the treatment of discoid lupus erythematosus, malaria, rheumatoid arthritis, and antiphospholipid syndrome [3]. Nevertheless, it was reported that hydroxychloroquine showed several adverse effects such as gastrointestinal disorders, myopathy, retinopathy, and hepatic failure [4]. In order to diminish them and to reduce the frequency of drug daily dosage, it is suggested to apply ordered mesoporous silicas as drug carriers. These nanomaterials can be used as ideal candidates for hosting active compounds mainly due to their nontoxicity, high stability, well-developed surface area, and great pore volume [5]. The aim of this study was to apply mesoporous silicas in the adsorption and release of hydroxychloroquine. The SBA-15 and SBA-16 materials were selected to be modified with 3-aminopropyltriethoxysilane and copper(II) chloride. The amino-functional groups were introduced to the surface of these materials to improve their sorption abilities towards the drug, while copper was chosen because it is reported that exhibited antiviral and antibacterial activity.

Experimental

Pristine and functionalized samples were synthesized and characterized by various techniques such as X-ray diffraction, small-angle X-ray scattering, low-temperature nitrogen sorption, transmission electron microscopy, X-ray photoelectron spectroscopy, infrared spectroscopy, laser diffraction, and elemental analysis. Next, these nanomaterials were applied as carriers for hydroxychloroquine. The drug loading into mesoporous silica was achieved in adsorption processes. Series of aqueous drug solutions with concentrations from the range of 6.25 to 125.00 mg/dm³ were prepared. 0.04 g of each nanomaterial (SBA-15, Cu/SBA-15-AS, SBA-16, and Cu/SBA-16-AS) were suspended in 50 cm³ of hydroxychloroquine solutions. As prepared samples were shaken steadily in a shaker for 24 h at room temperature. Afterward, the mixtures were filtered off and the concentration of HCQ found in the supernatant liquid was measured at the wavelength of 231 nm by spectrophotometer UV-Vis. Next, the release behavior of hydroxychloroquine from unmodified and modified materials was studied in three different conditions to simulate gastric fluid (pH 1.2), intestinal fluid (phosphate buffer of pH 5.8), and saliva (phosphate buffer pH 7.2).

Results and discussion

The results proved that both unmodified and modified mesoporous silicas were successfully obtained. Pristine SBA-15 and SBA-16 materials were characterized by high surface area, ranging from 703 to 727 m²/g, respectively. The modification of materials with aminosilane and copper(II) chloride led to decrease in the specific surface area and pore volume for both Cu/SBA-15-AS and Cu/SBA-16-AS. Based on small-angle X-ray scattering profiles and transmission electron microscopy images it was found that pristine SBA-15 and SBA-16 had highly ordered mesoporous structure, while for the modified materials the

degree of mesostructure ordering decreased. The results revealed that the adsorption process of hydroxychloroquine was more efficient on the surface of copper and aminosilane modified materials only at low drug concentrations (Fig.1A). It was found that pore volume is the significant parameter that had an influence on the drug sorption capacity. The highest amount of HCQ was adsorbed on SBA-15 with the largest pore volume ($0.614 \text{ cm}^3/\text{g}$) compared to other ordered mesoporous silica materials obtained. The results proved that the release behavior of hydroxychloroquine from ordered mesoporous silica was determined by different factors including pH conditions, textural parameters, surface charge, and presence of surface functional groups. The biggest differences in the HCQ release profiles were found at pH 7.2 (Fig. 1B).

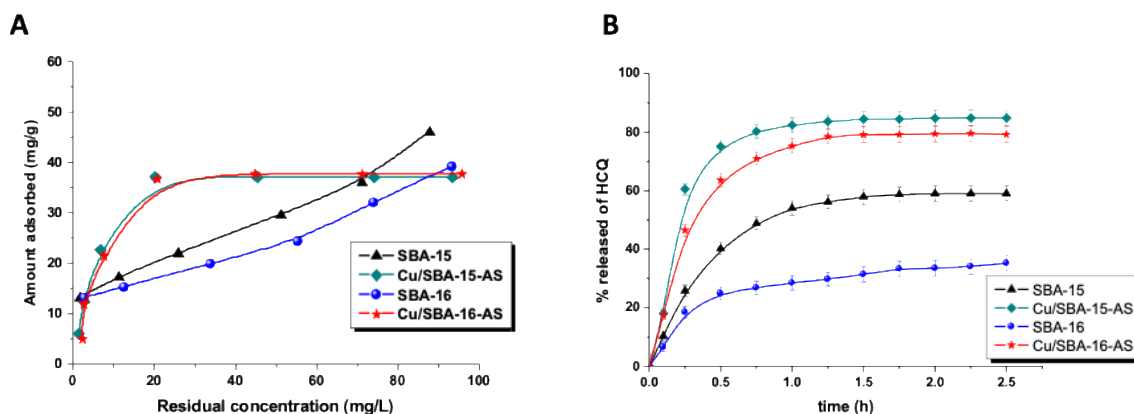


Figure 1. Adsorption isotherms of HCQ on modified and non-modified ordered silica materials (A) and release profiles of HCQ from modified and non-modified mesoporous silica materials at pH 7.2 (B).

Conclusions

Based on these findings it is suggested that functionalized mesoporous silica materials could be applied as smart carriers for hydroxychloroquine that will enable the release of the antiviral drug at the chosen location of the body in a controlled manner.

Acknowledgements

Financial support from Polish Ministry of Science and Higher Education is acknowledged.

References

- [1] Lajoie, J., Mwangi, L., Fowke, K.R., *AIDS Research and Therapy*, 14 (2017), 1-5.
- [2] Arshad, S., Kilgore, P., Chaudhry, Z.S., Jacobsen, G., Wang, D.D., Huitsing, K., Brar, I., Alangaden, G.J., Ramesh, M.S., McKinnon, *International Journal of Infectious Diseases*, 97 (2020), 396-403.
- [3] Rainsford, K.D., Parke, A.L., Clifford-Rashotte, M., Kean, W.F., *Inflammopharmacology*, 23 (2015), 231-269.
- [4] Srinivasa, A., Tosounidou, S., Gordon, C., *The Journal of Rheumatology*, 44 (2017), 398.
- [5] Wang, S., *Microporous and Mesoporous Materials*, 117 (2009), 1-9.

Metal-organic frameworks as diclofenac nanocarriers to treat migraine

Aleksandra Galarda, Joanna Goscińska*

Adam Mickiewicz University in Poznań, Faculty of Chemistry, Department of Chemical Technology, Uniwersytetu Poznańskiego 8, 61-614 Poznań, Poland
e-mail: asiagosc@amu.edu.pl

Introduction

Migraine is now the sixth most common disease in the world. The drugs usually applied during migraine attacks are non-steroidal anti-inflammatory drugs, which include, *i.e.* ketoprofen, diclofenac, and naproxen [1]. Despite a large amount of anti-migraine substances, it was still not possible to find the ideal drug. Current migraine treatment and prevention strategies focus on finding solutions that will simultaneously increase the effectiveness and absorption rate of the drugs taken, as well as reduce their side effects. Therefore, the best idea is using porous nanomaterials whose unique physicochemical properties make them promising drug carriers. Metal-organic frameworks (MOFs) are good candidates for biomedical applications due to their porous nature, modular structure, and readily chemical functionalizability. They can be commonly used as active compound carriers, bioimaging and therapeutic agents. The porosity and topology of MOFs can be modulated through post-synthetic modification, variations of the metal-node and pre-designed ligand geometries. Organic linkers (*e.g.*, carboxylates, imidazolates, or phosphonates) in the hybrid structure of MOFs provide biocompatibility and high sorption capacity towards different drugs, while inorganic groups can be optimized for controlled release profiles [2-4]. The aim of the study was to synthesize MOF materials with different morphology and porosity, and to evaluate the importance of their physicochemical properties during the adsorption and release of diclofenac.

Experimental

Metal-organic frameworks were synthesized under solvothermal conditions in autoclaves. Obtained MOFs included MIL-88A, MIL-101(Fe) and MIL-53(Fe). These materials consisted of iron cations and organic linkers, *i.e.* terephthalic acid and fumaric acid. The materials were subjected to detailed physicochemical characteristics using X-ray diffraction, low-temperature nitrogen adsorption/desorption, elemental analysis, scanning and transmission electron microscopy. To determine the adsorption properties of selected MOFs, a series of adsorption experiments were conducted at room temperature. 25 mg of each nanomaterial were suspended in 50 mL of diclofenac solutions. As prepared samples were shaken steadily in a shaker (KS 4000i control, IKA, Germany) for 24 h. Afterward, the mixtures were filtered off and the concentration of drug found in the supernatant liquid was measured at the wavelength of 276 nm by spectrophotometer UV-Vis (Cary 60, Agilent). The release experiments of diclofenac from MOF materials were performed in the conditions to simulate intestinal fluid (phosphate buffer of pH 5.8). The receptor fluids were maintained at $37.0\text{ }^{\circ}\text{C} \pm 0.50\text{ }^{\circ}\text{C}$ with the stirring of speed 100 rpm.

Results and discussion

Scanning electron microscopy images of the resulting products revealed the formation of hexagonal rods in case of MIL-88A. MIL-53(Fe) and MIL-101(Fe) show an octahedral morphology. MIL-101(Fe) had the highest surface area ($584\text{ m}^2/\text{g}$) and pore volume ($0.54\text{ cm}^3/\text{g}$) among synthesized adsorbents. The isotherms of diclofenac adsorbed on the surface of MOF materials are depicted in Fig. 1. It was observed that at low initial drug concentrations the active sites of samples were highly accessible for drug loading and its adsorption was

random. With increase in diclofenac concentration, the drug molecules were tightly packed on the surface of MOFs. At high diclofenac concentration the sorption capacity was constant because all available active sites were occupied either by drug molecules that could compete with each other or with water molecules. It was observed that the amount of diclofenac adsorbed is significantly different depending on the selected material. MIL-88A is the most effective adsorbent of the drug, even though it is characterized by the smallest specific surface area ($10 \text{ m}^2/\text{g}$). This could be explained by the electrostatic interactions between the positively charged amine groups derived from diclofenac and the negatively charged carboxylic groups from fumaric acid present in linker of MIL-88A.

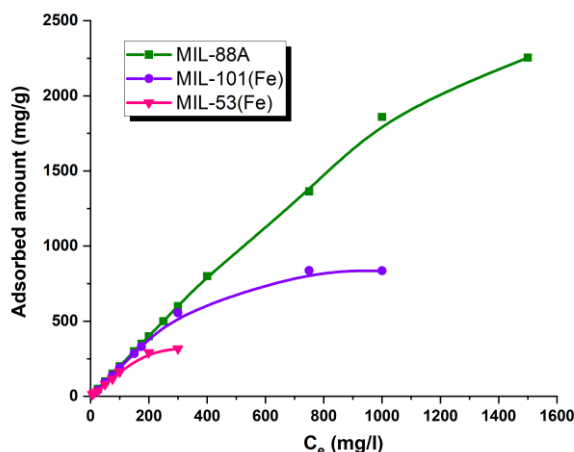


Figure 1. Adsorption isotherms of diclofenac onto metal-organic frameworks.

Conclusions

Metal-organic frameworks have been found promising adsorbents of diclofenac. The highest amount of drug was adsorbed on MIL-88A. Morphological irregularities and specific functional groups created new adsorption sites for diclofenac, supporting host-guest interactions that enable high drug loading. Additionally, it was found that the diclofenac release rate exhibited pH sensitivity. These phenomena allow control of the experiment according to the needs.

References

- [1] Negro, A., Martelletti, P., Expert Opinion on Investigational Drugs, 28 (2019), 555-567.
- [2] Wang, Z., Cohen, S.M., Chemical Society Reviews, 38 (2009), 1315-1329.
- [3] Yang, J., Yang Y.W., Small, 16 (2020), 1906846.
- [4] Ejsmont, A., Andreo, J., Lanza, A., Galarda, A., Macreadie, L., Wuttke, S., Canossa, S., Ploetz, E., Goscianska, J., Coordination Chemistry Reviews, 430 (2021), 213655.

Magnetic core-multi-shell nanocomposites for green oxidation process of glucose

Magdi El Fergani, Iunia Podolean, Nicolae Guzo, Simona M. Coman, Madalina Tudorache, Vasile I. Parvulescu, Natalia Candu*

Department of Organic Chemistry, Biochemistry and Catalysis, Faculty of Chemistry, University of Bucharest, Bdul Regina Elisabeta 4-12, Bucharest 030016, Romania

e-mail: natalia.candu@chimie.unibuc.ro

Introduction

In the past few years, a big attention has been paid to valorizing terrestrial biomass as renewable and inexpensive feedstock for producing chemicals and fuels for replacing fossil-based ones [1]. The valorization of glucose to its oxidation products, such as gluconic acid (GLA) or glucaric acid (GA) is quite interesting and promising as such processes can easily be integrated in already existing carbohydrate technologies [2]. GLA and GA are used in many fields, including construction industries, food additives, pharmaceutical, raw materials, textile and paper industries [3]. In this respect, many studies on catalytic oxidation were made by using noble metals (*i.e.* Pt, Au or Pd) supported on different carriers and in the presence of aqueous alkali solutions [4]. However, the high price of noble metals demands innovating cheap alternatives where transition metal-based heterogeneous catalysts would be preferred [5]. Also, for environmentally friendly considerations (*i.e.* high stability, reusability, inexpensive and ease of separation from the reaction media), the use of heterogeneous catalysts based on core magnetite has been developed [6]. By rationally tuning the shells of such materials, a range of core-shell nanoparticles can be produced with tailorable properties such as; acid-base and/or redox properties that can play important roles in various catalytic reactions which can offer green and sustainable solutions for the environmental problems [7].

In this context, the use of these materials for transformation of bio-renewable feedstock to highly attractive bio-chemicals are becoming an effective method of minimizing pollution and improving the efficiency of energy utilization [8].

In this work, we aimed to synthesize highly performance, cheaper, excellent stability and convenient recycling catalytic system based on $\text{Fe}_3\text{O}_4@\text{S}@\text{A}@\text{M}(5\%)\text{O}_x$ (where S: SiO_2 , CeO_2 and ZrO_2 , A: 3-aminopropyltriethoxysilane and M: Cu, Co and Ni). Obtained catalytic systems have been applied in the selective oxidation of D-glucose to carboxylic acid products (*i.e.* GLA, GA).

Experimental

All the catalysts were prepared by using the procedure described as following: the magnetic core was prepared by coprecipitation method ($\text{Fe}^{+3}/\text{Fe}^{+2}$), followed by adding the first shell (SiO_2 , CeO_2 and ZrO_2) by precipitation. After that APTES was linked to the shell in the presence of toluene for 24 h at 80 °C and mild stirring. Finally, the metal oxides were deposited on the support by using metal precursor salts in the basic aqueous solution for 24 h at room temperature. The solids were separated, washed, dried and calcined under inert atmosphere for 3 h at 250 °C. The catalytic oxidations of glucose to carboxylic acids were carried out using a 16 mL autoclave reactor in water as solvent and oxidants like O_2 or H_2O_2 . The reactions were carried out under 0-5 bar of O_2 , at different temperatures and reaction times. Reaction products were analyzed by GC-MS and HPLC.

Results and discussion

Prepared catalysts were exhaustively characterized before and after catalytic test by XRD, DRIFT, TG-DTA, etc. The obtained results from XRD and FTIR spectra indicated that

the magnetic core was successfully covered by all types of the shells (SiO_2 , CeO_2 and ZrO_2). Also, APTES were strongly linked to both the first shell and the deposited metal oxides. No specific diffraction lines for MO_x were evidenced, which indicated their formation as small crystals uniformly dispersed. The TG-DTA shows that all the prepared catalytic samples were stable under the reaction conditions. The catalytic results revealed different oxidation products as a function of support/metal oxides combination and the reaction conditions. In case of $\text{SiO}_2/\text{CoO}_x$ based catalyst, for instance, the mainly product was gluconic acid which transformed into glucaric acid by increasing the reaction time. For the $\text{SiO}_2/\text{CuO}_x$ based catalyst, on the other hand, the oxidation takes place towards low molecular acids, such as glycolic acid. The catalysts were recycled more than four times without losing their efficiency.

Conclusions

The relationship between the $\text{Fe}_3\text{O}_4@\text{S}@\text{A}@\text{M}(5\%)\text{O}_x$ catalysts structures and their catalytic performance was investigated. The characterization results show the successful homogeneously incorporated metal oxides with high dispersion on the shells. The catalytic results strongly depend on the nature of the support, metal oxides and the reaction conditions. Optimal catalytic features and reaction conditions as well as the catalytic performances – catalytic properties correlation will be discussed in detail. The new proposed catalytic systems do not contain noble metals, are highly efficient, can be separated by applying an external magnetic field and are recyclable.

Acknowledgements

This work was supported by a grant of the Romanian Ministry of Education and Research, CNCS-UEFISCDI, project PN-III-P1-1.1-TE-2019-1933, Nr.69/2020, within PNCDI III.

References

- [1] Corma, A., Iborra, S., Velty, A., *Chemical Reviews*, 107 (2007), 2411-2502.
- [2] Baatz, C., Thielecke, N., Prüße, U., *Applied Catalysis B: Environmental*, 70 (2007), 653-660.
- [3] Qi, P., Chen, S., Chen, J., Zheng, J., Zheng, X., Yuan Y., *ACS Catalysis*, 5 (2015), 2659-2670.
- [4] Rass, H.A., Essayem, N., Besson, M., *Green Chemistry*, 15 (2013), 2240-2251.
- [5] Delidovich, I., Hausoul, P., Palkovits, R., *Chemical Reviews*, 116 (2016), 1540-1599.
- [6] Rajabi-Moghaddam, H., Naimi-Jamal, M.R. & Tajbakhsh, M., *Scientific Reports*, 11 (2021), 2073.
- [8] Gawande, M.B., Goswami A., Asefa Tewodros., Guo, H., Biradar, A.V., Peng, D.-L., Zboril. R., Varma, Rajender S., *Chemical Society Reviews*, 44 (2015), 7540-7590.
- [9] Qi P., Chen S., Chen, J., Zheng, J., Zheng, X., Yuan, Y., *ACS Catalysis*, 5 (2015), 2659-2670.

Protein based byproducts conversion into advanced materials

Carmen Gaidau¹, Mihaela Niculescu¹, Maria Stanca^{1,*}, Cosmin-Andrei Alexe¹, Maria Rapa²
¹*R&D National Institute for Textiles and Leather-Division Leather and Footwear Research, Bucharest, Romania*

²*University POLITEHNICA of Bucharest, Bucharest, Romania*

email: maria.stanca@icpi.ro

Introduction

Collagen and keratin based biomass is an important bioresource with potential to be recovered and reused in advanced materials in the frame of circular economy concept. Leather industry processes a by-product from meat industry which if it were not capitalized it would cost US\$1040 million per year adding ground, water and air pollution [1]. In the last 18 years [2] hide processing has made many advances in terms of environmental impact, water consumption has fallen 2.5 times, energy consumption has fallen 1.96 times, and solid waste has remained at the same level. Wool represents a recent waste due to its low quality, unsuitable for textile industry. At the EU level, a resource of 150,000 tons of unmarketable wool, which represents about 75% of total wool production per year, becomes waste. The paper presents results obtained for the extraction, solubilization and refining of collagen and keratin hydrolysates and the obtaining of value-added products that have been tested as plant growth biostimulants, nanostructures for skin cellular restoration or organic tanning material for hide and leather processing.

Experimental

Collagen based waste was supplied by a local tannery and wool waste from sheep breeders. Chemical reagents of analytical grade (CaO, NaOH, H₂SO₄, CH₃COOH) were purchased from Chimopar SA Bucharest, Romania, poly(ethylene oxide)-PEO was supplied by Alpha Aesar and Alcalase 2.5L with activity of 2.4 AU-A/g was purchased from Novozymes. Whey and mimosa vegetable tannin, two renewable materials were purchased from Deco and Silvateam Italy. Collagen hydrolysates (CH, CHC) were obtained from tanned waste by alkaline-enzymatic hydrolyses according to the method previously described [3]. Keratin hydrolysate was solubilized from degreased wool by alkaline hydrolysis with 10% sodium hydroxide at 800 °C for 4 hours (KH, KHL) [4]. The characterisation of the protein hydrolysates was performed by standard methods for dry substance, nitrogen, protein, ash, cysteine, sulphur content and pH. The molecular weight was determined by gel permeation chromatography (GPC) using an Agilent Technologies instrument (1260 model) equipped with PL aqua gel-OH MIXED-H column and multi-detection unit. Depending on molecular weight the protein hydrolysates were used for preparation of plant biostimulation and nutrition product, nanofibers for wound dressings and organic tanning materials. Plant biostimulants were prepared by mixing collagen and keratin hydrolysates with low molecular weight with macro and micronutrients based on P, K, N, Cu, Fe, Mg, Mn, Mo, Zn and B and were tested on maize plant foliar fertilization in comparison with water treated plants. The chlorophyll content and weight of the combs were the indexes for biostimulation efficiency identification. High molecular weight collagen and keratin hydrolysates were used for nanofibre fabrication for new wound dressing design by using uniaxial electrospinning equipment (TL-Pro-BM, China) with a flow rate of 1-3 mL/h, voltage of 18-25 kV and distance from the needle to collector from 10-12 cm. In view of spinnability improvement collagen hydrolysate was mixed with 1.5% w/v chitosan solution and keratin hydrolysate was mixed with 10% w/v PEO. Collagen and keratin hydrolysates were mixed with whey and mimosa vegetable tannin in view of a new renewable tanning material development as

alternative to metal based tannins. The tanning properties were tested by pre-tanning picked sheepskins followed by shrinkage temperature determination for collagen crosslinking assessment and organic retanning for full organic process demonstration as alternative to the use of basic chromium (III) salts.

Results and discussion

The main properties of collagen and keratin hydrolysates were listed in Table 1 and show that different protein hydrolysates can be tailored by alkaline and alkaline-enzymatic hydrolyses of leather industry waste and coarse wool. The potential of advanced materials preparation from low or high molecular weight proteins is shown in Fig. 1, from plant growth biostimulant (Fig. 1a,e), organic pre-tanning and retanning new material (Fig. 1b,f) to collagen and keratin based nanofibers for wound healing (Fig. 1c,d,e). Chlorophyll index was 10% higher as compared to control sample and the comb weight increased by 101.4%. Collagen shrinkage temperature of pretanned sheepskins was 69-720 °C which is acceptable for organic tanned leathers. The protein based mixtures were suitable for nanofiber mats development.

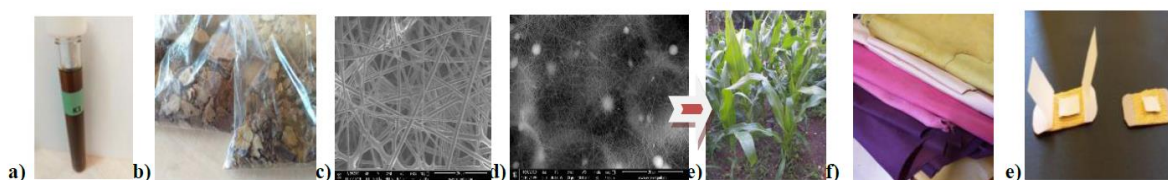


Figure 1: a, e) Plant biostimulant; b, f) organic tanning material; c, d, e) nanofibers for wound dressing

Conclusions

Advanced materials with bioactive properties and collagen crosslinking properties have been demonstrated by processing collagen and keratin-based by-products. The obtained products meet the requirements of the circular economy for the leather industry and agriculture.

Acknowledgements

The works were funded by grants of the Romanian Ministry of Research, Innovation and Digitalization, CCCDI-UEFISCDI, contract 5PTE, BIOTEHKER, contract 187/2020, E! 13359 KER_COL_CE and contract 127/2020, E!12610, FERTI-MAIZE, within PNCDI III. We are grateful to associate professor dr. Madalina Sandulescu from Department of Organic Chemistry, Biochemistry and Catalysis, Faculty of Chemistry from University of Bucharest, for GPC analysis.

References

- [1] Saiddain A., <https://internationaleathermaker.com/news/fullstory.php/aid/7289/19> August, (2019).
- [2] Tegtmeier D., Wynne B., 7th Freiberg Leather Days, Freiberg Germany, June 13 and 14, 2018.
- [3] Gaidau C., Ghiga M., Stepan E., Taloi D., Filipescu L., REV.CHIM.(Bucharest), 60 (2009), 501-507.
- [4] Gaidau, C., Stanca, M., Niculescu, M.-D., Alexe, C.-A., Becheritu, M., Horoias, R., Cioineag, C., Răpă, M., Stanculescu, I.R., *Materials*, 14 (2021) 4696.

A new generation of polysulfone membrane materials for hemodialysis

Mădălina Oprea^{1,*}, Ștefan Ioan Voicu^{1,2,*}, Andreea Mădălina Pandeale¹

¹University Politehnica of Bucharest, Faculty of Applied Chemistry and Material Science, Gheorghe Polizu 1-7, 011061, Sector 1, Bucharest, Romania

e-mail: madalinna.calarasu@gmail.com

²Advanced Polymers Materials Group, Gheorghe Polizu 1-7, 011061, Bucharest, Romania

e-mail: svoicu@gmail.com

Introduction

Heavy metal poisoning may occur as a result of industrial exposure, air or water pollution, contaminated medicines, improperly coated food containers, or the ingestion of lead-based paints. There are various methods for the removal of heavy metals from the human body, however, if the renal system is severely affected, hemodialysis is the most recommended one [1]. Amongst synthetic polymers used for the production of hemodialysis membranes, polysulfone (PSF) remarks itself in virtue of its appropriate physico-chemical and biological properties, such as good solubility in a large range of polar aprotic solvents, high thermal and mechanical resistance, chemical resistance on the entire range of pH and in oxidative medium, intrinsic biocompatibility, high permeability for low molecular weight proteins and high endotoxin retention ability [2]. In comparison with neat polymeric membranes, composite ones present clearer pore channels, higher porosity and show better results in terms of filtration rates and toxin retention [3]. According to various studies, the incorporation of carbonaceous compounds, particularly reduced graphene oxide (rGO), in polymeric membranes increases their thermal stability, improves bioactivity and mechanical properties [4]. The purpose of this study was the synthesis of a novel generation of composite membranes based on polysulfone and reduced graphene oxide. The membranes were obtained by blending polysulfone with reduced graphene oxide particles that were previously functionalized with 4'-aminobenzo-15-crown-5 ether (AB15C5) in order to provide them the ability to retain metal ions. Crown ethers are cyclic molecules that play a crucial role in the formation of host-guest complexes due to their ability to accommodate positive metal ions, coordinated to the ring of oxygen atoms inside their central cavity [5, 6] Therefore, these novel PSF-based membranes could be successfully used in "one day hemodialysis" procedures, employed in the case of heavy metals poisoning. The novelty degree of this study is represented by the functionalization method that ensures the formation of covalent bonds between the reduced graphene oxide and the complexation agent (AB15C5), thus preventing the release of the active compound in the bloodstream.

Experimental

First, reduced graphene oxide with surface amine groups (NH₂-rGO, Nanoinnova) was functionalized with 4'-aminobenzo-15-crown-5 ether (Sigma Aldrich) using cyanuric chloride (C₃Cl₃N₃, Sigma Aldrich) as binding molecule. The process was performed under magnetic stirring, for 4 hours, at temperatures ranging from 40 to 70 °C, depending on the reaction step. The obtained suspension was filtered and dried in a vacuum laboratory oven and the resulting powder was dispersed in the polysulfone (Sigma Aldrich) solution. Ultrasonication was employed for an even dispersion of the carbonaceous filler in the polymeric matrix. The polymer solution was casted on a glass plate, using an automated film applicator, and then immediately immersed into a coagulation bath (distilled water) in which the phase inversion process took place. The obtained membrane was washed with distilled water to remove residual solvents and dried at room temperature prior to characterization.

The chemical composition of the neat and composite membranes was investigated using FT-IR and dispersive Raman spectroscopy. SEM was employed to investigate the samples morphology, while their thermal stability was studied using TGA. The membranes ability to retain metal ions from synthetic feed solutions was determined by ICP-MS.

Results and discussion

The presence of two additional peaks at 1651 and 1735 cm^{-1} in the FT-IR spectrum and respectively the D and G bands in the Raman spectrum confirmed the successful incorporation of the functionalized graphene oxide in the membranes structure. TGA curves showed that the carbonaceous filler increased the thermal stability of PSF, $T_{d5\%}$ and T_{max} being shifted towards higher values compared to the neat samples. The filler also influenced the membranes morphology, the composite ones presenting an irregular pore distribution and a lower porosity. The ICP-MS analysis revealed that AB15C5-rGO modified PSF membranes had an up to three times increase in copper ions retention ability, compared to neat PSF.

Table 2. ICP-MS analysis results.

Sample	Copper concentration [$\mu\text{g/l}$]	Calcium concentration [$\mu\text{g/l}$]	Adsorbed copper [%]	Adsorbed calcium [%]
Synthetic feed solution	1133.13	208.12	0	0
PSF	1008.88	170.93	10.97	17.87
AB15C5-rGO/PSF	786.89	147.64	30.56	29.07

Conclusions

The AB15C5-rGO/PSF composite membranes synthesized in this study presented appropriate physico-chemical properties for metal ions retention. Future trends consist in hemocompatibility and hydrodynamic stability testing and also in the covalent attachment of other organic molecules on the surface of rGO, depending on the species that are intended to be separated.

Acknowledgements

This work was supported by a grant of the Ministry of Research, Innovation and Digitization, CNCS/CCCDI – UEFISCDI, project number PN-III-P4-ID-PCE-2020-1154, Hemodialysis combined with stimuli responsive drug delivery – a new generation of polymeric membranes for advanced biomedical applications within PNCIDI III.

References

- [1] Tchounwou, P.B., Yedjou, C.G., Patlolla, A.K., Sutton, D.J., *Experientia supplementum*, 101 (2012), 133-164.
- [2] Bowry, S.K., Gatti, E., Vienken, J., *Contribution to Nephrology*, 173 (2011), 110-118.
- [3] Eswari, S.T., Naik S., *Materials Science for Energy Technologies*, 3 (2020), 116-126.
- [4] Oprea, M., Voicu, S.I., *Materials* 13(23) (2020), 5347.
- [5] Potopnyk, M.A., Jarosz, S., *Advances in Carbohydrate Chemistry and Biochemistry*, 3 (2014), 227-295.
- [6] Davis, F., Higson, S., *Cryptands and Other Compounds*, 3 (2011), 34-76.

New approaches in synthesis of 2D LDH-type materials used in the Claisen-Schmidt condensation

Silvana-Denisa Mihăilă^{1,*}, Bogdan Cojocaru¹, Bogdan Jurca², Octavian-Dumitru Pavel^{1,*}, Gheorghita Mitran¹, Rodica Zăvoianu¹, Vasile I. Pârvulescu¹

¹University of Bucharest, Faculty of Chemistry, Department of Organic Chemistry, Biochemistry and Catalysis, 4-12 Regina Elisabeta, S3, Bucharest, Romania

²University of Bucharest, Faculty of Chemistry, Department of Physical Chemistry, 4-12 Regina Elisabeta, S3, Bucharest, Romania

e-mails: silvana_maria2012@yahoo.ro; octavian.pavel@chimie.unibuc.ro

Introduction

Layered Double Hydroxides (LDH) continue to be a fascinating class of materials due to their amazing properties that are important in various fields [1] such as environmental protection, medicine, pharmacy, catalysis, etc. Quaternary salts such as Tetra Methyl Ammonium Hydroxide (TMAH) represents a feasible alternative to traditional NaOH/Na₂CO₃ inorganic alkalis [2] for LDH-type materials synthesis. Usually, the washing step in the LDH synthesis *via* inorganic alkali generates a large amount of wastewater and its subsequent processing generates high costs. On the same note, the mechano-chemical method, highly demanded by the industry, leads to obtaining pure layered structures in low energy consumption conditions and the presence of a small number of specific vessels compared to the traditional route, co-precipitation [3]. Herein we report the results related to Y-modified LDH preparation using two methods, *e.g.* co-precipitation and mechano-chemical route, and also the obtaining of their corresponding mixed oxides by calcinations as well as the structural properties of these solids in correlation to their activity and selectivity in the Claisen-Schmidt condensation between benzaldehyde and cyclohexanone.

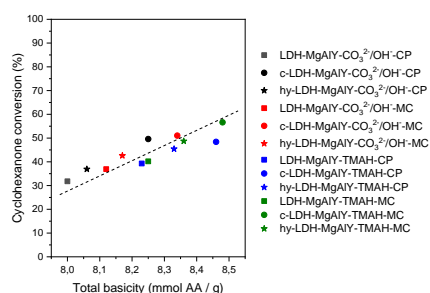
Experimental

Y-modified LDH (with Mg_{0.75}Al_{0.125}Y_{0.125} molar ratio) were prepared by two methods, co-precipitation and mechano-chemical, in the presence of inorganic Na₂CO₃/NaOH (as reference) as well as organic TMAH alkalis. The synthesis of the LDH in the inorganic alkali presence was carried out at pH of 10 under low super-saturation conditions using a solution **A** containing 1.5 M of Mg²⁺, Al³⁺ and Y³⁺ nitrates in distilled water and an equal volume of solution **B** containing 0.18 mol of Na₂CO₃ and 0.44 mol of NaOH in distilled water. The obtained gel was then aged, filtered, washed and dried. The synthesis of the LDH in the organic alkali presence was performed identically to the procedure described above with exception that instead of the inorganic base previously introduced this procedure required a volume of TMAH solution such that the pH during preparation would be maintained at 10. The synthesis by mechano-chemical route in the inorganic alkali presence was carried out in a mortar with pestle by mixing the required amounts of Mg, Al and Y nitrates as well as Na₂CO₃ and NaOH for 1 h without the addition of water. The white paste obtained was then filtered, washed and dried. The synthesis in the organic alkali was carried out in the same way like in the inorganic route with the only exception being the replacement of the inorganic base with a suitable volume of TMAH solution in order for the working pH to hit a constant value of 10. All samples were calcined at 460 °C for 18h and reconstructed by memory effect. Claisen-Schmidt condensation was carried out for 2 h at 120 °C by placing a mixture of benzaldehyde (10 mmoles) and cyclohexanone (5 mmol) under batch and solvent-free conditions with a specified amount of catalyst (benzaldehyde/catalyst ratio of 10/1). At the end of reaction time, 1 mL of toluene

was added to solubilize the reaction mixture, which became solid at room temperature. The mixture was analyzed using a GC-FID Thermo Quest Chromatograph.

Results and discussion

The XRD patterns of the sample obtained by co-precipitation using inorganic alkalis revealed the formation of a layered structure with the presence of $Y(OH)_3$ as impurity. This phase transforms into the corresponding mixed oxide via calcination and does not participate in the process of reconstruction despite being present in the reconstructed sample. The same behavior is observed in the sample obtained using inorganic alkalis through mechano-chemical mixing. In the samples obtained in organic alkalis by co-precipitation, $Y(OH)_3$ is totally under amorphous form, its presence being marked by the obtaining of Y_2O_3 in the calcined material. The samples obtained through mechano-chemical mixing using organic alkalis revealed the formation of a layered structure with the presence of $Mg(OH)_2$. Their calcination generates a solid solution of MgO-periclase type under the formula $Mg(Al^{3+}/Y^{3+})O$ that is actually a defective structure with a certain degree of cation vacancies generated by the introduction of trivalent cations in octahedral sites. The memory effect is highlighted in the case of the traditional preparation method. DRIFT spectra highlight the presence of small amounts of TMAH in the solids pores, regardless of the preparation method. It is completely removed from solids by calcination. Regardless of the preparation method or the alkalis type used, the specific surfaces areas corresponding to the reconstructed samples have drastically lower values than those of the dried materials. Mixed oxides shows



surfaces of about $200 \text{ m}^2/\text{g}$, being in accordance with the literature [2,3]. The variation of basicity keeps the trend of mixed oxides > reconstructed > dried; the preparation with TMAH generates a slight increase in its value. All catalysts yield 2,6-dibenzylidenecyclohexanone. The conversion variation remains in the same trend with the values of total basicity. There is not presence the benzoic acid, a by-product that can appear very easily due to the presence of air in the work installation.

Conclusions

The Y-modified LDH can be prepared by both co-precipitation and mechano-chemical methods. The XRD patterns prove the layered structure of dried samples contaminated with Y or Mg impurities phases. Basicity keeps the trend: mixed oxides > reconstructed > dried samples. The catalytic activity for aldol condensation shows linearity between conversion of cyclohexanone and total basicity with selectivity toward di-condensated compound of 100%.

Acknowledgements

This work was supported by a grant of the Ministry of Research, Innovation and Digitization, CNCS/CCCDI – UEFISCDI, project number PCE 235 / 2021, within PNCDI III. Also, this work was supported by a grant from the Romanian Ministry of Education and Research, CNCS–UEFISCDI, project number PNIII-P4-ID-PCE-2020-0580, within PNCDI III.

References

- [1] Wang, Q., O'Hare, D., Chemical Reviews, 112 (2012), 4124.
- [2] Pavel, O.D., Stamate, A.-E., Bacalum, E., Cojocaru, B., Zăvoianu, R., Pârvulescu, V.I., Catalysis Today, 366 (2021), 227-234.
- [3] Pavel, O.D., Zăvoianu, R., Birjega, R., Angelescu, E., Pârvulescu V.I., Applied Catalysis A, General, 542 (2017), 10-20.

New coordination compounds based on Cu(II) and 1,3-bis(4-pyridyl)propane as a divergent ligand

Petre-Cristian Mitroi, Augustin Mădălan, Delia-Laura Popescu*

University of Bucharest, Faculty of Chemistry, Department of Inorganic Chemistry, 23 Dumbraava Roşie, 020462-Bucharest, Romania

emails: petre.mitroi@s.unibuc.ro, delia.popescu@chimie.unibuc.ro

Introduction

Copper coordination polymers have attracted considerable interest as functional materials due to their structural diversities and also to their remarkable properties, including gas storage, catalysis, magnetism, luminescence, electrical conductivity, and ion exchange [1-3].

Experimental

The reagents used in the syntheses were 1,3-bis(4-pyridyl)propane (bpp), $\text{Cu}(\text{CF}_3\text{SO}_3)_2 \cdot 6\text{H}_2\text{O}$ and $\text{Cu}(\text{BF}_4)_2$ 45% aq. sol. The solvent used was methanol. All chemicals were obtained from commercial sources (Sigma-Aldrich and Alfa Aesar) and were used without further purification. The UV-Vis spectra were recorded in solid phase by the diffuse refracting technique in 200-1800 nm employing the JASCO V670 UV-Vis-NIR spectrophotometer, which uses magnesium oxide as reference, and Spectra Manager Software. The IR spectra were recorded in the 4000-400 cm^{-1} domain using MB3000 spectrophotometer with Fourier transform (FT-IR) purchased from ABB, which uses Horizon Software and KBr pills as a reference. Single crystal X-ray diffraction was performed using the Rigaku XtaLAB diffractometer Synergy S with Mo-Ka source ($\lambda = 0.71073 \text{ \AA}$) of microfocus type. Solving the structures being made through the SHELXT-2018 program and their refinement was done with the program SHELXL-2018. Graphic representations were made using Diamond, Mercury and Origin programs.

Results and discussion

New coordination polymers, $^1_\infty[\text{Cu}(\text{bpp})(\text{H}_2\text{O})_2(\text{BF}_4)_2]$ (**1**), $^1_\infty[\text{Cu}(\text{bpp})(\text{NH}_3)_2(\text{BF}_4)_2]$ (**2**), and $^1_\infty\{[\text{Cu}_2(\text{bpp})_2(\text{CF}_3\text{SO}_3)_2(\mu_2\text{-OCH}_3)_2](\text{S})\} + ^2_\infty\{[\text{Cu}_2(\text{bpp})_2(\text{CF}_3\text{SO}_3)_2(\mu_2\text{-OCH}_3)_2](\text{S})\}$ (**3**), where $\text{S} = \text{CH}_3\text{OH}$, have been obtained from reaction of Copper(II) salts with the divergent, flexible organic ligand 1,3-bis(4-pyridyl)propane (bpp), by slow evaporation method. X-ray diffraction on single crystal, as well as spectroscopic techniques (FT-IR and UV-Vis) were used to obtain the required data for characterization.

The structural diversity of the new compounds depends on the starting Cu(II) salts, conducting to 1-D and 2-D extended structures [4]. Compounds **1** and **2** are 1-D zigzag polymeric chains in which one molecule of bpp acts as bridging ligand. The chain-like structure of compound **1** is depicted in Fig. 1. Compound **3** has an interesting and not very common structure in which coexist, as parallel layers, 2-D grid-like structures with 1-D linear coordination polymers. The X-ray diffraction reveals a significant influence of the nature of counter-anions on the obtained coordination frameworks, conducting to 1-D and 2-D extended structures. Therefore, we can conclude that the structural diversity of the new compounds depends on the starting Cu(II) salts.

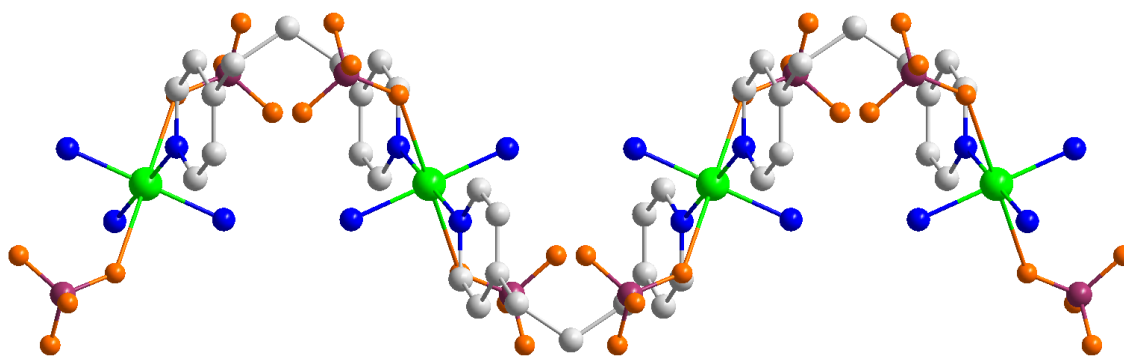


Figure 1. The 1-D structure of compound **1**, view on *a* axis (Hydrogen atoms were omitted for clarity).

Conclusions

Copper(II) coordination polymers reported here demonstrate that 1,3-bis(4-pyridyl)propane is an excellent, flexible, divergent ligand for the self-assembly of extended structures with various dimensionalities.

References

- [1] Amo-Ochoa, P., Castillo, O., Gómez-García, C.J., Hassanein, K., Verma, S., Kumar, J., Zamora, F., *Inorganic Chemistry*, 52(19) (2013), 11428-11437.
- [2] Alikani, M., Hakimi, M., Moeini, K., Eigner, V., Dusek, M., *Journal of Inorganic and Organometallic Polymers and Materials*, 30 (2020), 2907-2915.
- [3] Saghatforoush, L. A., Mehdizadeh, R., Chalabian, F., *Journal of Chemical and Pharmaceutical Research*, 3 (2011), 691-702.
- [4] Mondal, R., Basu, T., Sadhukhan, D., Chattopadhyay, T., Bhunia, M.K., *Journal of the American Chemical Society*, 9 (2009), 2015-2023.

Synthesis of barbituric acid graphene hybrids

Maria N. Psarrou*, Solon Economopoulos

Norwegian University of Science and Technology, Department of Chemistry, Norway

e-mail: maria.psarrou@ntnu.no

Introduction

The barbituric acid building block, apart from being extensively studied as a precursor for neurochemical medicine, it is a useful building block in supramolecular and coordination chemistry, having 5 metal binding sites and possessing multiple sites for hydrogen bonding [1].

Experimental

In our effort to develop graphene hybrids for photocatalysis, barbituric acid moiety was covalently attached on to exfoliated graphene. The graphene was produced *via* tip sonication-assisted liquid exfoliation, which is an effective and environmentally friendly method. The synthesis was done by one step microwave [2+1] cycloaddition of the barbituric acid on to graphene in the presence of carbon tetrabromide (CBr₄) and 1,8-diazabicycloundec7-ene (DBU) [2,3]. The resulting hybrid has good dispersibility in *e.g.*, DMSO which belongs in the group of green solvents.

Results and discussion

One of the aspects of green chemistry is to reduce the use of harmful solvents and perform reactions in milder ones. As the exfoliation of graphene is a subject of intense interest towards mass production of the material, the possibility to use DMSO and barbituric acid for the exfoliation of the graphite was investigated as an environmentally friendly alternative. The exfoliation of graphite in saturated solutions of barbituric acid in DMSO resulted in a stable dispersion (Figure 1, C) in straight contrast to pure DMSO in which the exfoliation of graphite was unsuccessful (Figure 1, B). Filtration, extensive wash with DMSO to remove the excessive barbituric acid and redispersion in DMSO resulted in non-covalent barbituric acid/graphene nanoensembles (Figure 1, D). Finally, the produced exfoliated graphene and the hybrids were characterized by Raman spectroscopy and thermogravimetric analysis (TGA).

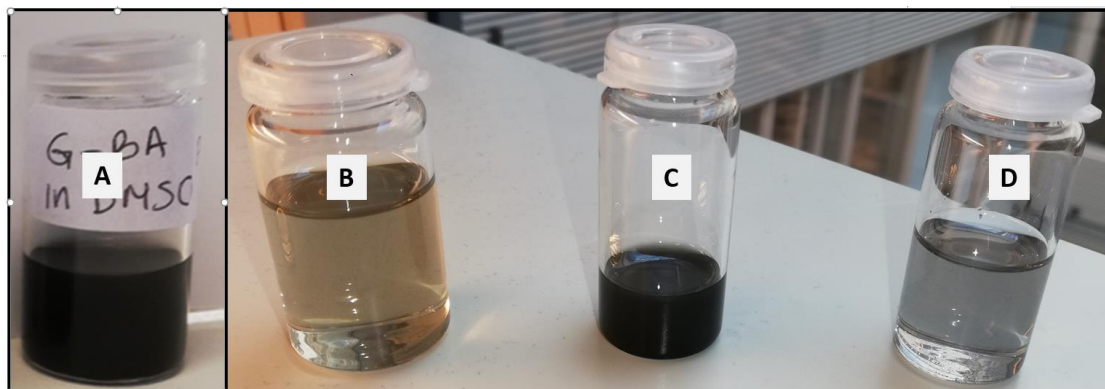


Figure 1. Dispersion of covalent barbituric acid-Gr hybrid (A), dispersion of exfoliated graphene in DMSO (B), dispersion of exfoliated graphene in DMSO/barbituric acid (C), non-covalent barbituric acid-Gr hybrid (D).

Acknowledgements

The study was financially supported internally by Department of Chemistry Norwegian University of Science and Technology.

The Research Council of Norway is acknowledged for the support to the Norwegian Micro- and Nano-Fabrication Facility, NorFab, project number 295864 and for financial support. Through the ACT programme (Accelerating CCS Technologies, Horizon2020 Project No 294766).

References

- [1] Mahmudov, K.T., Kopylovich, M.N., Maharramov, A.M., Kurbanova, M.M., Gurbanov, A.V., Pombeiro, A.J.L., *Coordination Chemistry Reviews*, 265 (2014), 1-37.
- [2] Bingel, C., *Chemische Berichte*, 126 (1993), 1957-1959.
- [3] Economopoulos, S.P., Rotas, G., Miyata, Y., Shinohara, H., Tagmatarchis, N., *ACS Nano*, 12 (2010), 7499-7507.

Imidacloprid removal using activated carbons

J. Farrando-Pérez, A. Garcia-Ripoll, E.O. Jardim, J. Silvestre-Albero*

Departamento de Química Inorgánica-Instituto Universitario de Materiales, Universidad de Alicante, Spain

e-mail: joaquin.silvestre@ua.es

Introduction

For decades, human beings have produced and used various types of chemical products both for their daily comfort and for the development of industrial activity. In recent years, water analysis have found the presence of a large number of pollutants in water, which are directly related to numerous health problems in both animals and humans [1]. One of the most prominent groups of pollutants are pesticides, which are not only harmful to living beings, but also cannot be easily and effectively eliminated from water systems [2]. Imidacloprid, a pesticide belonging to the neonicotinoid group, is mainly used for insect and pest control, both in agriculture and in parks and lawns etc [3]. Exposure to this substance in high doses can lead to degenerative changes in vital organs of the body. The main problem with imidacloprid is its ability to accumulate in nature, which makes most of the removal techniques used (advanced oxidation, photocatalytic degradation, nano-membrane filtration, ozonation etc.) unsuitable as they generate equally harmful by-products [4]. For this reason, much research has been focussed on the use of adsorption to remove the compound from water, rather than degradation. Adsorption using nanoporous materials has a number of advantages such as low cost, reasonable removal values, high surface area available and a large number of active sites for adsorption [5]. One of the most widely used adsorbents in water treatment is activated carbon. Due to the slow kinetics in liquid-phase, activated carbons have to be designed with a proper porous structure combining micropores (adsorption sites) and mesopores (diffusional channels). Based on these premises, the main goal of the present study is the evaluation of the adsorption performance of a micro/mesoporous activated carbon, RGC-30 (from Nuchar), in the removal of imidacloprid in liquid phase.

Experimental

Imidacloprid quantification was performed based on a UV-Vis spectroscopy method. A 100 ppm stock solution was prepared dissolving 0.1 g of Imidacloprid in a 1000 ml of ultrapure water. The calibration curve was developed measuring concentrations from 1 to 50 ppm using the UV-Vis Spectrophotometer. Measurements were made at a fixed wavelength (270 nm) with 3 cycles of measurements with an interval of 5 seconds between each cycle. To evaluate the adsorption process, adsorbent dosage and volume of solution studies were carried out to determine the effect of these parameters on the process. The adsorbent dosage effect was investigated by adding different amounts of RGC-30 as an adsorbent to the fixed concentration of Imidacloprid solutions (from 2.5 to 30 mg). The volume effect was investigated by adding the same amount of RGC-30 to different volumes (from 50 to 100 ml) of Imidacloprid solutions. All experiments were left under stirring until equilibrium was reached. Aliquots were taken at different times to evaluate the kinetic behaviour of RGC-30. The activated carbon reaches complete adsorption equilibrium after 48 hours.

Results and discussion

The adsorption results are displayed in Fig. 1. As it can be observed, the adsorption kinetics are very promising with more than 70% removal in less than 10 h. Interestingly, the amount of imidacloprid adsorbed does not scale with the amount of sorbent incorporated. In

general, the adsorption capacity at equilibrium (mg/g) decreases with the amount of RGC-30, except for the experiment with 2.5 mg. Most probably at low carbon dose diffusional limitations are important, thus limiting the adsorption performance. A closer look to the removal capacity shows that 30 mg are able to remove 100 % of the pesticide in less than 10 h. A much smaller amount of sorbent (5 mg) exhibits an optimum performance with close to 92% removal efficiency after 25 h and a total capacity of ca. 500 mg/g. In the case of the effect of the volume of the initial solution, the results were as expected. An increase in the concentration of pesticide molecules present in the medium causes an increase in the adsorption capacity of the adsorbent, while the performance is worse under diluted conditions.

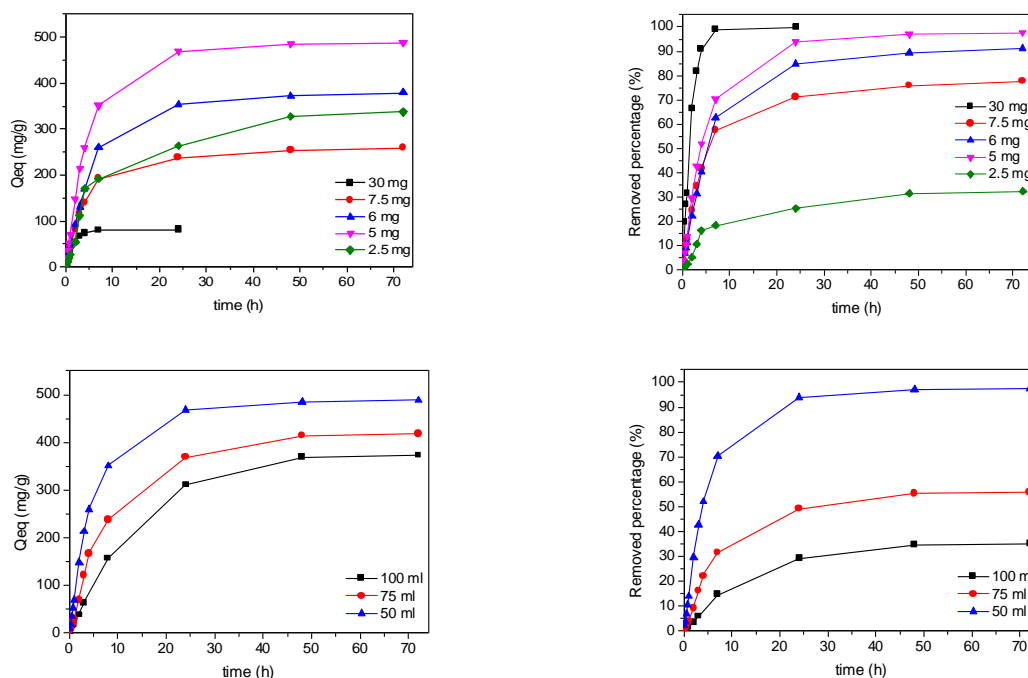


Figure 1. Effect of (a-b) amount of RGC-30 incorporated and (c-d) volume of initial solution of Imidacloprid in the adsorption performance (amount adsorbed at equilibrium – Q_{eq} , and removal percentage). Experiments are performed at 25 °C.

Conclusions

These results anticipate that an activated carbon with a properly designed porous structure combining micro and mesopores exhibits a promising performance for the removal of pesticides with high efficiency (close to 100%), excellent kinetics (less than 10 h) and a high adsorption capacity (up to 500 mg/g).

Acknowledgements

Authors acknowledge financial support from the MINECO (Projects PID2019-108453GB-C21 and PCI2020-111968/ERANET-M/3D-Photocat).

References

- [1] Yong Kim, K., Dominic Ekpe, O., Lee, H.J., Oh, J.E., *Journal of Hazardous Materials*, 400 (2020), 123235.
- [2] Nault, B.A., Taylor, A.G., Urwiler, M., Rabaey, T., Hutchison, W.D., *Crop Protection*, 23 (2004), 147-154.
- [3] Segura, C., Zaror, C., Mansilla, H.D., Mondaca, M.A., *Journal of Hazardous Materials*, 150 (2008), 679-686.
- [4] Singh, S., Kaushal, S., Kaur, J., Kaur, G., Mittal, S.K., Singh, P., *Chemosphere*, 272 (2021), 129648.
- [5] Gupta, V.K., Gupta, B., Rastogi, A., Agarwal, S., Nayak, A., *Water Research*, 45 (2011), 4047-4055.

Environmental friendly solid catalytic systems for HMF production

Magdi El Fergani^{1,*}, Natalia Candu¹, Madalina Tudorache¹, Pascal Granger², Vasile I. Parvulescu¹, Simona M. Coman¹

¹University of Bucharest, Faculty of Chemistry, Department of Organic Chemistry, Biochemistry and Catalysis, 4-12 Regina Elisabeta Av., Bucharest 030018, Romania

²Univ. Lille, CNRS, Centrale Lille, ENSCL, Univ. Artois, UMR 8181 – UCCS – Unité de Catalyse et Chimie du Solide, F-59000 Lille, France

e-mail: magdi.belkassim@drd.unibuc.ro

Introduction

It is widely acknowledged that there is a growing research efforts aiming to developed new processes based on biomass as a renewable source for production of chemicals and energy, with environmentally acceptable in the chemical industry [1]. Therefore, transformation of biomass to high-value furan compounds such as 5-hydroxymethylfurfural (HMF) has recently awakened considerable interest.

HMF platform molecule which synthesized by dehydration of monosaccharides under acidic conditions, can be converted into a bunch of useful chemicals such as 2,5-furandicarboxylic acid (FDCA), diformylfuran (DFF) and levulinic acid (LA). The demanding on the efficient HMF production has become important and full of challenges like substrates, solvents, catalyst and the reaction conditions [2,3]. In this context, the significant aims of the solid acid catalysts development have dovetail with one of the green chemistry principles, due to several advantages such as easily separated from liquid medium, recycling, highly selective, works under mild reaction conditions, non-corrosive and safer to handled compared with homogeneous ones (*e.g.* H₂SO₄) [4].

In this context we will present the one-pot conversion of glucose to HMF in biphasic systems over niobia-based catalysts with two different types of supports such as Beta-zeolites and humins (*by-products biomass treatment*).

Experimental

All the synthesis reagents were of analytic purity (Sigma-Aldrich). The two catalytic systems were prepared by following procedures: (i) The zeolite-based catalysts were synthesized through a two-step post synthesis methodology, involving a dealumination of H-Beta zeolite (different Si/Al ratios) with nitric acid followed by its impregnation with Nb ethoxide (0.02 and 0.05 mol% Nb), then calcined in static air [5]. (ii) For niobia-supported onto humins, humins prepared by heating up glucose solution with H₂SO₄ were impregnated with ammonium niobate oxalate hydrate (0.03 and 0.04 mol% Nb), then calcined in the inert atmosphere (N₂) [6].

All the synthesized catalysts were exhaustively characterized using XRD, TG-DTA, XPS, CO₂/NH₃-TPD, DLS, SEM/EDX, SSNMR and IR spectroscopy.

Results and discussion

The characterization results revealed the formation of the mesoporous Nb-Beta zeolites with residual framework Al-acid sites, extra-framework isolated Nb(V) and Nb₂O₅ pore-encapsulated clusters in which Nb(V)O-H (DRIFT and XPS analysis) exhibit moderate strength Brønsted acidity. In the case of Nb-humins catalysts the characterizations shows that for the same concentration of surface niobium (*i.e.* 2.4 at% from XPS analysis) deposited on, a relatively more homogeneous distribution (SEM analysis) as –Nb-OH and Nb=O species (DRIFT analysis) leads to an efficient catalyst, while the agglomeration in relatively rich areas determines an appreciable decrease of the HMF yield. Also, the relative base/acid sites

ratio (CO₂/NH₃-TPD) is influenced by the distribution of niobium, the formation of Nb-rich particles corresponding to an increased ratio.

Catalytic tests showed that the differences in the yield of HMF highly depend on both the location of the catalyst and the intrinsic catalytic features: (i) the dehydration of glucose onto the Nb/Beta-zeolites occurred with a selectivity of 84.3% in HMF for a glucose conversion of 97.4%. This result has been obtained in a biphasic (3.5 ml H₂O [(NaCl 20%)]/1.5 ml MIBK) solvents at 180 °C, after 12 h. (ii) the GHNb1.2 catalyst exhibited excellent catalytic ability and efficiency for dehydration of glucose to HMF with a 96% yield, under the following reaction conditions: 3.5 ml H₂O [(NaCl 20%)]/1.5 ml TBP at 180 °C, for 8h.

Conclusions

Obtained results show that humins (by-products of renewable biomass-based technologies), may offer valuable solutions for the production of functional materials with catalytic application. The preparation procedure induced structural modifications of the humins carrier with the formation of a highly hydrophobic graphite-like carbon structure and acid-base functionalities, on which niobium is dispersed on. These structural features are responsible for the high yields to HMF. Moreover, zeolites, some of the most widely used catalysts in petrochemicals, can be modified in such a way as to become efficient catalysts for biorefinery. In this case, the residual framework Al-acid sites prevent the solubilization of the zeolite framework in hot water, while their improved acidity and the mesoporous texture generates an efficient environment for the dehydration of glucose to HMF.

Acknowledgements

Simona M. Coman kindly acknowledges UEFISCDI for the financial support (project PN-III-P4-ID-PCE-2016-0533, Nr. 116/2017). Magdi El Fergani kindly acknowledges ERASMUS and the PICS “Nanocat” N°230460 for supporting and partially funding this work.

References

- [1] Sudarsanam, P., Zhong, R., Bosch, S. V. d., Coman, S. M., Parvulescu, V. I., Sels, B.F., *Chemical Society Reviews*, 47 (2018), 8349-8402.
- [2] Hu, D., Zhang, M., Xu, H., Wang, Y., Yan, K., *Renewable and Sustainable Energy Reviews*, 147 (2021), 111253.
- [3] Lai, F., Yan, F., Wang, P., Li, C., Shen, X., Zhang, Z., *Journal of Cleaner Production*, 316 (2021), 128243.
- [4] Mustansar, C. H., Sudarsanam P., (Eds.), *Advanced Functional Solid Catalysts for Biomass Valorization*, Elsevier, 2020, Ch. 2–5.
- [5] Fergani, M.E., Candu, N., Tudorache, M., Bucur, C., Djelal, N., Granger, P., Coman, S. M., *Applied Catalysis A: General*, 618 (2021), 118130.
- [6] Candu, N., Fergani, M. E., Verziu, M., Cojocaru, B., Jurca B., Apostol, N., Teodorescu, C., Parvulescu, V.I., Coman, S.M., *Catalysis Today*, 325 (2019), 109-116.

OF SYSTEMS

Catalin Mirica*, Sales director

OF Systems SRL

e-mail: catalin.mirica@yahoo.com

O F Systems is Romanian private company, whose main activity is the supply of laboratory equipment, process equipment, industrial scales and product inspection.

Ever since the company was founded in 1992 O F Systems has been and has remained strictly customer oriented and needs.

O F Systems is the place where any specialist can find reliable information, the company providing not only laboratory equipment but also good ideas, practical solutions rather than theoretical approaches service and know how based on the experience of his team.

O F Systems delivers complete, integrated solutions for professionals to enhance their performance and competitiveness, from designing the laboratory to the smallest detail to warranty and post warranty services.

Over the years O F Systems added to the honorable partnership with METTLER TOLEDO (the company is the sole representative, for almost 30 years, of METTLER TOLEDO in Romania) successful collaborations with leading manufacturers, representative of the market Büchi, Sotax, Thermo Scientific, Binder, Elga Veolia, Parr, ERLAB, Integra, Novasina, etc

We offer high-end products in order to help our customers to streamline processes, enhance productivity, reach compliance with regulatory requirements and optimize cost.



Synthesis and Characterization of Several New 1-D, 2-D, and 3-D Coordination Polymers

Traian-Dinu Pasatoiu^{1,*}, Radu Cristian Dascalu², Catalin Maxim¹, Augustin Madalan¹, Marius Andruh^{1,*}

¹University of Bucharest, Faculty of Chemistry, Department of Inorganic Chemistry, 23 Dumbrova Roşie, 020464-Bucharest, Romania

²National Institute for Research and Development in Electrical Engineering ICPE-CA, Splaiul Unirii 313, Bucharest, 030138, Romania

e-mail: traiandp@yahoo.com

Introduction

The progress of a technology-driven society, such as ours, requires the development of materials with enhanced capabilities and new properties. Among the alternatives, coordination polymers are one interesting candidate. The design and synthesis of porous coordination polymers is often based on the *node and spacer* approach proposed by Robson [1].

Experimental

We herein describe new coordination polymers obtained starting from Cu^{II} or Zn^{II} salts, mandelic acid and its derivatives, and various exobidentate ligands with nitrogen donor atoms (4,4'-bipyridine, 1,2-bis(4-pyridyl)ethane, 1,2-bis(4-pyridyl)ethylene, or 4,4'-azopyridine) or hexamethylenetetraamine. All reactions were performed at room temperature and single-crystals suitable for X-Ray diffraction have been collected after several days.

Results and discussion

Depending on the reaction conditions and spacer used, different 1-D, 2-D, or 3-D coordination polymers have been obtained. All of them have been structurally characterized through single crystal and powder X-Ray diffraction, UV-VIS and IR spectroscopy. The thermal stability of some of the new coordination polymers has also been investigated. In case of the 3-D coordination polymers, one of which is the MOF illustrated in Figure 1, the solid-state architecture proved to be quite robust.

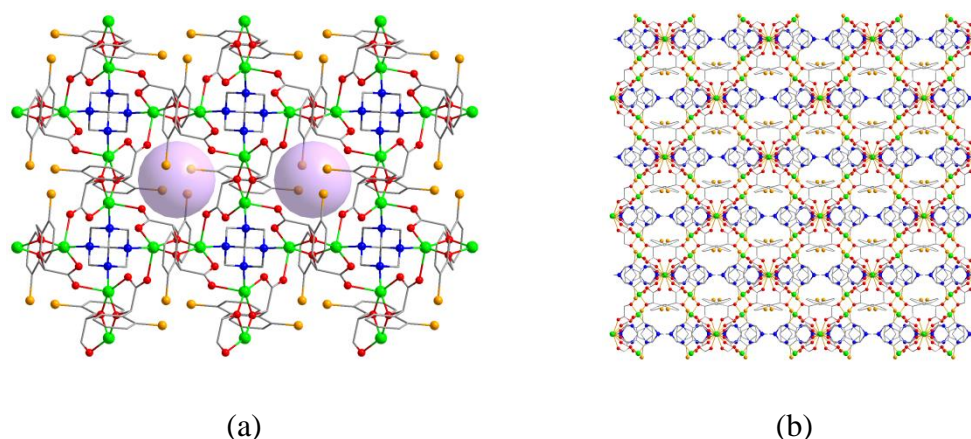


Figure 1. Voids in the solid-state structure of $\infty[\text{Cu}_2(2\text{-Cl-mand})_2(\text{hmt})]$
(2) View along the crystallographic *c* axis; (b) View along the crystallographic *a* axis.

Conclusions

The *node* and *spacer* approach proved to be still an efficient method for the synthesis of coordination polymers. However, it has been observed that slight changes in the experimental conditions can lead to different dimensionalities of the final solid-state structure. When 3-*D* structures are obtained, the solid-state architectures are quite robust which makes them good candidates for gas storage, separation, catalysis, or biomimetic design.

Acknowledgements

Financial support from PN-III-P1-1.1-TE-2019-1534 research grant is gratefully acknowledged.

References

[1] Hoskins, B.F., Robson, R., *Journal of the American Chemical Society*, 112 (1990), 1546-1154.

Synthesis, Characterization, and Bioactivity of New Oxidovanadium(V) Compounds based on Salicylaldehyde-derivatives Schiff Bases

Oana Petcuță^{1,*}, Mihai Bordeiașu¹, Mihaela Turtoi², Augustin M. Mădălan¹, Cătălin Maxim¹, Delia-Laura Popescu^{1,*}

¹University of Bucharest, Faculty of Chemistry, Department of Inorganic Chemistry, 23 Dumbrova Roșie, 020464-Bucharest, Romania

²Institute of Cellular Biology and Pathology "Nicolae Simionescu" of the Romanian Academy, 8 B.P. Hasdeu Street, 050568-Bucharest, Romania

e-mails: adipetcuta@yahoo.com, delia.popescu@chimie.unibuc.ro

Introduction

Vanadium is a trace element, which may be beneficial and possibly essential in humans, but it is certainly essential for some living organisms. With its unique features, vanadium(V) receives a great deal of attention from chemists, biologists, biochemists, toxicologists, and pharmacologists. Studies carried out so far have demonstrated an essential role of this element in the metabolism of carbohydrates (through the effects on the glycolysis, glycogenolysis, glycogenogenesis, and gluconeogenesis pathways), lipids (by stimulation of lipogenesis and inhibition of lipolysis), phospholipids, and cholesterol. Vanadium salts and well-known vanadium coordination compounds have shown antibacterial, antifungal, antitumor, and antidiabetic activities when investigated by various biological methods [1-3].

Experimental

The reagents used in the synthesis of the new oxidovanadium compounds were: L-/D-/L,D-valine (2-amino-3-methylbutanoic acid), sodium hydroxide (NaOH), vanadyl sulfate ($\text{VOSO}_4 \cdot 3\text{H}_2\text{O}$), and 5-X-salicylaldehyde (X = H, Cl, Br, I), and they were all purchased from Sigma-Aldrich. All manipulations were carried out with no special solvent and reagent purification. Elemental analysis was performed on a EuroEA Elemental Analyser (soft Callidus™) system. The electronic spectra of the complexes were determined by UV-Vis spectroscopy with a Jasco V580 spectrophotometer. The infrared spectra were recorded in KBr pellets, at room temperature, by using the FT-IR Bruker Tensor-V-37 spectrometer. Data processing was done with OPUS program. The circular dichroism (CD) spectra of vanadium complexes were measured on a Jasco J-1500 spectrophotometer. X-ray diffraction measurements were performed on a STOE IPDS II diffractometer and SHELX-2013 crystallographic software package was employed for calculations. The cytotoxicity of tested compounds was assessed by the XTT cell viability assay.

Results and discussion

Reaction between $\text{VOSO}_4 \cdot 3\text{H}_2\text{O}$ and the ONO donor Schiff base H_2L , where L is X-sal-val, with X = H, Cl, Br, or I, a series of Schiff bases obtained by condensation of 5-X-salicylaldehyde and L-/D-/L,D-valine, respectively, resulted, upon their aerial oxidation in methanol, in the formation of a family of new coordination compounds with the general molecular formula $(S/R/rac)-[(\text{V}^{\text{V}}\text{O})(\text{X-sal-val})(\text{CH}_3\text{O})(\text{CH}_3\text{OH})]$. All compounds are characterized in the solid state and in solution, by elemental analysis, spectroscopic techniques (IR, UV-Vis, circular dichroism), single crystal and powder X-ray diffraction analysis, as well as a set of biological activity tests. The structures of oxidovanadium(V) complexes containing the Schiff base Cl-sal-val and octahedral coordinated vanadium centers are shown in Fig. 1.

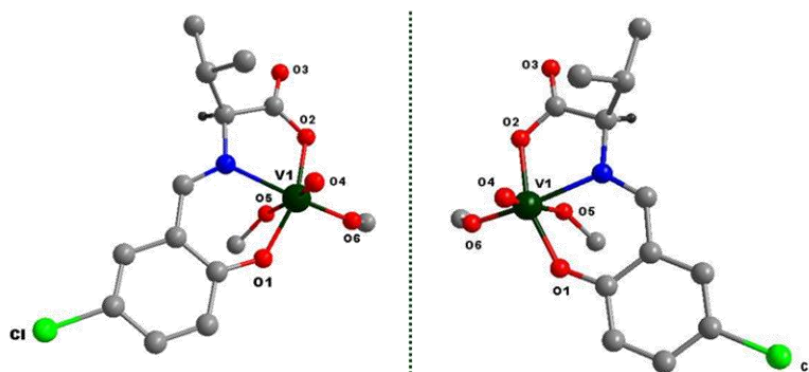


Figure 1. Crystal structures of (S/R) - $[(VO)(Cl\text{-}sal\text{-}val)(CH_3O)(CH_3OH)]$.

Conclusions

In the present study, we have synthesized a new family of compounds by condensation of 2-hydroxybenzaldehyde (salicylaldehyde, sal) and its 5-chloro-, 5-bromo-, and 5-iodo- derivatives with L-valine, D-valine, or D,L- valine, respectively, followed by coordination with $VOSO_4 \cdot 3H_2O$. All obtained compounds have been characterized by elemental analysis, single-crystal and powder X-ray diffraction, IR and UV-Vis spectroscopies, as well as circular dichroism measurements. The biological activity of these new synthesized compounds is investigated; some preliminary results will be discussed. We hope this work would provide new insight for potential applications of vanadium complexes as antimicrobial, antidiabetic, antineoplastic, antibacterial and antifungal materials.

References

- [1] Crans, D.C., Smee, J.J., Gaidamauskas, E., Yang, L., *Chemical Reviews*, 104 (2004), 849-902.
- [2] Sakurai, H., Katoh, A., Yoshikawa, Y., *Bulletin of the Chemical Society of Japan*, 79 (2006), 1645-1664.
- [3] Ścibior, A., Pietrzyk, Ł., Plewa, Z., Skiba, A., *Journal of Trace Elements in Medicine and Biology*, 61 (2020), 126508-126533.

Enzymatic degradation of PET

Andreea-Iuliana Ftodiev*

University of Bucharest, Faculty of Chemistry, 4-12 Regina Elisabeta Av., 030018, Bucharest, Romania

e-mail: andreea.ftodiev1@gmail.com

Introduction

Due to the fact that PET is almost impossible to degradate and has such a negative impact on the environment, new methods for PET recycling are constantly being search. In order to improve the degradation process and to prevent the release of microplastics in the natural environment, it is important to understand the degradation process [1].

Experimental

BHET hydrolysis

BHET was used for optimizing the system for future use in PET degradation. An attempt was made to build reaction systems based on different types of DES. Six types of DES were created starting from the solubility of BHET in different solvents. The system of BHET and DES was completed by adding free (lipase from *Aspergillus niger*) and immobilized enzymes (Lypozime RMIM, Lypozime TLIM, Novozyme 425 and Transenzyme) as catalysts.

PET degradation

PET from four different sources and with different durity was used in the experimental processes: ST (PET from a bottle of juice), TA (PET from a packing tray), CU (PET from an ice cream box) and CF (PET from a bottle of Cif). The PET was cut into pieces of around 0.5 cm x 0.5 cm. The catalyst used in the degradation of PET was the enzyme *Aspergillus niger*. After the reaction, the PET pieces were washed with distilled water and then weighed. Their final weight was compared with their initial weight.

Results and discussion

BHET hydrolysis

After the HPLC analysis, the conversion for each type of DES and each type of enzyme was calculated. Graphics were made to see which type of DES is the best system for each enzyme. As a general remarks analysing the graphics, the best systems are: DES 1, 3 and 5 with Transenzyme, DES 6 with Lypozime TLIM, DES 5 with Novozyme 425 and DES 5 and 6 with Lypozime RMIM.

PET degradation

It can be observed that first and third method have the biggest sums of relative areas, so the degradation went better in these conditions. Although the second method had an error (the liquid phase of the CF reaction evaporated), it can be considered a valid method.

CoSolMat

	Method 1				Method 2			
	ST	TA	CU	CF	ST	TA	CU	CF
Before reaction (mg)	0.0122	0.0159	0.0197	0.0420	0.0220	0.0216	0.0276	0.0326
After reaction (mg)	0.0130	0.0163	0.0194	0.0418	0.0240	0.0216	0.0272	0.0328
Difference (mg)	+0.8	+0.4	-0.3	-0.2	+2	0	-0.4	+0.2

	Method 3				Method 4			
	ST	TA	CU	CF	ST	TA	CU	CF
Before reaction (mg)	0.0106	0.0163	0.0197	0.0321	0.0218	0.0197	0.0284	0.0369
After reaction (mg)	0.0112	0.0170	0.0194	0.0320	0.0220	0.0201	0.0283	0.0373
Difference (mg)	+0.6	+0.7	-0.3	-0.1	+0.2	+0.4	-0.1	+0.4

Method 5											
Simple				Distilled water				Hydrogen peroxide			
ST	TA	CU	CF	ST	TA	CU	CF	ST	TA	CU	CF
0.0186	0.0193	0.0256	0.0429	0.0286	0.0148	0.0262	0.0553	0.0259	0.0213	0.0260	0.0498
0.0196	0.0193	0.0255	0.0430	0.0305	0.0159	0.0260	0.0555	0.0275	0.0216	0.0260	0.0498
+1	0	-0.1	+0.1	+1.9	+1.1	-0.2	0	+1.6	+0.3	0	0

Pretreatment method 1, 2 and 3 allowed achieving the most degraded PET surface. Positive difference between masses could be the effect of DMC attached on the PET surface (carboxy methylation).

Conclusions

The study will be continued on both directions: BHET system in DES will be optimized and adapted for PET degradation. Also, sample pretreatment of the PET will be coupled to the degradation system in order to improve the accessibility of the enzyme on the PET surface for a better PET degradation.

References

[1] Sang, T., Wallis, C.J., Hill, G., Britovsek, J.P.G., European Polymer Journal, 136 (2020), 109873.

Crystalline Cu(II)-based coordination polymers with Kagomé architecture

Mihai Bordeiasu^{1,*}, Yangyang Sun², Mihai Răducă¹, Augustin M. Mădălan¹, Christoph Janiak², Delia-Laura Popescu^{1,*}

¹University of Bucharest, Faculty of Chemistry, Department of Inorganic Chemistry, 23 Dumbrova Roşie, 020464-Bucharest, Romania

²Heinrich-Heine-Universität, Institut für nanoporöse und nanoskalierte Materialien, Universitätsstr. 1, D-40225 Düsseldorf, Germany

e-mails: bordeiasu.mihai@yahoo.com, delia.popescu@chimie.unibuc.ro

Introduction

Porous coordination polymers (PCPs) are a class of materials formed by self-assembly of metal ions or clusters and different types of ditopic organic ligands [1]. Due to their structural properties, namely high regularity, tunable pore sizes, and adjustable internal surfaces, PCPs are used in various application areas: heterogeneous catalysis, magnetism, sensor technology, biomedical application and adsorption, separation and storage of gases [2,3]. Emphasizing the storage application, PCPs can be used as a sequestration method for greenhouse gases. CO₂, for example, is the most abundant greenhouse gas and can be stored within the framework of a PCP via chemical fixation, as well as physical adsorption [4,5].

Experimental

The employed reagents were: 1,2-bis(4-pyridyl)ethane (bpe), 1,2-bis(4-pyridyl)ethylene (bpy), 4,4'-azopyridine (azopy), Copper(II) tetrafluoroborate hexahydrate (Cu(BF₄)₂·6H₂O), Copper(II) perchlorate hexahydrate (Cu(ClO₄)₂·6H₂O), and aqueous ammonia solution (25% NH_{3(aq)}). All reagents were procured from Sigma-Aldrich and used without any further purification. X-ray diffraction measurements were carried out using a Rigaku XtaLAB Synergy-S diffractometer and calculations were performed using ShelX crystallographic software for single crystal determinations and a Proto AXRD Benchtop for powder determinations. PXRD data before and after the nitrogen physisorption isotherms were collected on Rigaku Miniflex 600 powder diffractometer. The infrared spectra were recorded by a Fourier Transformer Tensor 27 Spectrometer (FT-IR) using OPUS software. The UV-Vis spectra were recorded in solid state with a JASCO V-670 spectrophotometer. Thermogravimetric analysis (TGA) was performed on a Netzsch TG209 F3 Tarsus device under nitrogen conditions. The nitrogen physisorption isotherms were carried out at 77 K using a Quantachrome Autosorb 6 instrument within a partial pressure range of $p/p_0 = 10^{-3}$ –1 bar.

Results and discussion

Three-dimensional Cu(II)-based PCPs were obtained using a modified Solvay process in which NH_{3(aq)} is added to a suspension formed by the reaction between the Cu(II) salts and the exo-bidentate bipyridine-based ligands (bpe, bpy, azopy). The X-ray diffraction revealed that all compounds are isostructural, having the general formula $\{[\text{Cu}_3(\text{CO}_3)_2(\text{L})_3](\text{Y})_2\}_n$, where L = bipyridine-based ligand and Y = ClO₄⁻ or BF₄⁻ anions. The structure of the obtained compounds is presented in Figure 1. Two dimensional inorganic Cu(CO₃) layers with Kagomé arrangement are formed, in the basic ammonia solution, by direct fixation of atmospheric CO₂ as carbonate anion and are linked one to another via the organic pillars represented by bipyridine-based ligands, forming a cationic framework. Disordered counter anions are found along the channels and neutralize the charge excess. Thermogravimetric analysis revealed that all compounds have a thermal stability of approximately 300 °C.

Nitrogen adsorption isotherms have been recorded for all obtained compounds and showed that their porosity is not high, as expected for this type of materials.

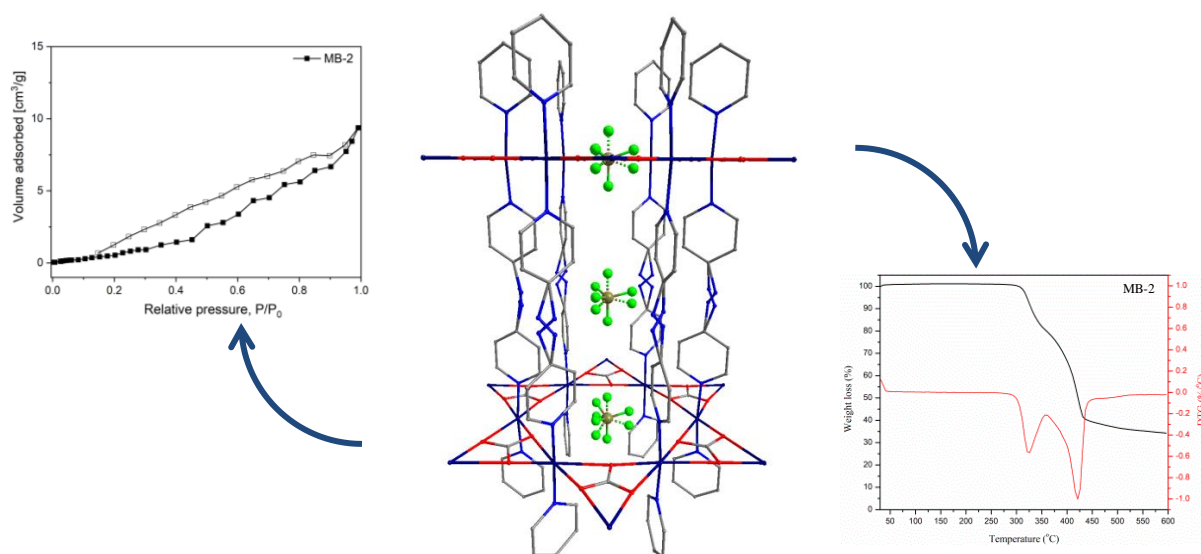


Figure 1. Crystal structure of $\{[Cu_3(CO_3)_2(L)_3](Y)_2\}_n$, hydrogen atoms omitted for clarity. TGA and N_2 adsorption isotherm of compound **2**.

Conclusions

Six isostructural Cu(II)-based PCPs with hybrid organic-inorganic structures were obtained following the chemical fixation of atmospheric CO_2 . The additional physical adsorption of CO_2 requires certain modifications of the obtained structure to increase the uptake, as a large part of the space along the hexagonal channels is occupied by counter anions.

Acknowledgements

This work was carried out as part of The Education, Scholarship, Apprenticeships and Youth Entrepreneurship Programmer—EEA Grants 2014-2021, Project No. 18-Cop-0041, project title: “Cooperation and partnership strategy for the enhancement of the education quality of strategic master Chemistry of Advanced Materials in line with Green Chemistry requirements – Green Chemistry of Advanced Materials“, acronym GREENCAM.

References

- [1] Zhou, H.-C., Long, J.R., Yaghi, O.M., *Chemical Reviews*, 112 (2012), 673-674.
- [2] Bon, V., Senkovska, I., Kaskel, S., Chapter 6: Metal-Organic Frameworks in Nanoporous Materials for Gas Storage, *Green Energy and Technology*, Ed. Springer, Singapore, 2019, pp. 137-172.
- [3] Janiak, C., Vieth, J.K., *New Journal of Chemistry*, 34 (2010), 2366-2388.
- [4] Keene, T.D., Murphy, M.J., Price, J.R., Sciortino, N.F., Southon, P.D., Kepert, C.J., *Dalton Transactions*, 43 (2014), 14766-14771.
- [5] De, D., Pal, T.K., Neogi, S., Senthilkumar, S., Das, D., Gupta, S.S., Bharadwaj, P.K., *Chemistry – A European Journal*, 22 (2016), 3387-3396.

Hydrothermal Synthesis of Equimolar Multicomponent Rare Earth Oxides

Simona Elena Bejan⁺, Cristina Florentina Ciobota⁺, Ioan Albert Tudor, Cristian Bogdanescu, Laura Madalina Cursaru, Roxana Mioara Piticescu, Radu Robert Piticescu*

National Research & Development Institute for Non-Ferrous and Rare Metals (INCDMNR-IMNR), Laboratories of Advanced and Nanostructured Materials, 102 Biruintei Blvd., Pantelimon, Ilfov, 077145, Romania

⁺ authors have equal contributed

e-mail: rpiticescu@imnr.ro

Introduction

For the first time, Rost et al [1] synthesized by solid state synthesis, a 5 equiatomic components single phase oxide ($\text{Mg}_{0.2}\text{Co}_{0.2}\text{Ni}_{0.2}\text{Cu}_{0.2}\text{Zn}_{0.2}\text{O}$) presenting rock salt structure. Berardan et al. [2] proposed the name of high entropy oxides (HEO's) analogous to high entropy alloys (HEA). The present work shows the results obtained by soft chemical synthesis of a new type of oxide (REO) nanocrystalline powder, containing 5 equiatomic rare earth elements ($(\text{La}_{0.2}\text{Sm}_{0.2}\text{Gd}_{0.2}\text{Yb}_{0.2}\text{Nd}_{0.2})\text{O}$).

Experimental

This powder was prepared in hydrothermal conditions, at high temperature and low pressure followed by a calcination at 1200 °C. X-ray diffraction identified the composition of the as obtained REO before and after calcination. It was observed that after heat treatment, a single phase $\beta\text{-Sm}_2\text{O}_3$ -type structure was successfully obtained. DSC/TG analysis was used to highlight the thermal stability of the powder in the range of 25-1200 °C after 4 cycles. Chemical composition was studied by ICP-OES and FT-IR analysis.

Results and discussion

It could be proved that the near-equiatomic rare earth powder was obtained, and that the peaks corresponding to OH groups (related to hydrothermal process) disappear after heat treatment. This fact also was proven by DSC/TG analysis. Measurements for thermal conductivity, thermal diffusivity and volumetric heat capacity were performed on pressed and 1200 °C sintered pellets. For the same type of pellets, impedance measurements in the range of 1kHz -100kHz, for 600 and 800 °C highlight a major change of the electrical behavior corresponding to temperature increase.

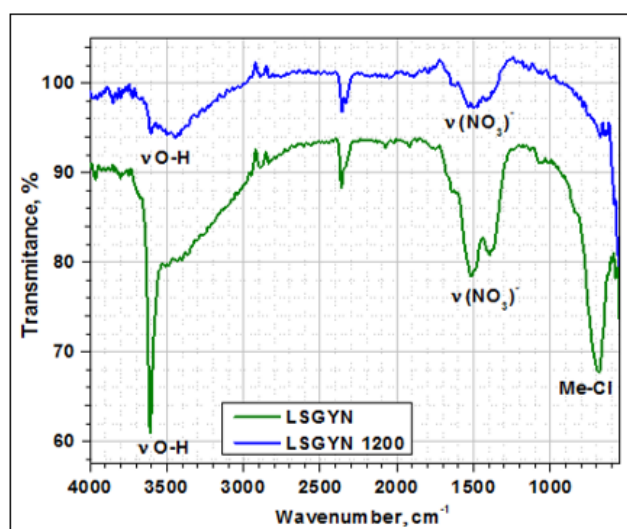


Figure 1. FT-IR spectra of LSGYN and LSGYN 1200.

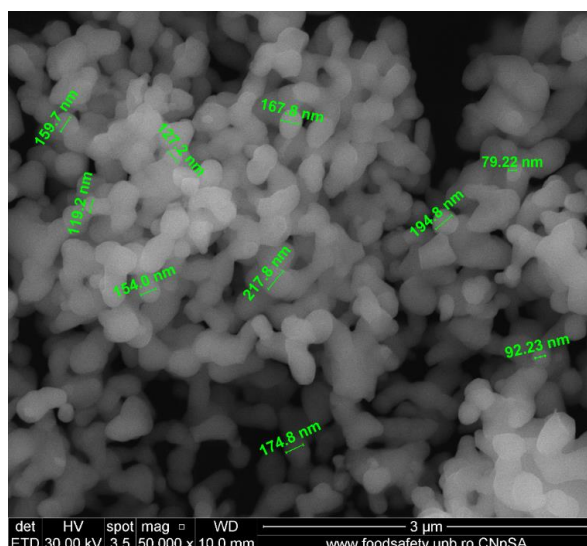


Figure 2. Scanning Electron Microscopy for LSGYN 1200.

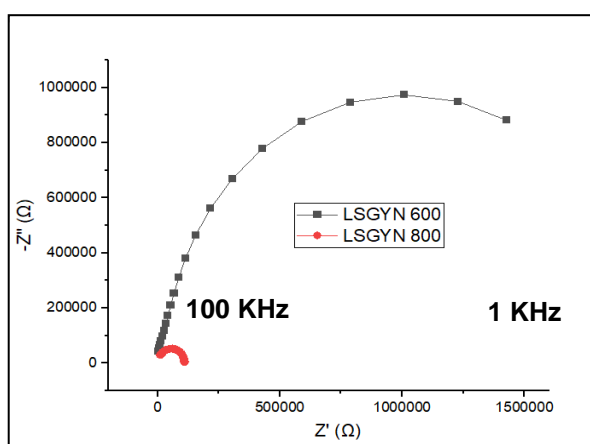


Figure 2. Nyquist plots for LSGYN at 600 °C and 800 °C.

Acknowledgements

The authors would like to thank to University Politechnica of Bucharest, dr. ing. Bogdan Vasile for Electron Microscopy and EDS analysis.

This work was supported by a grant from the Ministry of Research and Innovation, Program Nucleu, contract no. 6N/2019 (Project code PN 19 19 02 01/2019).

References

- [1] Rost, C., Sachet, E., Borman, T. Moballegh, A., Dickey, E.C., Hou, D., Jones, J.L., Curtarolo, S., Maria, J.-P., Nature Communications, 6 (2015), 8485.
- [2] Bérardan D., Franger S., Dragoie D., Kumar Meena A., Dragoie N., Physica Status Solidi (RRL), 10 (2016), 328-333.

New highly effective transition-metal-containing MgFe mixed oxides catalysts for benzyl alcohol hydrodeoxygenation

Alexandru-Tudor Toderasc¹, Adriana Urdă^{1,*}, Irina Atkinson², Daniela Culiță², Florica Papa², Gabriel Crăciun³, Ioan-Cezar Marcu¹

¹Laboratory of Chemical Technology and Catalysis, Department of Organic Chemistry, Biochemistry and Catalysis, Faculty of Chemistry, University of Bucharest, 4-12, Blvd. Regina Elisabeta, 030018 Bucharest, Romania

²“Ilie Murgulescu” Institute of Physical Chemistry, Romanian Academy, 202 Splaiul Independentei, 060021, Bucharest, Romania

³National Institute for Research and Development in Microtechnology – IMT Bucharest, 126A Erou Iancu Nicolae Street, 077190, Voluntari, Romania

e-mail: adriana.urda@chimie.unibuc.ro

Introduction

Nowadays, hydrodeoxygenation (HDO) is employed for converting oxygenated compounds into hydrocarbons through treatment at moderate temperatures and pressures by means of C-O bond scission [1]. Copper-containing mixed metal oxides seem to be interesting catalysts for this kind of reactions due to their significant hydrogenolysis activity and limited propensity for complete hydrogenation of aromatic substrates [2]. These materials can provide a cheaper, efficient alternative to noble metal catalysts or to typical sulphided hydrotreatment catalysts commonly used for converting biomass into biodiesel [3]. In this work, several transition-metal-containing M-MgFeO mixed oxides, with M = Cu, Ni, Co, Ag or Ce, were prepared, characterized and tested in the HDO reaction of benzyl alcohol.

Experimental

The layered double hydroxides (LDH) precursors, with Mg/Fe = 3 and 10 at. % M or, for M = Cu from 2.5 to 20 at. %, were prepared through coprecipitation at a constant pH of 10 using Mg, Fe and M nitrates as starting materials. The synthesized LDH were dried and then calcined at 500 °C for 5 h. The LDH precursors and the mixed oxides were characterized by XRD, N₂ adsorption-desorption, H₂-TPR, CO₂-TPD and SEM-EDX techniques. The obtained mixed oxides were tested in the HDO reaction in an autoclave reactor at 230 °C, under 5 atm of H₂ for 3 hours, with 1 ml of benzyl alcohol and 50 mg catalyst. For the Cu-containing catalysts, the influence of Cu loading (2.5 – 20%), reaction temperature (150-230 °C), reaction time (15 min – 5 h) and catalyst weight (25 – 100 mg) were also investigated. Catalytic tests were also performed with benzaldehyde, benzyl benzoate and toluene substrates in order to propose a reaction pathway for the HDO of benzyl alcohol.

Results and discussion

The XRD patterns of the LDH precursors showed typical reflections for the LDH structure, with similar crystallite sizes of 6.1-7.1 nm. No segregated phases were detected, except for the sample with 20% Cu. After calcination, the mixed oxides showed, besides the periclase phase, the presence of MgFe₂O₄. The samples with 20% Cu and 10% Ag additionally showed diffraction lines for CuO and metallic Ag, respectively. All mixed oxides presented high specific surface areas (97-185 m²/g) and mesoporous structures, with relatively narrow distributions for the mesopores. Cu-modified samples showed the highest hydrogen consumption in H₂-TPR measurements, in strong correlation with the catalytic results.

Their catalytic performance strongly depended on both the nature and the content of transition metal. Among them, Cu-MgFeO with 10 at.% Cu gave the best results, with 93,8%

alcohol conversion and 93,8% selectivity for toluene. The Ag-MgFeO sample reached 62% conversion, but with only 61% selectivity for toluene, while Co, Ni and Ce-modified samples showed poor results (less than 30 % conversion). Considering the excellent performance of the copper-containing catalyst, the influence of the copper content of the mixed oxides was then studied by preparing a series of Cu_x-MgFeO catalysts, where x = 2,5; 5; 7,5; 15 and 20 at.%. The sample with 10 at.% Cu still showed the best results, and the influence of reaction temperature, reaction time, catalyst weight were studied on this catalyst. Benzaldehyde and benzyl benzoate were considered reaction intermediates, and catalytic tests using them as reactants confirmed this hypothesis. Based on the products observed, a reaction pathway has been proposed.

Acknowledgements

Dr. Bogdan Cojocaru is kindly acknowledged for providing the XRD analyses of some of the materials.

References

- [1] Rizescu, C., Sun, C., Popescu, I., Urdă, A., Da Costa, P., Marcu, I-C., *Catalysis Today*, 366 (2021), 235-244.
- [2] Deutsch, K.L., Shanks, B.H., *Applied Catalysis A: General*, 447-448 (2012), 144-150.
- [3] Yakovlev, V.A., Khromova, S.A., Sherstyuk, O.V., Dundich, V.O., Ermakov, D.Yu., Novopashina, V.M., Lebedev, M.Yu., Bulavchenko, O., Parmon, V.N., *Catalysis Today*, 144 (2009), 362-366.

Novel coordination polymers of Co(II) with 4,4'-oxy(bis)benzoic acid and auxiliary N,N'-donor ligands

Voinea Denisa, Cătălin Maxim, Delia-Laura Popescu*

University of Bucharest, Faculty of Chemistry, Department of Inorganic Chemistry, 23 Dumbraava Roşie, 020464-Bucharest, Romania

emails: denisa.voinea@s.unibuc.ro, delia.popescu@chimie.unibuc.ro

Introduction

Cobalt(II) coordination polymers have lured the attention of many researchers worldwide due to an unlimited diversity of their structural types, architectures, topologies, as well as important properties and applications of these functional solids [1-3].

Experimental

The starting reagents used in the syntheses: 4,4'-oxy(bis)benzoic acid (obb), 4,4'-bipyridine (bipy), 1,2-di(4-pyridyl) ethylene (bpe), and cobalt perchlorate hexahydrate, $\text{Co}(\text{ClO}_4)_2 \cdot 6\text{H}_2\text{O}$, are all commercially available and purchased from Sigma-Aldrich. They were of reagent grade and used as received. All the synthetic operations were carried out at room temperature, under air atmosphere. The synthesized compounds were characterized by elemental analysis, single crystal and powder X-ray diffraction, as well as IR spectroscopy and solid-state diffuse-reflectance UV-Vis. The elemental analysis was performed using the Euro EA Elemental Analyzer (Euro Vector) and Callidus software. Molecular structures were determined by single-crystal X-ray diffraction with a STOE IPDS II diffractometer using the SHELX-97 and Diamond 3 softwares for calculations and graphical representations. A XRD Benchtop Powder Diffraction system was used to acquire the powder diffraction data, which were processed with NIST software. IR spectra were recorded on a Bruker Fourier Transformance Tensor V-37 spectrophotometer, using OPUS software. Solid-state electronic spectra were recorded using the UV-Vis-NIR Jasco V670 spectrophotometer, equipped with Spectra Manager software.

Results and discussion

Systematic studies of the self-assembly process between the Cobalt(II) salt, $\text{Co}(\text{ClO}_4)_2 \cdot 6\text{H}_2\text{O}$, 4,4'-oxy(bis)benzoic acid (oba) ligand, and the auxiliary N,N'-donor building block 1,2-bis(4-pyridyl)ethylene (bpe), have been carried out in order to investigate the influence of the mixed ligands and their molar ratio on the properties and construction of coordination frameworks. Three new coordination polymers, two tridimensionals $^3_\infty\{[\text{Co}(\text{oba})(\text{bpe})(\text{H}_2\text{O})_2] \cdot (\text{H}_2\text{O})_4\}$ (**1**), $^3_\infty\{[\text{Co}_2(\text{oba})_2(\text{bpe})_2]\text{H}_2\text{O}\}$ (**2**), and a cocrystal of two monidimensional polymers, $^1_\infty[\text{Co}_2(\text{oba})_2(\text{bpe})_{2.5}(\text{H}_2\text{O})_5] \cdot ^1_\infty[\text{Co}_2(\text{oba})_2(\text{bpe})_3(\text{H}_2\text{O})_4](\text{bpe}) \cdot x\text{H}_2\text{O}$ (**3**), were successfully obtained by slow evaporation method. The crystal structures of the resulting assemblies have been determined and the intermolecular interactions of the compounds in the crystalline phase have been investigated. Structure of compound $^3_\infty\{[\text{Co}(\text{oba})(\text{bpe})(\text{H}_2\text{O})_2] \cdot (\text{H}_2\text{O})_4\}$ is depicted in Fig. 1.

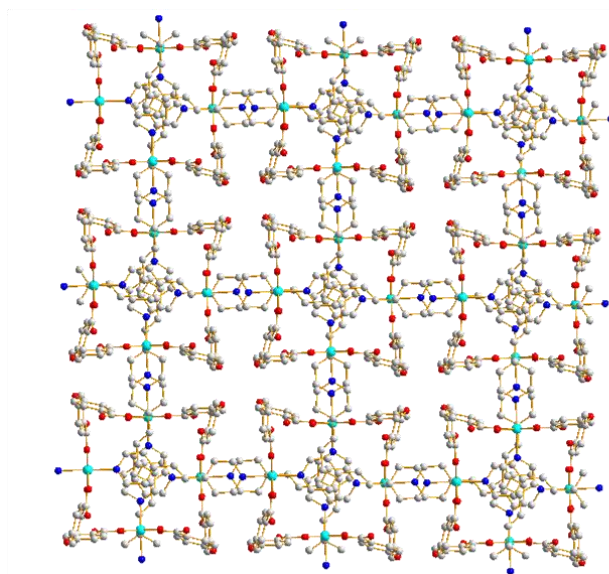


Figure 1. Structure of the 3-D coordination polymer ${}^3_{\infty}\{[\text{Co}(\text{oba})(\text{bpe})(\text{H}_2\text{O})_2]\cdot(\text{H}_2\text{O})_4\}$ (Hydrogen atoms were omitted for clarity).

Conclusions

The results revealed that the flexible V-shaped dicarboxylate ligand obtained by deprotonating the 4,4'-oxy(bis)benzoic acid (oba), along with auxiliary N,N'-donor ligand 1,2-bis(4-pyridyl)ethylene (bpe) are effective building blocks in constructing new Co(II) coordination polymers with diverse architectures.

References

- [1] Chin T.C., Kenneth S., Coordination Chemistry Reviews, 128(1-2) (1993), 293-322.
- [2] Sareeya B., Satoru J., Susumu K., Science and Technology of Advanced Materials, 9(1) (2008), 014108-014119.
- [3] Kim, H.C., Mitra, S., Veerana, M., Lim, J.-S., Jeong, H.-R., Park, G., Huh, S., Kim, S.-J., Kim, Y., Scientific Reports, 9 (2019), 14983-14995.

POSTER PRESENTATIONS

New extended structures of organotin(IV) with dicarboxylic acids

Ariadna-Elena-Maria Benes, Cătălin Maxim, Andrei A. Pătrașcu, Delia-Laura Popescu*
*University of Bucharest, Faculty of Chemistry, Department of Inorganic Chemistry, 23
Dumbrava Roșie, 020464-Bucharest, Romania,*
emails: benesariadna@gmail.com, delia.popescu@chimie.unibuc.ro

Introduction

Organotin(IV) coordination polymers have been considered for their ability to stabilize specific stereochemistry and to induce diverse dimensionalities in their complexes, for their outstanding applications in agriculture, industry, biology, medicine, as well as in the synthesis of various types of chemical compounds [1-3]. Several new extended structures have been synthesized by slow evaporation method, at room temperature, in the reaction of ${}^n\text{Bu}_3\text{SnCl}$ with deprotonated dicarboxylic acids employed as linkers.

Experimental

The reagents employed in this study were purchased from commercial sources and used without further purification. Elemental analyses (C, H, N) were performed on a EuroEA Elemental Analyzer. The IR spectra of the samples were recorded in the range 4000-400 cm^{-1} using a Tensor 27 spectrophotometer with Fourier transform (FTIR) from Bruker, OPUS software, and KBr pills as a reference. The structures of the compounds were determined by single-crystal X-ray diffraction with a STOE IPDS II diffractometer, operating with Mo-K α ($\lambda = 0.71073 \text{ \AA}$) X-ray tube with graphite monochromator. ShelX-97 and Diamond 3 crystallographic software packages were used for calculations and graphical representations.

Results and discussion

The objectives of the study were the synthesis and characterization, followed by the evaluation of biological activity of new polynuclear systems of Sn(IV), in which organotin nodes are joined by organic ligands derived from dicarboxylic acids, which act as linkers. To obtain such compounds we used the reaction of organotin halides with deprotonated carboxylic ligands. Starting from Ph_3SnCl along with the dianions adipate (adp), fumarate (fum), 1,4-cyclohexanedicarboxylate (1,4-chd), and biphenyl-4,4'-dicarboxylate (bpdc) employed as divergent spacers, four new organotin polynuclear coordination compounds were obtained in the form of colorless crystals, during 25-40 days of slow evaporation. They are stable in and out of the solution. The characterization of these new structures is very important and was carried out by elemental analysis, single crystal and powder X-ray diffraction, as well as through the FTIR spectrophotometric method. In Fig. 1 is presented the molecular formula of the compound ${}^2_\infty[(n\text{Bu}_3\text{Sn})_2(\text{adp})]$.

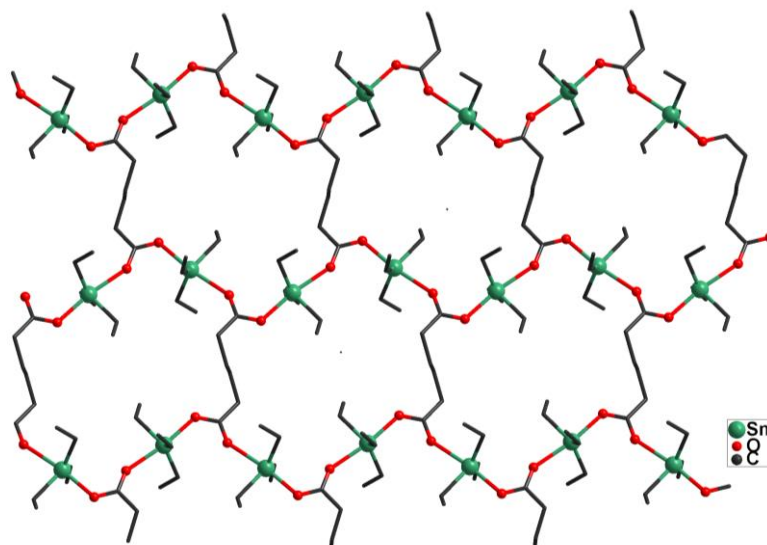


Figure 1. Molecular structure of compound $2_{\infty}[(n\text{Bu}_3\text{Sn})_2(\text{adp})]$.

Conclusions

A series of new polynuclear complexes with *n*-tributyltin(IV) nodes and deprotonated dicarboxylic acids as organic spacers have been synthesized. All compounds were obtained as colorless single crystals and characterized in solid state by elemental analysis, FTIR spectroscopy, as well as single crystal and powder X-ray diffraction. Obtaining various polynuclear organotin compounds is based on the proper choice of organotin(IV) precursors that act as nodes in extended structures, but also of the ligands that act like spacers. The crystallographic investigation of the new compounds reveals novel network topologies.

References

- [1] Kadu, R.; Roy, H.; Singh, V.K., *Applied Organometallic Chemistry*, 29 (2015), 746-755.
- [2] Awang, N.; Zakri, N.H.; Zain, N.M., *Journal of Chemical and Pharmaceutical Research*, 8 (2016), 862-866.
- [3] Iornumbe, E.N.; Yiase, S.G.; Sha'Ato, R., *International Journal of Science and Research*, 5 (2016), 1610.

Decorated Multi-Walled Carbon Nanotubes Dispersed in PHBHV for Wood Preservation

Madalina Elena David^{1,2,*}, Rodica-Mariana Ion^{1,2}, Lorena Iancu¹, Ramona Marina Grigorescu¹

¹National Institute for Research and Development in Chemistry and Petrochemistry – ICECHIM, 202 Spl. Independentei, 6th district, 060021, Bucharest, Romania

²Valahia University, Doctoral School of Materials Engineering Department, 13th Aleea Sinaia, Targoviste, Romania

e-mail: madalina.e.david@gmail.com

Introduction

Wooden artifacts are subjected to several degradation factors, which affect more or less their structural integrity and mechanical strength. Thus, the consolidation of wood artifacts has become a global problem and new systems are investigated in order to find a capable consolidate that ensures better durability over time [1]. In this study, nanocomposites based on multi-walled carbon nanotubes (MWCNTs) decorated with hydroxyapatite (Hap), zinc oxide (ZnO), or silver (Ag) nanoparticles (NPs) were dispersed in poly(3-hydroxybutyrate-co-3-hydroxyvalerate) (PHBHV) solution in order to study their ability as consolidate for wood.

Experimental

Each type of nanocomposites (at different concentrations 0.1, 0.2 and 0.4%) was dispersed in a solution of 2% PHBHV in chloroform, with the purpose of obtain a better dispersion of the nanomaterials. After the solutions were obtained, young oak wood pieces were treated by brushing – in three layers, to investigate the potential of the obtained solutions. Artificial aging test by exposure to temperature variations (cold-check test, different from freeze-thaw test) were carried out in order to investigate the color changes for each wood sample at different conditions. The total color difference ($\Delta E_{x\text{final}}$) was recorded before and after ageing, according to ASTM 2244 [2], and calculated according to Equation (1).

$$\Delta E_{x\text{ final}} = (\Delta L_x^2 + \Delta a_x^2 + \Delta b_x^2)^{1/2} \quad (1)$$

Artificial aging test by exposure to temperature variations consists in 20 alternative cycles, of three steps each; step I consisted of drying the wood samples for one hour at a temperature of 50 °C; step II, the samples were conditioned in a laboratory environment for 1 hour ($T = 25 \pm 2$ °C), and step III consisted of keeping the samples in the freezer at a temperature of -20 ± 2 °C, according to ASTM D1211-97 [3]. After the 20 alternative cycles, colorimetric parameters, mechanical resistance and contact angle tests were investigated in order to study if the obtained treatments were time-resistant.

Results and discussion

The environmental conditions to which the wood is subjected causes wood discoloration, and this degradation takes place in shades of gray, brown, yellow or red, depending on the type of wood. The process of wood discoloration takes place due to environmental factors that play an important role in the degradation of lignin or hemicellulose in the cell wall of the wood material. After cold-check test, the control sample showed the highest change of ΔE_x , which showed a slight discoloration over time and

exceeds the visible limit (of 2.5). This means that the color change after the cold-check test is significantly visible (Table 1).

Table 1. Total color difference calculated (ΔE_x) after cold-check test reported to the initial chromatic parameters of the samples

Treatment	ΔL_x	Δb_x	Δa_x	ΔE_x
Untreated wood	1.54	0.19	2.89	3.28
0.1% MWCNT+ PHBHV	0.40	1.58	2.29	2.81
0.2% MWCNT+ PHBHV	0.92	0.56	1.96	2.24
0.4% MWCNT+ PHBHV	0.23	0.68	2.16	2.28
0.1% MWCNT_ZnO+ PHBHV	0.35	0.48	2.46	2.53
0.2% MWCNT_ZnO+ PHBHV	0.16	0.43	2.26	2.31
0.4% MWCNT_ZnO+ PHBHV	0.80	0.73	2.75	2.96
0.1% MWCNT_Hap+ PHBHV	0.75	0.01	2.25	2.37
0.2% MWCNT_Hap + PHBHV	0.36	0.54	2.27	2.36
0.4% MWCNT_Hap + PHBHV	0.82	0.58	2.15	2.38
0.1% MWCNT_Ag+ PHBHV	0.49	0.42	2.25	2.34
0.2% MWCNT_Ag + PHBHV	0.10	0.31	2.35	2.38
0.4% MWCNT_Ag + PHBHV	0.20	0.15	2.33	2.34

where: ΔL is the difference in lightness, calculated with the formula: $\Delta L = L_{\text{treated sample}} - L_{\text{untreated sample}}$; Δa is the chromatic deviation of the coordinates of a* coordinates, calculated with the formula: $\Delta a = a_{\text{treated sample}} - a_{\text{untreated sample}}$; and Δb is the chromatic deviation of the b* coordinates, calculated with the formula: $\Delta b = b_{\text{treated sample}} - b_{\text{untreated sample}}$.

Subsequently, contact angle tests performed on the untreated and treated samples, after cold-check test. It was observed that the value of the contact angle for untreated wood decreases significantly, in 30 seconds reaching 0° , while for the treated samples, the contact angle value after 1 minute remained above 150° . Also, mechanical tests were performed and it was observed that the applied treatments protected the wood material even after it was exposed to temperature variations, the treated samples showing superior mechanical properties compared to the untreated sample.

Conclusions

The obtained treatments have the ability to protect the wooden material, even after it was exposed to extreme conditions, maintaining its mechanical properties and a hydrophobic character for a long time.

Acknowledgements

This work was supported by Romanian Ministry of Research and Innovation, CCCDI – UEFISCDI, by the contract 567 PED/2020.

References

- [1] David, M.E., Ion, R.M., Grigorescu, R.M., Iancu, L., Holban, A.M., Nicoara, A.I., Alexandrescu, E., Somoghi, R., Ganciarov, M., Vasilievici, G., Gheboianu, A.I., *Nanomaterials*, 11 (2021), 1415.
- [2] ASTM, D. (2013). 2244. Standard Practice for Calculation of Color Tolerances and Color Differences from Instrumentally Measured Color Coordinates.
- [3] Budakçi, M., Korkut, D. S., *African Journal of Biotechnology*, 9 (2010), 3595-3602.

Chiral-copper(II) complexes anchored on carboxylated graphene oxide for catalytic applications

Diana-Ioana Eftemie^{1,*}, Adela-Maria Spinciu¹, Cătălin Maxim¹, Zinnia Arora², Ana-Maria Hanganu^{2,3}, Madalina Tudorache², Bogdan Cojocaru², Octavian D. Pavel², Pascal Granger⁴, Marius Andruh^{1,3}, Vasile I. Pârvulescu²

¹University of Bucharest, Faculty of Chemistry, Department of Inorganic Chemistry, 4-12 Regina Elisabeta Av., S3, 030018, Bucharest, Romania

²University of Bucharest, Faculty of Chemistry, Department of Organic Chemistry, Biochemistry and Catalysis, 4-12 Regina Elisabeta Av., S3, 030018, Bucharest, Romania

³Institute of Organic Chemistry "C. D. Nenitzescu", Romanian Academy, 202B Spl. Independenței S6, 060023, Bucharest, Romania

⁴Univ. Lille, CNRS, Centrale Lille, Univ. Artois, UMR 8181 – UCCS – Unité de Catalyse et Chimie du Solide, F-59000 Lille, France

e-mail: deftemie@yahoo.com

Introduction

Immobilization of metal complexes on solid supports is an efficient method for the synthesis of hybrid catalysts, combining the advantages of homogenous and heterogenous catalysis. In this study, two new chiral hybrid systems, GO-COOH/(Cu(D-valmet) and GO-COOH/Cu(L-valmet), were synthesized and they were further investigated for their catalytic activity.

Experimental

The chiral compounds [Cu(D-valmet)(H₂O)]·H₂O, [Cu(L-valmet)(H₂O)]·H₂O were synthesized following a procedure described in the literature [1]. Graphene oxide (GO) was prepared using the modified Hummers' method as previously reported [2]. The number of carboxyl groups present on the surface of graphene oxide was increased using a derivatization method with chloroacetic acid [3]. The hybrid systems GO-COOH/(Cu(D-valmet) and GO-COOH/Cu(L-valmet) were synthesized by anchoring the copper(II) complexes onto the surface of carboxylated graphene oxide through covalent and non-covalent interactions. The catalytic activity of the new materials was investigated for the asymmetric Henry reaction of benzaldehyde with nitro-methane.

Results and discussion

The newly obtained compounds (Fig. 1) have been characterized by FTIR, Raman, Circular Dichroism and SEM-EDX spectroscopy. The carboxyl groups act as linkers for the immobilization of the complexes via coordination to the copper centers. The attachment of [Cu(D-valmet)(H₂O)]·H₂O and [Cu(L-valmet)(H₂O)]·H₂O onto the surface of carboxylated graphene oxide can be also supported by π - π interactions established between the phenyl rings of the ligands and the basal plane of GO-COOH. For the reaction of benzaldehyde and nitromethane in water, catalytic testes showed that the newly obtained composites led to a high conversion and enantioselectivity (92.5%, with an ee of 95.8%).

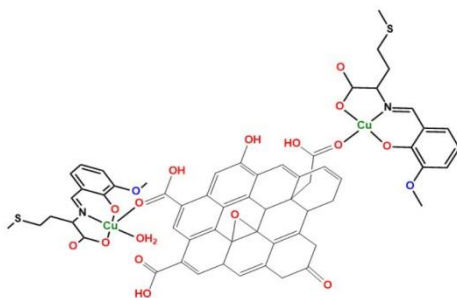


Figure 1. Schematic illustration of the hybrid systems.

Conclusions

In this study, two new hybrid materials were successfully synthesized and their catalytic activity has been investigated. The immobilization of chiral copper(II) complexes onto the surface of carboxylated graphene oxide was an efficient method for the preparation of new heterogenous catalysts for the asymmetric Henry reaction.

Acknowledgements

The authors thank the UEFISCDI for continued funding through the projects PN-III-337 P1-1.2-PCCDI-2017-0541 1/2018, PN-III-P4-IDPCCF-2016- 338 0088 17/2021, and PN-III-P4-ID-PCE-2020-1532.

References

- [1] Ene, C.D., Maxim, C., Rouzières, M., Clérac, R., Avarvarei, N., *Chemistry – A European Journal*, 24 (2018), 8569-8576.
- [2] Hummers, W.E., Offeman, R.E., *Journal of the American Chemical Society*, 80 (1958), 1339-1339.
- [3] Guo, S., Raya, J., Ji, D., Nishina, Y., Menard-Moyon, C., Bianco, B., *Nanoscale Advances*, 2 (2020), 4085-4092.

Removal of Sunset Yellow FCF from aqueous solutions using modified NaX zeolite and MCM-41 silica obtained from fly ash

Agata Jankowska^{1,*}, Rafał Panek², Wojciech Franus², Joanna Gościańska¹

¹Adam Mickiewicz University in Poznań, Faculty of Chemistry, Laboratory of Chemical Technology, Uniwersytetu Poznańskiego 8, 61-614 Poznań, Poland

²Lublin University of Technology, Department of Geotechnical Engineering, Nadbystrzycka 40, 20-618 Lublin, Poland

e-mail: agachel@amu.edu.pl

Introduction

The economic development of the world has contributed to a significant deterioration of the environment. Water bodies are polluted with various compounds, including organic dyes, that threaten wildlife and human health. These contaminants are difficult to remove *via* conventional methods such as mechanical and biological treatment, chemical coagulation or sludge digestion, hence adsorption processes are most often used. For this reason, it is important to search for new porous adsorbents that would effectively remove dangerous substances from water. Fly ash is a solid residue obtained from the energetic combustion of coal in power plants and thermal power plants. The wide range of its applications is related to its characteristic physicochemical properties (such as chemical composition, bulk density, particle size, porosity, water holding capacity or specific surface area). Therefore, fly ash is currently used in the synthesis of zeolites and ordered mesoporous silicas [1-3]. In the following work, research concerning the effectiveness of pure and modified NaX zeolite and MCM-41 silica obtained from fly ash in removing Sunset Yellow FCF from aqueous solutions is presented.

Experimental

During the studies, the pure materials were functionalized with different amounts of (3-aminopropyl)trimethoxysilane (APTMS) and (3-aminopropyl)triethoxysilane (APTES). The modifications were carried out in order to obtain materials with higher sorption capacities towards selected azo dye. The samples were characterized using low-temperature nitrogen adsorption/desorption method. Acidic and basic oxygen groups located on the surface of all samples were determined. The influence on sorption capacities of pure and modified zeolites and silicas at different pH (2, 3, 5, 7, 9) and temperatures (25 °C, 35 °C, 45 °C) was also investigated. Subsequently, the synthesized materials were applied in the removal of Sunset Yellow FCF from the liquid phase using adsorption processes. A series of dye's water solutions of different concentrations (12.5–900 mg/l) were prepared in order to obtain isotherms of Sunset Yellow FCF adsorption on pure and modified NaX and MCM-41.

Results and discussion

The modification of NaX and MCM-41 has led to obtaining new materials with improved adsorption properties, making them applicable in Sunset Yellow FCF removal. Functionalization with APTMS and APTES resulted in the decrease of their specific surface area as well as pore volume and the generation of basic oxygen functional groups on the surface. The studies concerning the impact of pH and temperature revealed that the materials have the highest sorption capacities at pH 2 and room temperature. This showed that the adsorption process is exothermic. In acidic environment, the surface of zeolites and silicas is protonated. Because of the electrostatic attraction between the negatively charged dye's molecules and positively charged surface of the materials, the bigger amount of dye can be adsorbed in the lower pH. The isotherms of Sunset Yellow FCF adsorption are displayed in

Fig. 1. The amount of adsorbed dye increased with the increase of concentration of its solutions due to the enhanced interaction of dye molecules with the adsorbent surface.

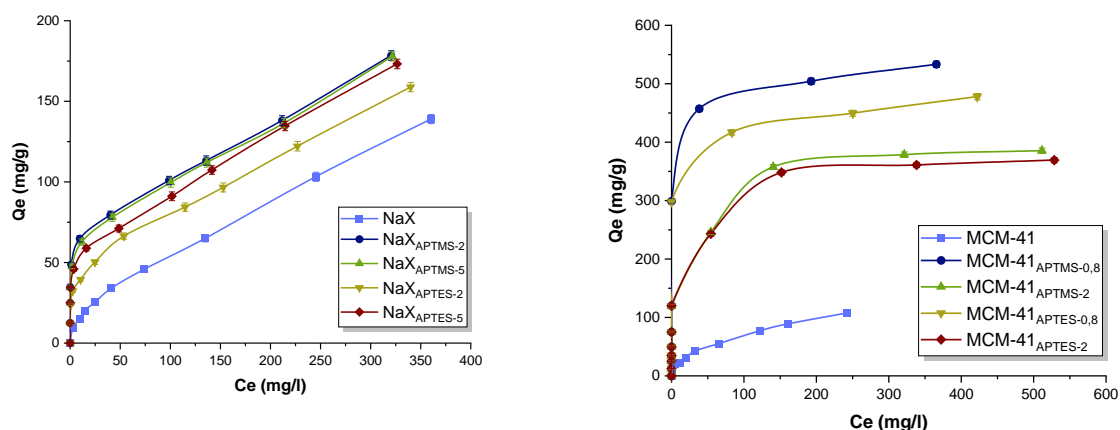


Figure 1. Isotherms of Sunset Yellow FCF adsorption onto NaX, NaX_{APTMS-2}, NaX_{APTMS-5}, NaX_{APTES-2}, NaX_{APTES-5}, MCM-41, MCM-41_{APTMS-0,8}, MCM-41_{APTMS-2}, MCM-41_{APTES-0,8}, and MCM-41_{APTES-2}.

Conclusions

The pH value and the temperature of the adsorption process as well as the acid-base properties of studied zeolites and silicas have a significant influence on their sorption capacities towards Sunset Yellow FCF. The best results were obtained at room temperature in acidic environment what arise from the exothermic nature of the process and electrostatic attraction between Sunset Yellow FCF molecules and adsorbents. Research proved that the modified NaX and MCM-41 can effectively remove the analyzed azo dye from aqueous solutions and are promising adsorbents for other pollutants endangering the environment.

References

- [1] Bonilla-Petriciolet, A., Mendoza-Castillo, D.I., Reynel-Avila, H.E., Introduction, Adsorption Processes for Water Treatment and Purification, Springer International Publishing (2017), 1-18.
- [2] Bello, M., Raman, A., Adsorption and Oxidation Techniques to Remove Organic Pollutants from Water, Green Adsorbents for Pollutant Removal, Springer International Publishing (2018), 249-300.
- [3] Belviso, C., State-of-the-art applications of fly ash from coal and biomass: A focus on zeolite synthesis processes and issues, Progress in Energy and Combustion Science, 65 (2018), 109-135.

Photocatalytic decontamination of wastewaters using hybrid organic inorganic magnetic supramolecular catalysts

Razvan Mihailescu*, Octavian D. Pavel, Sabina Ion, Madalina Tudorache, Simona M. Coman, Vasile I. Parvulescu, Bogdan Cojocaru*

University of Bucharest, Faculty of Chemistry, Department of Organic Chemistry, Biochemistry and Catalysis, 4-12 Regina Elisabeta Av., 030018, Bucharest, Romania

e-mails: bogdan.cojocaru@chimie.unibuc.ro; razvan.mihailescu09@gmail.com

Introduction

Pharmaceuticals, organic dyes, pesticides, phenolic compounds and many other hazardous chemicals are a silent enemy contaminating most of the fresh and salted water resources worldwide [1]. Current wastewater treatment technologies are unable to remove these toxic compounds which end up in the environment, posing a serious threat towards human life and the ecosystem. Antibiotics are one category of pharmaceutical compounds that have been recovered from aquatic systems. Because of their excessive use and the increasing demand of pharmaceuticals worldwide, their concentration in the environment is due to increase, currently being in the range of ppm-ppb making them hard to detect and degrade, affecting human health and also inducing an indirect antibiotic resistance to microbes [2,3]. One promising solution towards the decontamination of wastewaters is the usage of photocatalysts which use solar light as the energy source for the degradation process. While still emerging, Layered Double Hydroxides (LDHs) photocatalysts are currently researched towards accomplishing this goal [4,5]. The aim of this study is the synthesis of different magnetic Mg/Al LDHs incorporated with metallo-phthalocyanines (organic photosensitizers), their structural and functional characterization and the determination of the photocatalytic performance in β -lactam antibiotics photocatalytic degradation.

Experimental

A three-step synthesis was proposed. Firstly, six Mg/Al LDHs were synthesized via coprecipitation (pure LDH or doped with Fe^{2+} , respectively Fe^{3+}) while for the second and third steps, two strategies were followed in the preparation of the hybrid systems: in the first strategy the incorporation of Copper Phthalocyanine (CuPc) into the layered structure of the synthesized LDHs was done using the memory effect, followed by the insertion of Fe_3O_4 resulting in a magnetic supramolecular photocatalyst (HT CuPc/PM series – blue in Fig. 1.). The second strategy implied firstly the preparation of magnetite followed by the deposition of LDHs on it and, finally, the incorporation of CuPc into the layered structure (LDH/PM CuPc series – orange in Fig. 1). For the synthesized catalysts, the XRD, DR-UV-Vis, FT-IR and elemental analysis were used as characterization techniques. Catalysts were tested in the photodegradation of Oxacillin (Ox) from commercial drugs by using a solar simulator and also by irradiation at fixed wavelengths from the visible spectrum of light, in order to determine their activity and their best performance overall.

Results and discussion

Characterization data confirmed the success of the preparation: while the data obtained from XRD confirm the formation of the LDH structure and the insertion of magnetite; the DR-UVVis, FT-IR and elemental analysis results show the successful incorporation of the CuPc. The conversion in the degradation of Oxacillin after 60 minutes under simulated sun-light was high, with a maximum of about 90% for HT Fe^{3+} CuPc/PM

(Fig. 1). The HT CuPc/PM series (blue) exhibited higher activity than the LDH/PM CuPc series (orange).

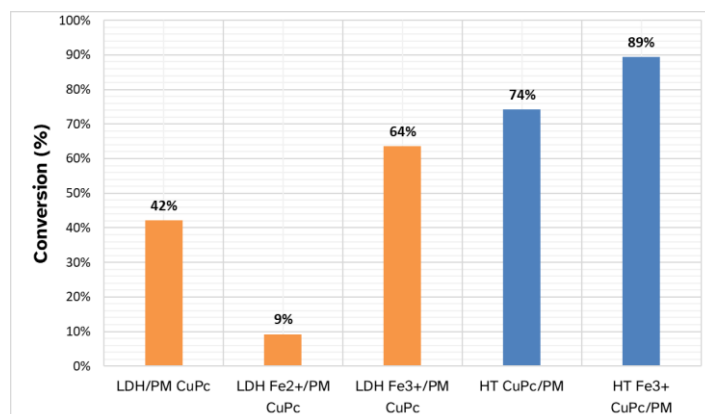


Figure 1. Oxacillin degradation after 60 minutes of simulated sunlight irradiation.

Conclusions

The hybrid organic-inorganic magnetic systems show promising activity in the photocatalytic degradation of β -lactam antibiotics under sun-light irradiation.

Acknowledgements

This work was supported by a grant of the Ministry of Research, Innovation and Digitization, CNCS/CCCDI – UEFISCDI, project number 235 / 2021 (PN-III-P4-ID-PCE2020-2207), within PNCDI III.

References

- [1] Varma, K.S., Tayade, R.J., Shah, K.J., Joshi, P.A., Shukla, A.D., Gandhi, V.G., *Water-Energy Nexus*, 3 (2020), 46-61.
- [2] Chatzidakis, A., Berberidou, C., Paspaltsis, I., Kyriakou, G., Sklaviadis, T., Poullos, I., *Water Research*, 42 (2008), 386-394.
- [3] Giraldo, A.L., Peñuela, G.A., Torres-Palma, R.A., Pino, N.J., Palominos, R.A., Mansilla, H.D., *Water Research*, 44 (2010), 5158-5167.
- [4] Maretti, L., Carbonell, E., Alvaro, M., Scaiano, J.C., Garcia, H., *Journal of Photochemistry and Photobiology A: Chemistry*, 205 (2009), 19-22.
- [5] Perez-Bemal, E., Ruano-Casero, R., Pinnavaia, T.J., *Catalysis Letters*, 11 (1991), 55.

Homo and heteroclusters of Mn(II/III) and Co(II/III) containing aminoalcohols and carboxylate anions

Andreea-Maria Pîrvu*, Violeta Tudor*, Cătălin Maxim*

University of Bucharest, Faculty of Chemistry, Department of Inorganic Chemistry, 23 Dumbrava Roşie, 020464-Bucharest, Romania

e-mails: andreea.pirvu@s.unibuc.ro, violeta.tudor@chimie.unibuc.ro,

catalin.maxim@chimie.unibuc.ro

Introduction

Magnetic clusters, meaning molecular assemblies consisting of a finite number of coupled paramagnetic centers, are currently receiving much attention in several active fields of research such as magnetism or biochemistry [1].

Of particular interest were Co/Mn heteroclusters due to the important and interesting applications that these metallic compounds present: catalysis, molecular magnetism, mimicking of active sites in biological systems.

Experimental

New Co/Mn heteroclusters were synthesized using cobalt perchlorate ((Co(ClO₄)₂·6H₂O), manganese perchlorate ((Mn(ClO₄)₂·6H₂O), triethanolamine (H₃tea), pivalic acid (Hpiv) and triethylamine (Et₃N) for deprotonation obtaining [Co^{II}₂Mn^{II}₂Mn^{III}₂(Htea)₄(piv)₆(Hpiv)₂]·8H₂O and the same salts, but changing the aminoalcohol with N-tertbutyldiethanolamine and using sodium acetate for [Co^{II}₃Mn^{II}₂Mn^{III}₂(N-tbdea)₄(AcO)₄(OH)₂(H₂O)₂]·2ClO₄·H₂O.

Results and discussion

In Fig. 1 is presented the structural unit in the compound [Co^{II}₂Mn^{II}₂Mn^{III}₂(Htea)₄(piv)₆(Hpiv)₂]·8H₂O.

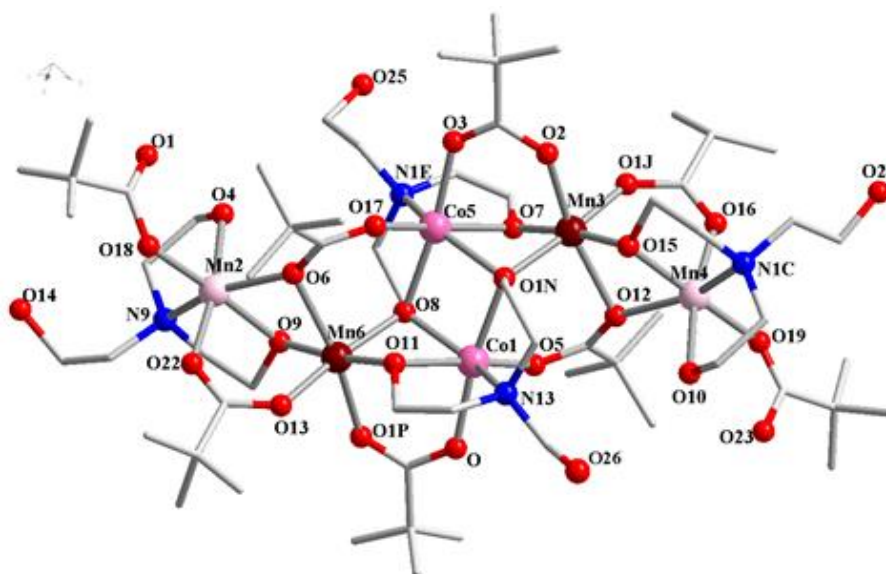


Figure 1. Structural unit in the compound [Co^{II}₂Mn^{II}₂Mn^{III}₂(Htea)₄(piv)₆(Hpiv)₂]·8H₂O

References

[1] Clemente-Juan, J. M., Coronado, E., Coordination Chemistry Reviews, 193-195 (1999), 361-394.

Plant based resins obtained from epoxidized linseed oil using a heterogenous hydrotalcite catalyst

Andrei Slabu, Florina Teodorescu *

“C.D. Nenitzescu” Center for Organic Chemistry, 202 B Spl. Independenței, S6, 060023 Bucharest, Romania

e-mail: florina.teodorescu@gmail.com

Introduction

Vegetable oil is an abundant renewable raw material which is considered for replacing petroleum based chemicals used industrially, with the intent of reducing pollution and can be used as such in the food industry and as bio lubricant [1]. The double bonds present in the alkyl chain of the unsaturated fatty acids present in vegetable oil open the possibility for obtaining a large variety of compounds using functionalization reactions such as metathesis, hydroformylation or epoxidation, leading to intermediaries that can be used as monomers in the polymer industry [2]. The epoxidation reaction is particularly important for the macro industry because it leads to versatile epoxidized vegetable oils that can be cured with a wide variety of compounds (amines, acids, anhydrides [3]) or that can undergo ring opening reactions, leading to interesting end-products and intermediaries. Anhydrides are some of the most efficient curing agents for epoxidized vegetable oils (EVO), leading to thermoset polymers with thermo-mechanical properties heavily influenced by the epoxy content of the vegetable oil and the anhydrides used [4]. The curing reaction is catalyzed by Lewis bases, such as tertiary amines or imidazole [5]. The goal of this study is obtaining materials through the curing of epoxidized linseed oil with phthalic anhydride (PA) using an affordable base heterogenous catalyst for achieving a cleaner and more environmentally friendly process. The catalyst is MgAl hydrotalcite, which is a layered double hydroxide (LDH), a class of materials with the $[M^{2+}_{1-x}M^{3+}_x(OH)_2]^{x+}[A^{n-}_{x/n}] \cdot mH_2O$ general formula. This catalyst was not previously reported in literature for this reaction, but it is instead well characterized [6] and used for a broad range of reactions [7].

Experimental

ELO and PA in different molar ratios were dissolved in toluene solvent. The MgAl LDH catalyst was added, and the mixture was heated to 100 °C and kept under constant magnetic stirring for 24 h. The solvent was evaporated, and the reaction mixture was processed. The obtained product was analyzed by 1H -NMR, IR spectroscopy, simultaneous thermogravimetric analysis (TGA) and differential scanning calorimetry (DSC) coupled with mass spectrometer (MS).

Results and discussion

The curing reactions were performed with different molar ratios between the ELO epoxy groups and PA. The average epoxy group content per triglyceride molecule was determined by adapting a previously described 1H -NMR method for the characterization of vegetable oils [8]. The molar ratio between reactants was adjusted for obtaining cured materials with different thermo-mechanical properties. Another curing reaction was also performed according to literature, using 1-methylimidazole as initiator. The FT-IR spectrum of the obtained solid product was compared with the spectra of the materials obtained by reacting ELO with PA in the presence of MgAl LDH, confirming the obtaining of cured resins. Modifying the molar ratio between ELO and PA led to products with different thermo-mechanical properties, as illustrated by the TGA thermogram presented below (Fig. 1). The

material obtained by using excess of PA (R2) has a higher thermal stability due to the higher degree of curing.

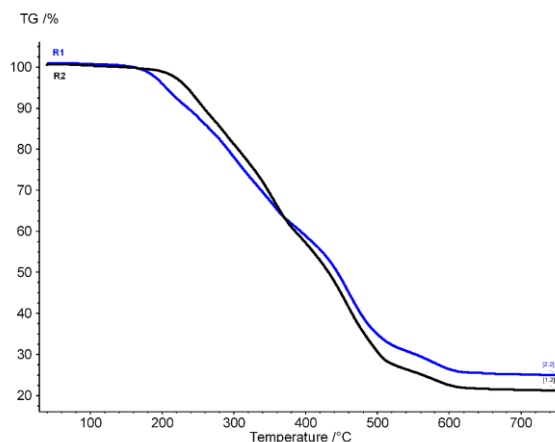


Figure 1. The TGA thermogram showing the degradation behavior of the resins at a heating rate of $10\text{ }^{\circ}\text{C} \cdot \text{min}^{-1}$, under He inert atmosphere.

Conclusions

Cured materials with different thermo-mechanical properties were obtained by reacting ELO and PA in different molar ratios, in the presence of a solid reusable catalyst, MgAl LDH. The curing was confirmed by FT-IR spectroscopy, TGA and DSC coupled with mass spectrometer. This shows that using MgAl LDH catalyst is a viable alternative for curing epoxidized vegetable oil with PA, in order to obtain interesting materials.

Acknowledgements

Financial support: PN-III-P2-2.1-PED-2019-4561, Executive Agency for Higher Education, Research, Development and Innovation (UEFISCDI)

References

- [1] Xia, Y., Larock, R.C., *Green Chemistry*, 12, (2010), 1893-1909.
- [2] Behr, A., Gomes, J.P., *European Journal of Lipid Science and Technology*, 112 (2010), 31-50.
- [3] Samper, M.D., Fombuena, V., Boronat, T., García-Sanoguera, D., Balart, R., *Journal of the American Oil Chemists' Society*, 89 (2012), 1521-1528.
- [4] Sedl, Z., *Journal of the American Oil Chemists' Society*, 79 (2002), 2333-2341.
- [5] Supanchaiyamat, N., Shuttleworth, P.S., Hunt, A.J., Clark, J.H., Matharu, A.S., *Green Chemistry*, 14 (2012), 1759-1765.
- [6] Debecker, D.P., Gaigneaux, E.M., Busca G, *Chemistry – A European Journal*, 15 (2009), 3920-3935.
- [7] Sels, B.F., De Vos, D.E., Jacobs, P.A., *Catalysis Reviews – Science and Engineering*, 43 (2001), 443-488.
- [8] Chira, N.A., Todasca, M.C., Nicolescu, A., Rosu, A., Nicolae, M., Rosca, S.I. *Revista de Chimie*, 62 (2011), 42-46.

Copper-based materials – new “green” electrochemical sensors for hydrogen peroxide

Adela Spinciu, Antonia Haddad, Diana Visinescu*, Cecilia Lete, Silviu Preda, Jose Calderon Moreno, Oana Carp

“Ilie Murgulescu” Institute of Physical Chemistry, Romanian Academy, Splaiul Independentei 202, Bucharest-060021

e-mail: dianavisinescu@icf.ro

Introduction

The obtaining of new “green” and sustainable electrochemical sensors for physiologically relevant electro-active analytes is challenging and stimulating. Copper is well-suited for designing electrochemical sensors, being highly reactive in electrocatalytic reactions (one-two electron pathway). Moreover, copper-based nanomaterials are generally low cost and show functional biocompatibility [1]. By using soft chemistry approaches, copper oxidic materials (CuO , Cu_2O) with various morphologies (nano-spheres, wires, cubes or rods or flower-like structures) were obtained and proved to be highly responsive to different analytes like glucose, uric acid, dopamine, ascorbic acid, and L-cysteine [1,2]. The polyol-based synthesis represents one of the most convenient and resourceful soft chemistry methods for the obtaining of well-crystallized metals or metal oxides with high compositional homogeneity, diversity of shapes and narrow size distributions [3]. Polyols can be considered green solvents being of low to moderate toxicity and highly biodegradable, with high boiling/flashing points. Polyols are the main source of oxygen for the formation of metal oxides, their specific properties (polarity, viscosity, and saturated vapour pressure) influencing the nucleation process, crystal growth, particle shapes, crystallite sizes and, therefore, their further aggregation into higher dimensional assemblies. Herein, we report on four new copper-based compounds obtained through polyol-based approach. Depending on the reaction parameters (precursor concentration, time/temperature of reaction), $\text{Cu}^{\text{II}}\text{O}$, mixtures $\text{Cu}^{\text{II}}\text{O}/\text{Cu}_2^{\text{I}}\text{O}$ and $\text{Cu}_2^{\text{I}}\text{O}/\text{Cu}^0$ and metallic copper nanoparticles were obtained. Their optical, morpho-structural, textural and electrochemical properties will be discussed.

Experimental

Copper-based particles were obtained through a 1,4-butanediol-assisted precipitation, as a result of the hydrolysis of $\text{Cu}(\text{CH}_3\text{COO})_2$, with different concentrations (0.1-0,5 M), at 140 and 180 °C. In a typical synthesis, an amount of $\text{Cu}(\text{CH}_3\text{COO})_2$ is dissolved in a known volume of 1,4-butanediol. The mixture was heated under stirring at the reaction temperature, in a round-bottom flask fitted with a reflux column, for 6–12 hours. The precipitation of copper-based particles occurred after 30 minutes. After cooling at room temperature, the solid phases were collected by centrifugation and washed with ethanol.

Results and discussion

The hydrolysis of copper(II) acetate in 1,4-butanediol afforded four types of copper-based particles of which composition, morphology and texture depend on the reaction conditions. FTIR spectra indicate three typical stretching vibrations of $\text{Cu}^{\text{II}}\text{-O}$ (covering 400-600 cm^{-1}) range and/or a strong peak attributed to $\text{Cu}^{\text{I}}\text{-O}$ bonds, at ca. 630 cm^{-1} . The XRD measurements show the formation of different crystalline phases depending on the precursor concentration and reaction parameters: a pure phase of monoclinic tenorite (CuO), a mixture of tenorite and cubic cuprite, $\text{Cu}_2^{\text{I}}\text{O}$, a mixture of cuprite and cubic metallic Cu^0 , as well as a pure phase of cubic copper particles. The SEM panoramic micrographs show the formation of large aggregates of nano-sized particles (see Fig. 1) of homogeneous phase (Fig. 1a), while,

for a different copper source concentration, the urchin-like particles of CuO co-exist with cubes of cuprite (Fig.1b). A higher reaction temperature led to the formation of porous aggregates of metallic copper particles (Fig. 1c). The electrochemical properties of CuO nanoparticles and their sensor applications were investigated through cyclic voltammetry and electrochemical impedance spectroscopy. The measurements indicate that the GCE/PEDOT-CuO sensor displayed better stability and enhanced electrochemical catalytic activity towards H_2O_2 reduction, with a linear response range towards hydrogen peroxide and a low detection limit (GCE – glassy carbon electrode; PEDOT – pre-electrodeposited polymeric coating made of poly(3,4-ethylenedioxythipohene)).

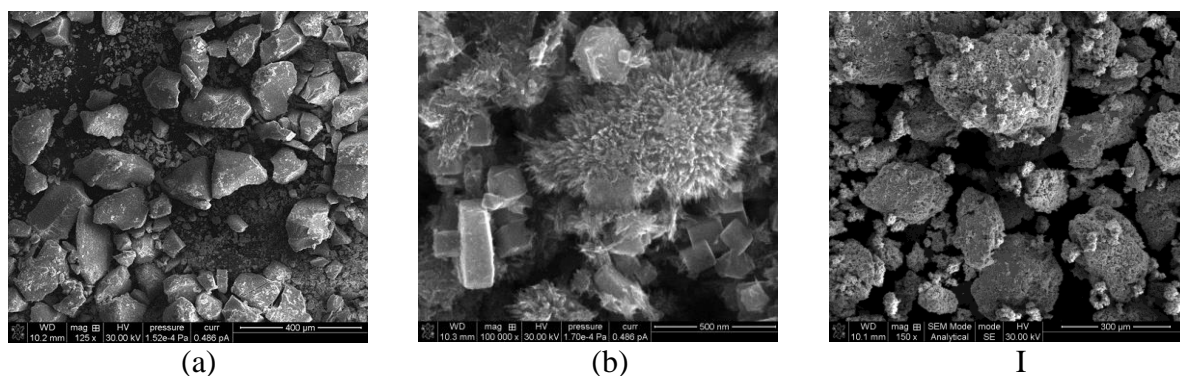


Figure 1. SEM panoramic micrographs for CuO, CuO/Cu₂O mixture and Cu⁰ metallic nanoparticles.

Conclusions

Copper-based particles were obtained through polyol-assisted method showing different compositions and morpho-structural properties, depending on reaction parameters. CuO nanoparticles proved to be a stable and electrochemically active toward hydrogen peroxide reduction.

Acknowledgements

This work was supported by a grant of the Romanian Ministry of Education and Research, CNCS – UEFISCDI, project number PN-III-P4-ID-PCE-2020-2324, within PNCIDI III.

References

- [1] Verma, N., Kumar, N., ACS Biomaterials Science & Engineering, 5 (2019), 1170.
- [2] Bhosale, M.A., Karekar, S.C., Bhanage, B.M., ChemistrySelect, 1 (2016), 6297.
- [3] Dong, H., Chen, Y.-C., Feldmann, C., Green Chemistry, 17 (2015), 4107.

Metal-containing ionic liquids used as catalysts in the recycling of PET waste

Robert-Andrei Tincu¹, Florina Teodorescu^{1,*}, Emeric Bartha¹

“C.D. Nenitzescu” Center for Organic Chemistry, 202 B Spl. Independenței, S6, 060023 Bucharest, Romania

e-mail: florina.teodorescu@gmail.com

Introduction

Poly(ethylene terephthalate), often known as PET, is a non-biodegradable post-consumer waste [1]. Glycolysis of PET wastes with various diols, employing a variety of catalysts, produces aromatic polyester-polyols (APPs) [2]. Inorganic metal salts or, more recently, organic molecules, are the most frequent catalysts used today (such as super-bases or ionic liquids). Ionic liquids have gained researchers' interest as suitable green solvents and/or catalysts due to their unique qualities, such as thermal stability, electrochemical stability, low flammability, and structural flexibility of the cation and anion. Polymer breakdown has been reported to use ionic liquids as solvents and/or catalysts. PET degrades efficiently with ionic liquids in a low-pressure, low-temperature environment without releasing harmful chemicals. The ionic liquid can be separated from the chemicals created by adding water via filtration, allowing the ionic liquid to be reused [3].

Experimental

In this study, various metal-containing ionic liquids and their precursors were synthesized using a 2-step experimental procedure. First, the 1,3-N,N-imidazolium salt was obtained by alkylation of N-methylimidazole with the corresponding organic halide, followed by the introduction of a metal, using the corresponding inorganic salt (ZnCl₂, CdCl₂ or ZnBr₂). To the best of our knowledge the use of [Bmim]ZnCl₃, [Ddmim]ZnCl₃, and [Bmim]CdCl₃ were not reported as catalyst for this reaction.

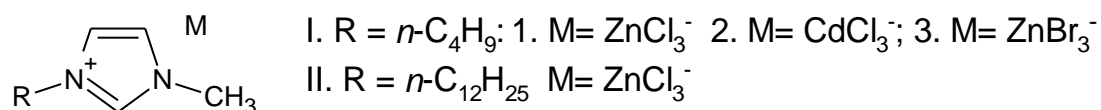


Figure 1. Formulas of the synthesized catalysts.

Following the synthesis, the compounds were analyzed by NMR, FTIR and MS and then tested for PET glycolysis using ethylene glycol (EG) as diol. After each reaction it was calculated the conversion (based on the quantity of PET unreacted) and the selectivity (based on the quantity of isolated monomer, by precipitation from cold water). In addition, some optimum reaction parameters were determined.

Results and discussion

The NMR analysis and FTIR spectra confirm the obtaining of compounds based on 1,3-N,N-disubstituted imidazolium salt. In addition, MS spectra show that these compounds have indeed the desired counter ions. The analysis of the precipitate indicates that beside the major product, bis-(2-hydroxyethyl)terephthalate (BHET), it contains around 20% of its dimer (bisBHET), fact that was not mentioned until now in the literature.

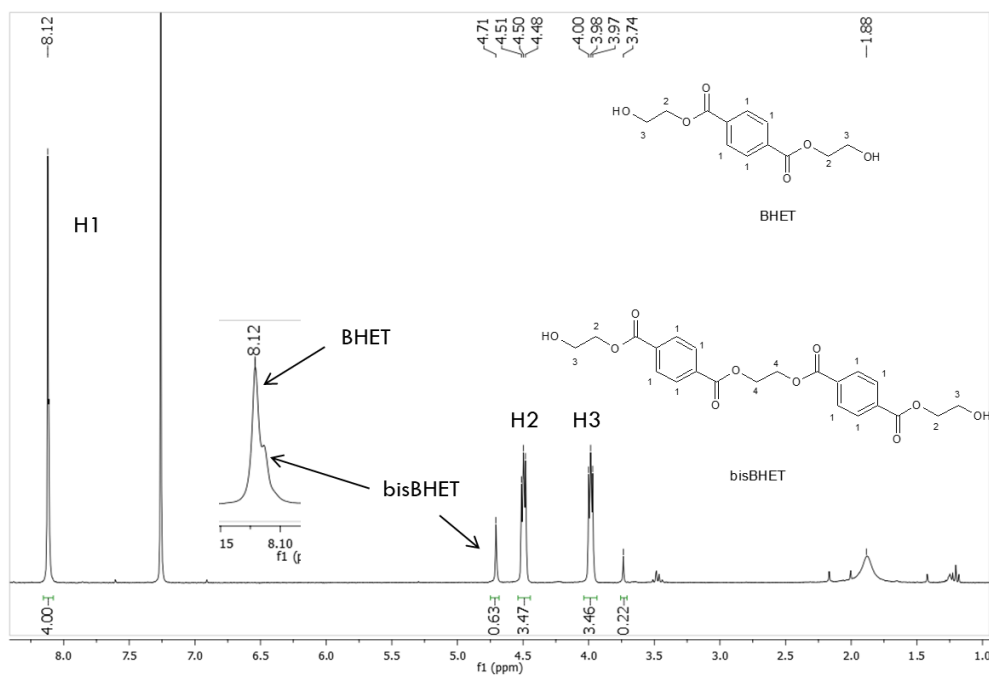


Figure 2. $^1\text{H-NMR}$ of the precipitate.

The parameters that were explored are the type of catalyst, the catalyst loading and the PET:EG molar ratio. The results show that the best selectivity in BHET is obtained using $[\text{Ddmim}]\text{ZnCl}_3$. This catalyst has also the advantages to be solid and more hydrophobic than $[\text{Bmim}]\text{ZnCl}_3$, hence it is more facile to use. Regarding the catalyst loading, the selectivity increases until 5% (molar), and then decreases, phenomena explained in the literature by the change in the equilibrium between BHET and its dimer, oligomers, etc. In addition, the selectivity increases with the molar ratio PET:EG, but above 1:10 the increase rate in BHET formation is insignificant so the usage of ratios above this value are not recommended.

Conclusions

In this study, four catalysts were synthesized and compared, three of them not being mentioned before in the literature. They were characterized by NMR, FTIR and MS, hence confirming the desired structure (1,3-N,N-disubstituted imidazolium salt). The glycolysis of PET using EG has the best selectivity in BHET using a catalyst ($[\text{Ddmim}]\text{ZnCl}_3$) loading of 5% molar with respect to PET and a molar ratio PET:EG=1:10.

Acknowledgements

This work was supported by the Executive Agency for Higher Education, Research, Development and Innovation (UEFISCDI): PN-III-P2-2.1-PTE-2019-0355.

References

- [1] George, N., Kurian T., *Industrial & Engineering Chemistry Research*, 53 (2014), 14185-14198.
- [2] Wang, H., Li, Z., Liu, Y., Zhang, X., Zhang S., *Green Chemistry*, 11 (2009), 1568-1575.
- [3] Shuangjun, C., Weihe, S., Haidong, C., Hao, Z., Zhenwei, Z., Chaonan, F., *Journal of Thermal Analysis and Calorimetry*, 143 (2021), 3489-3497.

ALFABETICAL INDEX OF AUTHORS

A		F	
Alexe C.-A.	53	Farrando-Pérez J.	23; 63
Andruh M.	68; 89	Franus W.	91
Antony J.	26	Frunza L.	11
Arora Z.	89	Ftodiev A.-I.	72
Atkinson I.	78		
B		G	
Badea M.	25	Gaidau C.	53
Bandyopadhyay S.	26	Galarda A.	49
Bartha E.	100	Ganes C.P.	11
Bălăşoiu M.	38	Garcia-Ripoll A.	63
Bărar A.	38	Gheorghita G.	40
Bejan S.E.	76	Ghetu M.C.	44
Benes A.E.M.	85	Gonzalez S.V.	26
Bogdanescu C.	76	Góra-Marek K.	21
Boquin L.H.Y.	4	Gościańska J.	32; 34; 47; 49; 91
Bordeiaşu M.	70; 74	Granger P.	65; 89
Boscornea C.	38	Greluk M.	21
		Grigorescu R.M.	87
		Grzybek G.	19; 21
		Guzo N.C.	32; 51
C		H	
Candu N.	51; 65	Haddad A.	98
Carp O.	98	Hanganu A.-M.	89
Cieź D.	16		
Ciobota C.F.	36; 76	I	
Ciszewska M.	16	Iancu L.	87
Cojocar B.	28; 30; 32; 42; 57; 89; 93	Ion R.-M.	87
Coman S.M.	6; 28; 32; 51; 65; 93	Ion S.	42; 93
Crăciun G.	78	Irimescu R.E.	36
Cuadrado-Collados C.	23		
Cucos A.	30	J	
Culiţă D.	78	Jacobsen E.E.	4
Cursaru L.M.	76	Janiak C.	74
		Jankowska A.	91
		Jardim E.O.	63
		Jurca B.	57
D		K	
Dascalu R.C.	68	Kadela K.	19
David M.E.	87	Kemnitz E.	6
		Klungseth K.	4
		Kotarba A.	21
		Kotula M.	34
		Kurniawan M.	13
E		L	
Economopoulos S.	61	Lete C.	98
Eftemie D.-I.	89	Lungu C.	46
Ejismont A.	34		
El Fergani M.	32; 51; 65		
Enculescu M.	11		

M		Purcarea C.	40
Majda D.	16	Pyra K.	21
Marcu I.-C.	78		
Martinez-	23	R	
Escandell M.		Radko M.	16
Maxim C.	68; 70; 80; 85; 89; 95	Rapa M.	53
Mădălan A.M.	59; 68; 70; 74	Răducă M.	74
Mănăilă-Maximean D.	38	Reljic S.	23
Mihailescu R.	93	Rønning M.	26
Mihăilă S.-D.	57	Rotko M.	21
Mirică C.	67	Ruwoldt J.	13
Mitran G.	57	S	
Mitroi P.C.	59	Silvestre-Albero J.	23; 63
Montero Amenedo J.	36	Simion C.E.	36
Moreno J.C.	98	Shova S.	30
		Skórkiewicz S.	16
N		Slabu A.	96
Niculescu M.	53	Slobozeanu A.E.	36
Norrman J.	13	Słowik G.	21
		Sobeŭkii A.	36
O		Spinciu A.-M.	89; 98
Oancea P.	28	Stanca M.	53
Olejnik A.	47	Stănoiu A.	36
Oliveira Jardim E.	23	Stelmachowski P.	19
Oprea M.	55	Stoian G.	28
Österlund L.	36	Sun Y.	74
		T	
P		Tarach K.	21
Pandele A.M.	55	Tennfjord A.L.	4
Panek R.	91	Teodorescu F.	96; 100
Papa F.	78	Toderaş A.-T.	78
Paraschiv C.	30	Troøyen S.H.	4
Parvulescu V.I.	3; 6; 28; 30; 32; 42; 51; 57; 65; 89; 93	Tudor I.A.	76
Pasatoiu T.-D.	68	Tudor V.	95
Paso K.G.	13	Tudorache M.	28; 40; 42; 44; 51; 65; 89; 93
Patulski P.	21	Turtoi M.	70
Pavel O.-D.	57; 89; 93		
Pătraşcu A.A.	85	Ț	
Petcuță O.	70	Țincu R.-A.	100
Piticescu R.M.	36; 76		
Piticescu R.R.	76	U	
Pîrvu A.-M.	95	Urdă A.	78
Popescu D.-L.	59; 70; 74; 80; 85		
Podolean I.	51	V	
Preda N.	11	Visinescu D.	98
Preda S.	98	Voicu Ş.I.	55
Psarrou M.N.	61	Voinea D.	80

Z

Zăvoianu R. 57

Zgura I. 11

Y

Yang J. 26

W

Węgrzyn A. 16